UNIVERSIDADE ESTADUAL DE CAMPINAS

INSTITUTO DE GEOCIÊNCIAS

PÓS-GRADUAÇÃO EM GEOCIÊNCIAS

ÁREA DE GEOLOGIA E RECURSOS NATURAIS

ALOÍSIO JOSÉ BUENO COTTA

DETERMINAÇÃO DE ELEMENTOS-TRAÇO EM ÁGUAS E ROCHAS POR ICP-MS QUADRUPOLAR COM CELA DE COLISÃO

Tese apresentada ao Instituto de Geociências como parte dos requisitos para obtenção do título de Doutor em Ciências.

Orientadora: Profª. Drª. Jacinta Enzweiler

CAMPINAS - SÃO PAULO

Dezembro – 2010

UNIVERSIDADE ESTADUAL DE CAMPINAS

INSTITUTO DE GEOCIÊNCIAS

PÓS-GRADUAÇÃO EM GEOCIÊNCIAS NA

ÀREA DE GEOLOGIA E RECURSOS NATURAIS

UNICAMP

AUTOR: Aloísio José Bueno Cotta

"Determinação de elementos-traço em águas e rochas por ICP-MS quadrupolar com cela de colisão".

ORIENTADORA: Profa. Dra. Jacinta Enzweiler
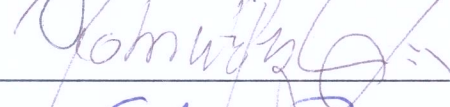
Aprovada em: 21/12/2010

EXAMINADORES:
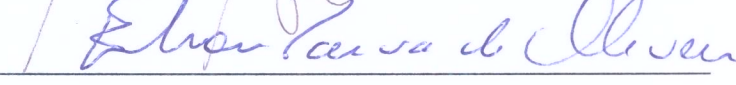
Profa. Dra. Jacinta Enzweiler   _____ - Presidente
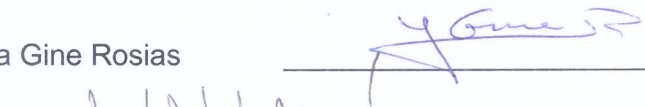
Prof. Dr. Roberto Perez Xavier   _____
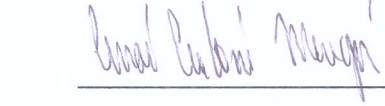
Prof. Dr. Élson Paiva de Oliveira   _____

Profa. Dra. Maria Fernanda Georgina Gine Rosias   _____

Prof. Dr. Amauri Antônio Menegario   _____

Campinas, 21 de dezembro de 2010.

AGRADECIMENTOS

BIOGRAFIA

Aloísio José Bueno Cotta é bacharel em química, graduado pela Universidade Federal de Viçosa-MG (2005) e mestre em Geociências pelo Instituto de Geociências da Universidade Estadual de Campinas-SP, IG-UNICAMP (2007). Possui artigos publicados nas áreas de produção e certificação de material de referência geoquímico (Basalto de Ribeirão Preto, BRP-1), tema de sua dissertação de mestrado. Possui também artigos nas áreas de geoquímica analítica descrevendo metodologias durante o doutoramento (2007-2010) no IG-UNICAMP para determinação de elementos-traço em águas e rochas após sua decomposição, além de diversas partições em congressos nacionais e internacionais na forma de pôster ou apresentação oral.

Índice

Lista de siglas

CC	Cela de colisão
CV	Coeficiente de variação relativo
GeoReM	Web site (http://georem.mpch-mainz.gwdg.de/)
HPA-S	High pressure asher-system
IAG	International Association of Geoanalysts
ICP-MS	Espectrometria de massas com plasma indutivamente acoplado
ICP-OES	Espectrometria óptica de emissão com plasma de Ar indutivamente acoplado
ICP-QMS	ICP-MS com analisador quadrupolar
ID	Diluição isotópica
IGGE	Institute of Geophysical and Geochemical Prospecting, People's Republic of China
IG/UNICAMP	Instituto de Geociências, Universidade Estadual de Campinas
INMETRO	Instituto Nacional de Metrologia, Normalização e Qualidade Industrial
ISO	International Organization for Standardization
KED	Discriminação por energia cinética
MR	Material de referência
NIST	National Institute of Standards and Technology
NRCC	National Research Council of Canada
US EPA	United States Environmental Protection Agency
USGS	United States Geological Survey
VIM	Vocabulário Internacional de Metrologia
XRF	Fluorescência de raios X

Materiais de referência (produtor)

BCR-2	Basalt, Columbia River (USGS)
BHVO-2	Basalt, Hawaiian Volcanic Observatory (USGS)
BIR-1	Icelandic Basalt (USGS)
BRP-1	Basalto de Rbeirão Preto (UNICAMP)
G-3	Granito (USGS)
GSP-2	Granodiorite, Silver Plume (USGS)
GSR-1	Granito (IGGE)
OU-6	Penrhyn Slate (IAG)
RGM-1	Rhyolite, Glass Mountain (USGS)
SLEW-3	Estuarine Water Reference Material for Trace Metals (NRCC)
SLRS-4	River Water Reference Material for Trace Metals (NRCC)
SRM 1640	Standard Reference Material 1640 Trace Elements in Natural Water (NIST)
SRM 1643e	Standard Reference Material 1643e Trace Elements in Water (NIST)

DETERMINAÇÃO DE ELEMENTOS-TRAÇO EM ÁGUAS E ROCHAS POR ICP-MS QUADRUPOLAR COM CELA DE COLISÃO

RESUMO

Aloísio José Bueno Cotta

A espectrometria de massas com plasma indutivamente acoplado (ICP-MS) possibilita determinações multielementares rápidas e com baixos limites de detecção numa variedade de matrizes, dentre elas as geológicas. Neste estudo, métodos comparativos utilizando um ICP-MS quadrupolar equipado com cela de colisão (CC) foram estabelecidos para determinar amplos conjuntos de elementos-traços em águas e em rochas. A aplicabilidade e as limitações da CC para atenuar interferências poliatômicas sobre os isótopos empregados foram amplamente investigadas. Em condições ótimas, muitas interferências puderam ser eliminadas ou significativamente atenuadas, o que tornou os métodos menos dependentes de correções matemáticas. Para a análise de rochas, técnicas clássicas de dissolução envolvendo misturas ácidas, como HF/HNO_3, foram utilizadas e um novo procedimento com equipamento que possibilita efetuar a digestão sob pressão de até 13 MPa é proposto. Nesse caso, a precipitação de AlF_3, o qual retém alguns elementos-traço, principalmente Co, Sr, Ba e Pb, foi o maior obstáculo à recuperação quantitativa dos analitos. A formação de AlF_3 foi evitada com a adição de Mg à porção teste e com o controle da temperatura de digestão. A decomposição por sinterização com peróxido de sódio foi também investigada e verificou-se que a inclusão de uma etapa de aquecimento da dispersão resultante da dissolução do sinterizado em água, antes da separação do precipitado de hidróxidos de Fe e Ti, o qual retém os elementos-traço, auxilia na co-precipitação de Ni, Zr, Nb, Cd, Sn, Sb, Hf, Pb e Th e permite acrescentá-los à lista de elementos determináveis. Os métodos foram validados pela análise de um conjunto de materiais de referência (MR), alguns deles certificados. Os resultados obtidos demonstraram que os métodos desenvolvidos para águas e rochas apresentaram tendência e coeficientes de variação menores que 5% para a maior parte dos mensurandos. Os resultados obtidos para os MR certificados de rochas, BRP-1 e OU-6, foram utilizados para calcular a incerteza do método ao nível aproximado de confiança de 95%. A técnica de diluição isotópica foi aplicada para determinar Cr, Ni, Cu, Zn, Sr e Sn em alguns MR de rochas em uso e em candidatos a MR, com o objetivo de estabelecer o método e contribuir com novos valores para esses MR. As incertezas de todas as etapas do procedimento foram estimadas. Os resultados obtidos evidenciam que o valor certificado de Cr em BRP-1 deveria ser revisto e confirmam a necessidade do estabelecimento da rastreabilidade metrológica durante a certificação de MR.

TRACE ELEMENTS DETERMINATION IN WATER AND ROCKS BY QUADRUPOLE ICP-MS WITH COLLISION CELL

ABSTRACT

Aloísio José Bueno Cotta

Inductively coupled plasma mass spectrometry (ICP-MS) is suited for fast multi-trace element determinations with low detection limits in a variety of matrices, including geological samples. In this study we established comparative analytical methods for the determination of an expressive number of trace elements in water and rock samples using an ICP-MS equipped with collision cell (CC). The applicability and limitations of CC for polyatomic interference attenuation over the isotopes used were widely investigated. Under optimized conditions, many interferences were eliminated or significantly attenuated, so these methods depend less on mathematical corrections. For rock analyses, classical multi-acid decomposition techniques, with mixtures like HF/HNO_3, were used, and a new procedure with equipment that allows digestion at 13 MPa is proposed. In this case, the precipitation of AlF_3, which retains some trace elements like Co, Sr, Ba and Pb preferentially, was the major drawback in achieving quantitative recoveries. The formation of AlF_3 was inhibited by adding Mg to the test portion and controlling the temperature of digestion. Sample decomposition by sintering with sodium peroxide was also tested and was demonstrated that including a heating step of the sinter dispersion obtained after dissolution in water and before the separation of the precipitated Fe and Ti hydroxides, which retain many trace elements, helps to achieve a quantitative co-precipiation of Ni, Zr, Nb, Cd, Sn, Sb, Hf, Pb and Th and allows to include them to the list of determinable elements. The methods were validated by analysis of a set of reference materials (RM) some of them certified. Relative standard deviations and bias of the results were less than 5% for most of the measurands. The results obtained for the certified RM BRP-1 and OU-6 were used to calculate the measurement uncertainty at the approximate 95% confidence interval. The isotope dilution technique was applied to determine Cr, Ni, Cu, Zn, Sr and Sn in some geochemical RM in use and in candidate RM, with the objective of establishing the method to contribute with new values for the analysed RM. The uncertainties of the whole analytical procedure were estimated. The results obtained show that the certified value of Cr in BRP-1 should be reviewed and confirm the need of establishing the metrological traceability during the certification of RM.

1. APRESENTAÇÃO DO TRABALHO

O presente texto visa atender aos requisitos para obtenção do título de Doutor em Ciências. A seguir há uma introdução, acompanhada dos objetivos e conclusões desta pesquisa. As investigações realizadas durante o estabelecimento de métodos analíticos para a determinação de elementos-traço em águas e rochas são apresentadas e seus resultados discutidos nos Anexos I, II, III e IV respectivamente, um artigo completo publicado, um resumo expandido, um artigo aceito para publicação e um manuscrito em preparação.

2. INTRODUÇÃO

2.1. Introdução à instrumentação

Valores de concentração para elementos-traço presentes em águas, solos, sedimentos e rochas são amplamente utilizados para investigar processos geológicos, bem como, para garantir e monitorar a qualidade ambiental de sistemas aquáticos e terrestres. A espectrometria de massas com plasma indutivamente acoplado (ICP-MS) se destaca dentre as técnicas instrumentais disponíveis para tais fins quando os limites de detecção, rapidez e diversidade de elementos determináveis numa única análise são considerados.

A ICP-MS concilia a alta eficiência e estabilidade do plasma de argônio na produção de íons monopositivos com a simplicidade de interpretação do espectro de massas (Houk *et al*. 1980). Líquidos, gases e sólidos podem ser analisados diretamente empregando diferentes técnicas de introdução de amostra, das quais a nebulização é a mais simples (Taylor 2001). Uma descrição detalhada sobre os principais componentes e o funcionamento de um ICP-MS está além do escopo deste texto, mas pode ser encontrada nos mais recentes livros dedicados ao tema (Taylor 2001, Nelms 2005, Becker 2007) e no artigo de revisão de Linge e Jarvis (2009).

Um esquema simples de um ICP-MS é mostrado na Figura 1. Nas determinações realizadas nesta pesquisa, a amostra foi introduzida empregando-se um nebulizador concêntrico para produção de um aerossol, das gotículas desse, as maiores foram eliminadas sob ação da câmara de nebulização. A temperatura da câmara de nebulização foi mantida, por efeito *peltier*, em torno de 4 ℃ para eliminar uma parte do vapor de água que compõe o aerossol. Esta dessolvatação parcial faz com que uma menor quantidade de água chegue ao plasma, e deste modo mais energia se torna disponível para ser empregada na dissociação de espécies poliatômicas e ionização dos analitos. Hutton e Eaton (1987) demonstraram que quando a temperatura da câmara de nebulização é diminuída de 20 para 5 ℃ há uma redução de 3 a 5 vezes na taxa interferentes poliatômicos na forma óxidos e um ganho similar em sensibilidade.
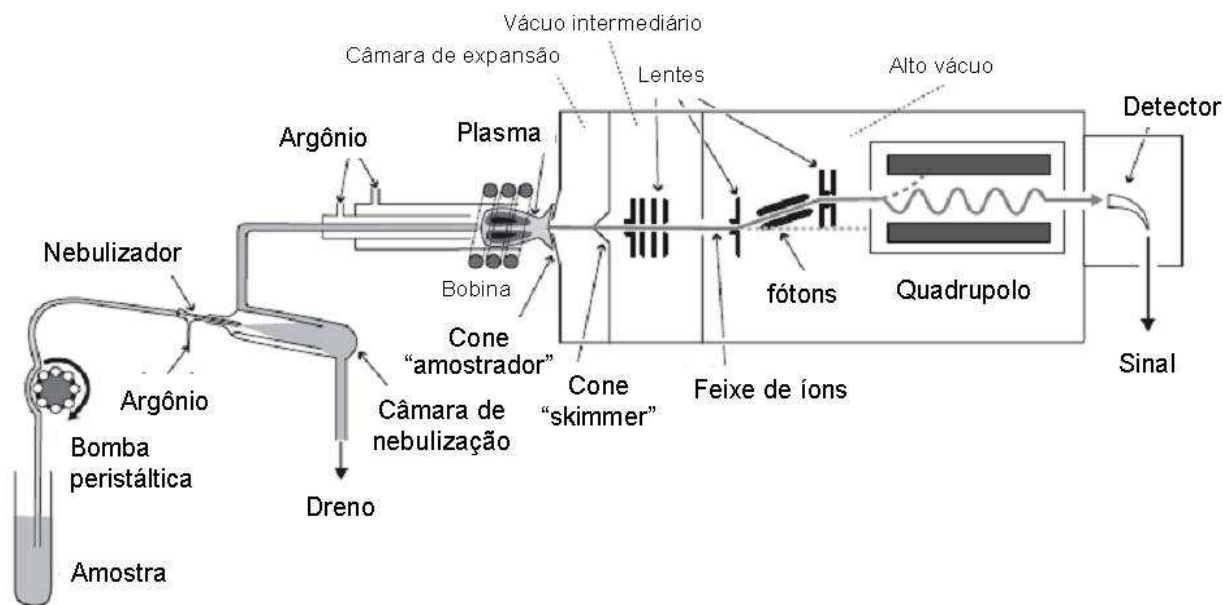
Figura 1. Esquema geral de um ICP-QMS simples com indicação dos componentes principais.

Depois da introdução da amostra no plasma mantido a pressão atmosférica, uma parcela dos íons produzidos é admitida no espectrômetro de massas através de uma interface composta por dois cones com orifícios milimétrico e sub-milimétrico, respectivamente, entre os quais há vácuo ($\leq$ 0,1 kPa). Em seguida o feixe de íons entra numa região de alto vácuo (0,001 Pa) e é direcionado através de lentes eletromagnéticas até o analisador. Os espectrômetros mais simples empregam analisador quadrupolar (ICP-QMS, modalidade utilizada neste trabalho) composto por dois pares de cilindros, paralelos e equidistantes, aos quais são aplicadas diferenças de potencial (ddp) alternadas (RF) e contínuas (DC) com amplitudes V e U, respectivamente. As ddp são aplicadas de modo que num dos pares o potencial elétrico combinado seja positivo e no outro negativo com igual amplitude. Os íons positivos de massa (m) ao entrarem no quadrupolo são atraídos com força proporcional a sua carga (z) e à intensidade do campo elétrico, adquirindo movimento acelerado para o cilindro de potencial negativo, ao mudar a RF para o semiciclo positivo o íon se afasta e assim avança seguindo trajetória em espiral. Deste modo, ao selecionar uma combinação de potenciais RF e DC apropriada apenas íons ressonantes (isto é, de razão m/z específica) com o campo elétrico oscilante serão capazes de percorrer todo quadrupolo e alcançar o detector. A faixa de potenciais capaz de transmitir íons é dita região de estabilidade, estas regiões são mostradas na Figura 2 para íons monopositivos de 1 a 5 a.m.u..
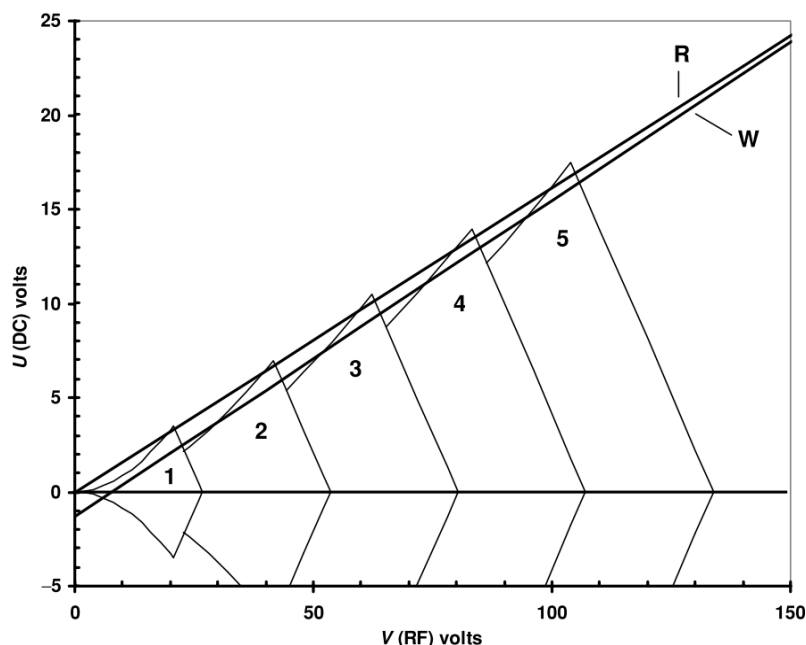
Figura 2. Diagrama de regiões de estabilidade para íons de *m/z* entre 1 e 5. A transmissão de íons de razão *m/z* específica é obtida pela combinação de potenciais que correspondem às cristas das regiões de estabilidade. A linha R indica varredura com resolução ($r = m/\Delta m$) constante, obtida variando-se U e V de modo que a razão U/V permaneça fixa. Desta forma, a largura dos picos é proporcional a massa do íon. A linha W indica a varredura que produz picos de largura constante através da aplicação de uma compensação (c) em (U/(V-c)), deste modo se obtém resoluções próximas à unidade para todo o espectro de massas. Reproduzido de Nelms (2005).

Os ICP-QMS apresentam elevada velocidade de varredura e são de simples operação, por isto são preferencialmente usados para medir concentrações. Instrumentos de alta resolução (HR-ICP-MS) têm ampla aplicação na determinação de concentrações e razões isotópicas, uma vez que quando operados em modo de baixa resolução oferecem sensibilidade e precisão superiores aos quadrupolares. Além disso, os HR-ICP-MS também são capazes de separar o sinal dos isótopos de interesse daquele causado por interferentes (isobáricos ou poliatômicos), em muitos casos. Contudo, seu custo comparado a um ICP-QMS, é mais elevado (Becker 2007).

Nas Figuras 3, 4, 5, 6 diversos ICP-QMS são apresentados esquematicamente. Primeiramente, os instrumentos da Thermo, Fig. 3, e da Agilent, Fig. 4, são mostrados dada similaridade entre eles, seguidos dos instrumentos de geometria ortogonal da Perkin Elmer, Fig. 5, e antiga Varian (atualmente Brucker, Fig 6). As imagens foram retiradas dos respectivos sítios eletrônicos.
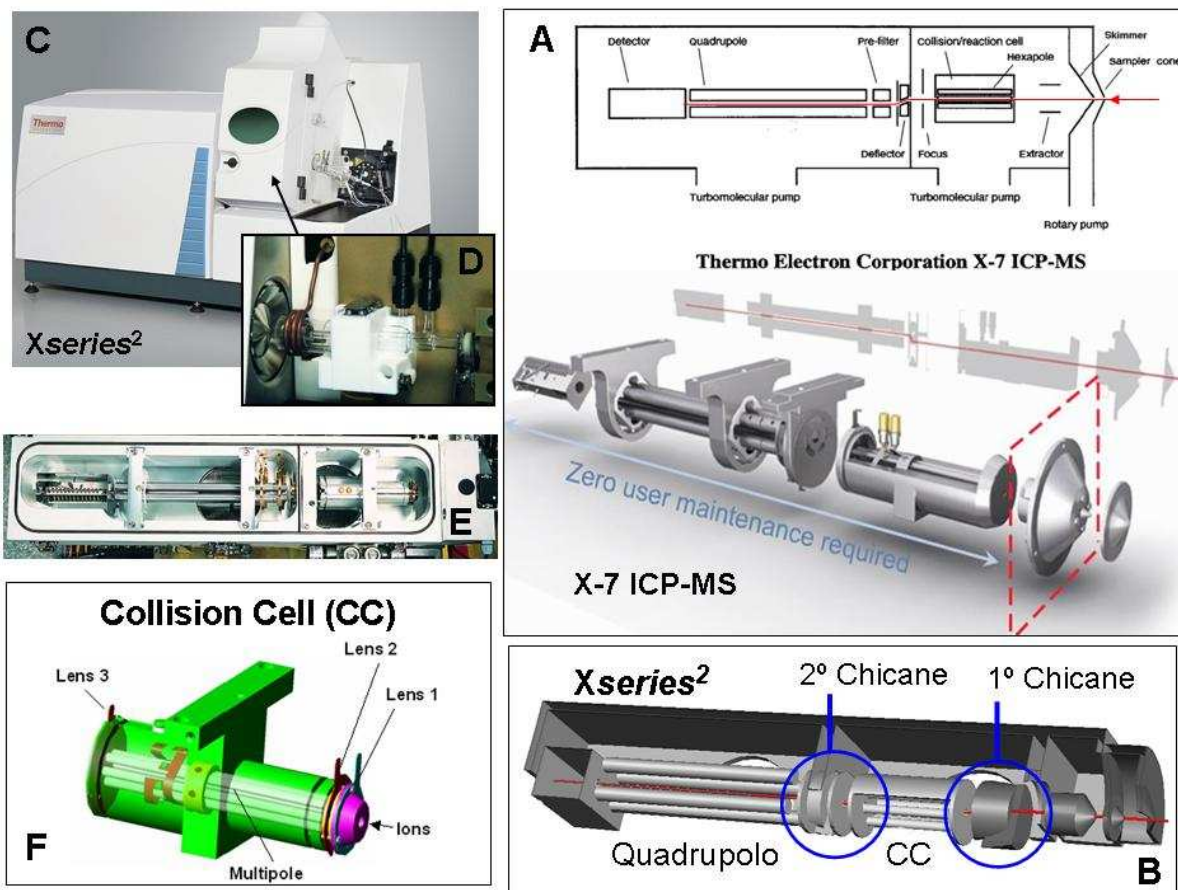
Figura 3. Esquema dos instrumentos X-7, lançado em 2001 e X*series*[II], 2005, ambos com cela de colisão (CC) hexapolar, Thermo Scientific. (A) esquema do X-7 indica o caminho do feixe de íons pelo espectrômetro com um arranjo de lentes (em chicana) após a CC; (B) esquema do X*series*[II] com duas chicanas, a primeira impede a entrada de espécies indesejadas (elétrons, fótons e espécies neutras) na CC, evitando reações indesejadas, e a segunda previne a entrada de espécies neutras no quadrupolo, o que reduz o background; (C, D, E) fotos do X*series*[II], montagem da tocha e compartimentos do espectrômetro e (F) esquema da cela de colisão.
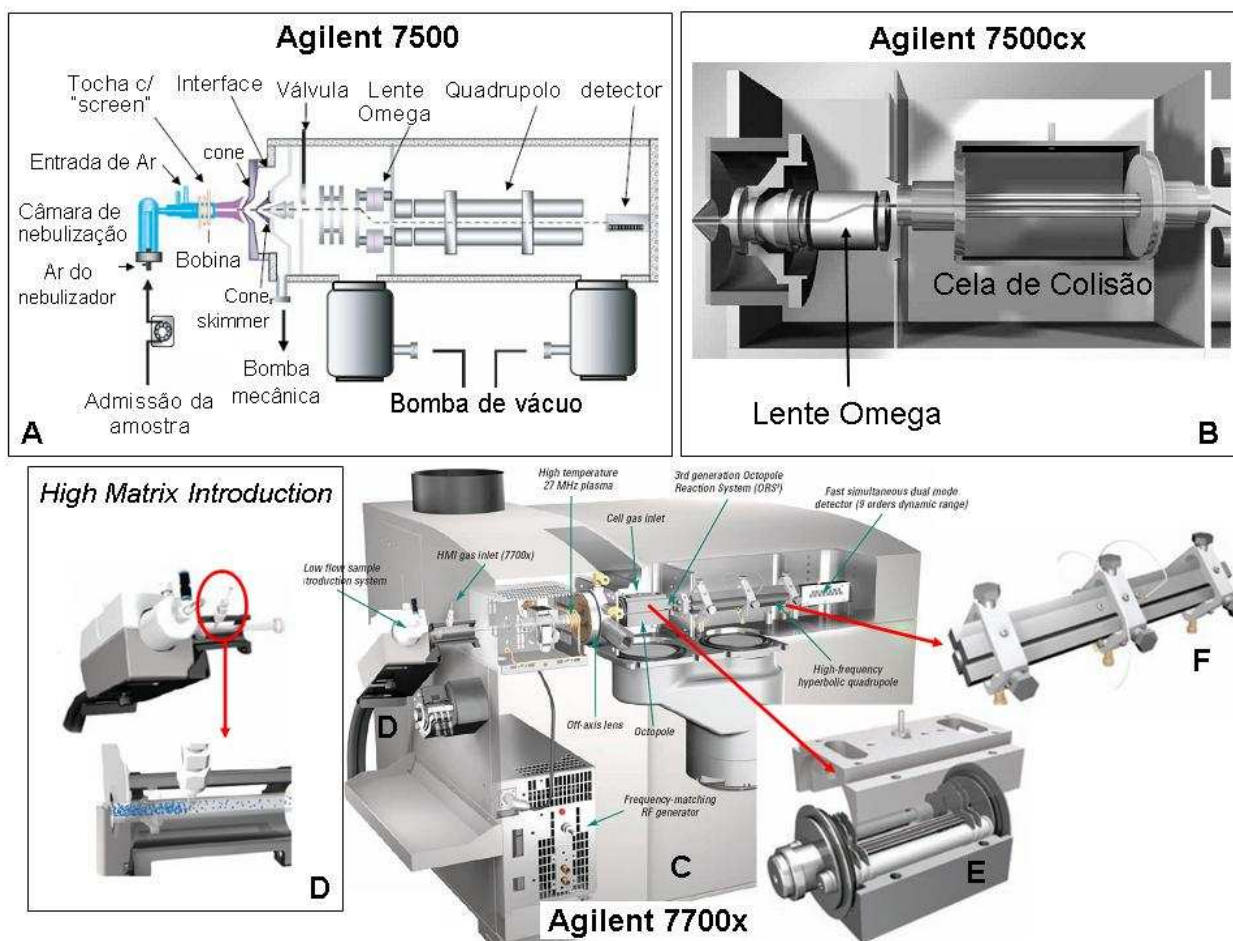
Figura 4. Esquema dos instrumentos Agilent 7500 (A), lançado em 2000; Agilent 7500cx (B), 2007; e Agilent 7700x (C), 2009, os dois últimos equipados com cela de colisão (CC) octopolar. Lente Omega (A, B e C) induz uma mudança na direção do feixe de íons e impede a passagem de espécies indesejadas para CC; (D) Câmara de nebulização resfriada, acima, e sistema para introdução de amostras com alto teor de sais (*High Matrix Introduction - HMI*), no qual um fluxo extra de Ar é admitido entre a câmara de nebulização e a tocha para diluição do aerossol da amostra, o que minimiza a deposição de material nos cones e os efeitos matriz; (E) cela de colisão pressurizada com He, cuja operação (idêntica à dos instrumentos da Thermo) envolve apenas o potencial RF para alcançar amplo espectro de transmissão; (F) quadrupolo de hastes hiperbólicas provê melhor resolução e transmissão do que arranjos cilíndricos.
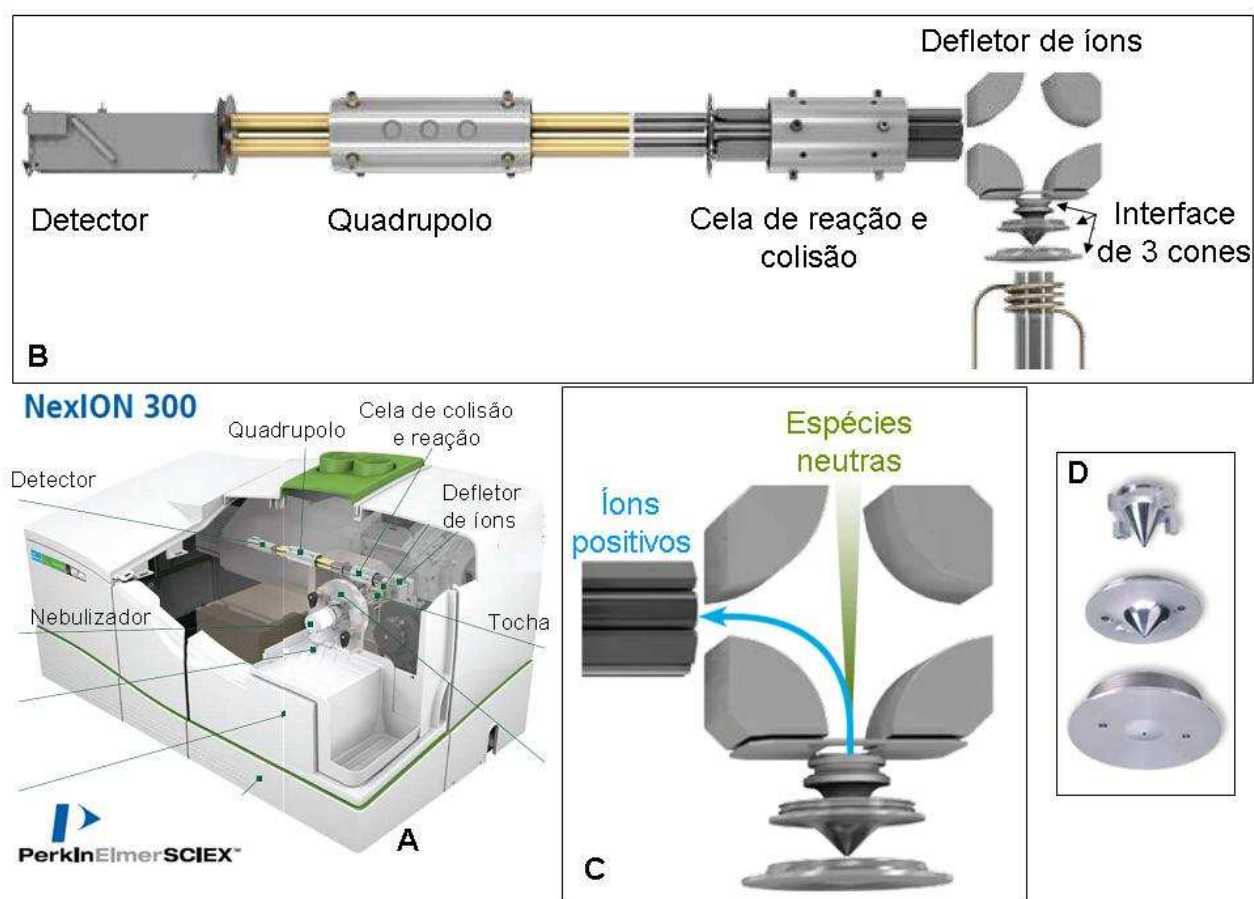
Figura 5. Ilustração do NexION da Perkin Elmer Sciex (A), lançado em 2010; (B) esquema interno do espectrômetro com geometria ortogonal; (C) defletor de íons, impede a entrada de espécies indesejadas na cela de reação/colisão (CRC) quadrupolar, a qual pode ser pressurizada com gases reativos (p. ex. NH_3 ou O_2) ou inerte (He), sendo o único instrumento projetado para operação em três modos a depender do uso da CRC: padrão, *i.e.* sem adição de gás, em modo de reação (RC) com NH_3 ou O_2 e de colisão (CC) com gás inerte. Diferentemente das celas mostradas anteriormente, esta permite o controle das condições de transmissão através do ajuste dos potenciais RF e DC, o que possibilita a exclusão seletiva de espécies poliatômicas formadas na cela e de precursores de interferentes. O gás a ser adicionado e as condições de operação são escolhidos de acordo com a interferência a ser removida que deve ser conhecida de antemão. Em oposição, a operação no modo CC emprega um gás inerte e a eliminação das interferências se dá através da discriminação feita com base nas diferenças de energia cinética entre interferentes poliatômicos e íons dos analitos; (D) foto dos três cones usados para extração dos íons.
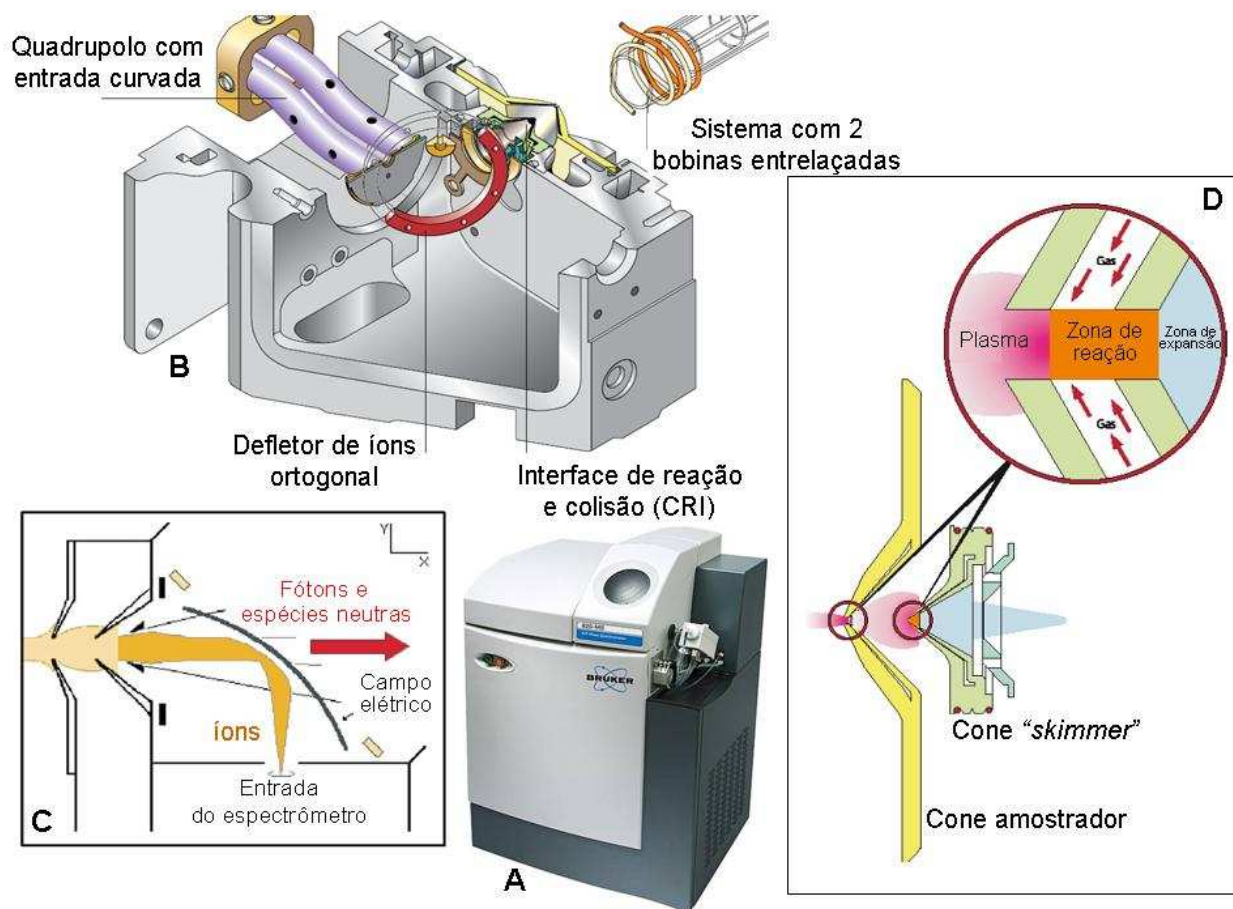
Figura 6. Foto do instrumento Brucker 820-MS (A), originalmente Varian 820-MS lançado em 2005; (B) esquema interno do espectrômetro com geometria ortogonal, defletor de íons impede o acesso de espécies indesejadas no quadrupolo de entrada curvada e sistema de bobinas entrelaçadas para geração e manutenção do plasma; (C) esquema da trajetória dos íons após extração; (D) esquema da interface composta por dois cones ocos que permitem a admissão de He e/ou H_2 ao material extraído do plasma, (*Collision Reaction Interface - CRI*) para remoção de interferências poliatômicas.

Embora a ICP-MS seja uma técnica extremamente sensível e versátil, esta também apresenta dificuldades. Por exemplo, a introdução de amostras líquidas ou dissolvidas implica na chegada de solvente (principalmente água) no plasma, o que propicia a formação de interferentes poliatômicos na forma de óxidos e hidróxidos (Vaughan e Horlick 1986). Adicionalmente, reações entre o argônio do plasma e os constituintes majoritários nas amostras ou dos ácidos utilizados contribuem para a formação de interferentes do tipo ArX^+, sendo X= Ar, O, H, N, S,

Cl, Na, Mg, Ti, entre outros. Embora muitas combinações ArX^+ sejam possíveis, a maioria delas esta restrita a faixa entre 40 e 80 a.m.u. (May e Wiedmeyer 1998).

Para a maior parte dos elementos, apenas íons monopositivos são produzidos quando a amostra alcança o plasma. Quantidades significativas de íons duplamente carregados originam-se de elementos cuja segunda energia de ionização é próxima da energia de ionização do Ar, o que faz de Ba e Sr os principais precursores de íons de duplamente carregados.

A ocorrência de íons poliatômicos ou de dupla carga, cuja massa nominal se sobrepõe à do(s) isótopo(s) medidos, constitui uma das maiores dificuldades encontradas na ICP-MS. Isso é especialmente verdade quando instrumentos quadrupolares são utilizados, uma vez que estes não possuem resolução suficiente para separar o sinal dos analitos do sinal gerado pelos interferentes. Contudo, a incorporação da cela de colisão (CC) tem possibilitado a atenuação de diversos interferentes poliatômicos, eliminando assim a necessidade por correções matemáticas ou a aplicação de técnicas de separação (Feldmann *et al*. 1999, McCurdy e Woods 2004). Embora exista uma vasta literatura sobre o uso de CC, o trabalho desenvolvido neste projeto para análise de águas (Cotta e Enzweiler 2009) foi o primeiro com o instrumento *Xseries^{II}*.

Uma cela de colisão consiste de um multipolo encapsulado, cuja operação envolve apenas o potencial RF para alcançar amplo espectro de transmissão, que é posicionado antes do quadrupolo e pode ser pressurizado para promover colisões entre os íons extraídos do plasma e o gás adicionado, geralmente, uma mistura de He/H_2 (Tanner *et al*. 2002). Como espécies poliatômicas têm seção transversal de colisão maior do que os íons monoatômicos, elas colidem mais frequentemente com os gases introduzidos na cela e por isso perdem mais energia cinética do que os analitos (Du e Houk 2000). A atenuação dos interferentes ocorre através da aplicação de um potencial positivo na CC em relação ao potencial do quadrupolo. Deste modo, é estabelecida uma barreira aos interferentes de baixa energia cinética que são impedidos de chegar ao detector. Este mecanismo, chamado de discriminação por energia cinética (KED), está ilustrado na Figura 7.

Durante uma sessão de medição num ICP-MS pode ocorrer variação de sensibilidade. Este efeito, dito *drift*, é mais severo quando amostras com elevado teor de sais dissolvidos são analisadas, dada a formação de um depósito que obstrui os orifícios dos cones e, por conseguinte dificulta o processo de extração dos íons. Como ao longo das análises mais material é depositado,

o efeito tende a ser progressivo e resulta numa perda sistemática da sensibilidade instrumental (Thompson e Houk 1987).
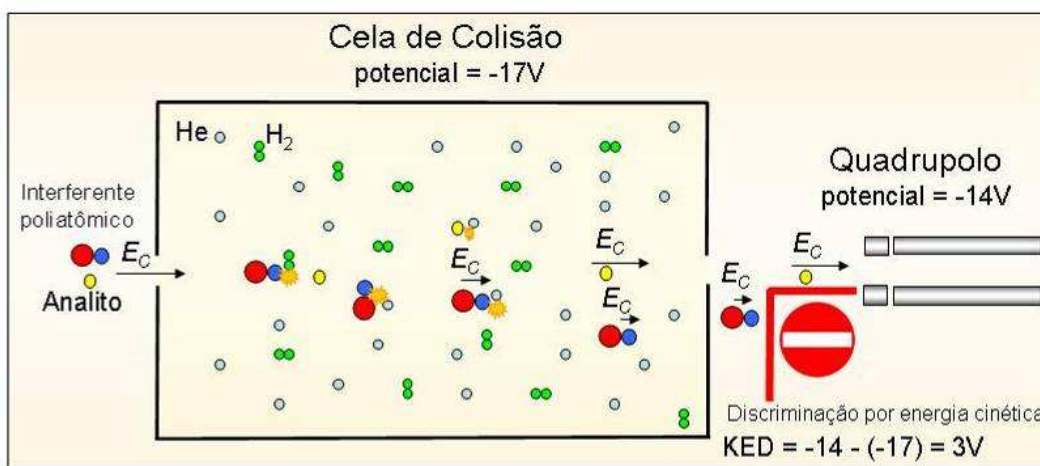
Figura 7. Ilustração do mecanismo de operação de uma cela de colisão com utilizado neste trabalho. Os interferentes poliatômicos são atenuados pela colisão com os gases na cela e a consequente diminuição de sua energia cinética (Ec) em relação à barreira aplicada (KED).

O controle e correção do *drift*, juntamente com o efeito matriz (o qual resulta da influência dos componentes majoritários da amostra sobre a eficiência dos processos de nebulização, ionização, extração e transmissão dos íons no espectrômetro) são especialmente importantes quando a quantificação dos analitos se dá por calibração externa, isto é, através de uma função que relaciona a resposta instrumental com a concentração de soluções-padrão. Nesse caso, qualquer alteração que resulte num ganho ou perda de sensibilidade entre amostras e padrões afetará a medição. A diluição apropriada das amostras, conjuntamente ao uso de um ou mais padrões internos, é a maneira mais recorrente para corrigir tais efeitos (Vanhaecke *et al*. 1992).

2.2. Materiais de referência: Usos, produção e revisão dos valores de referência

Idealmente a obtenção de resultados analíticos confiáveis para matrizes complexas por técnicas instrumentais pressupõe a correção dos efeitos matriz durante a calibração do instrumento. Em outras palavras, as curvas analíticas devem ser preparadas com padrões cuja composição global seja similar à das amostras. Essa similaridade pode ser obtida com o uso de materiais de referência certificados (MRC) para a matriz de interesse que disponham de valores certificados para os analitos objeto de determinação.

Um MR "*é um material suficientemente homogêneo e estável com respeito a uma ou mais propriedades especificadas, as quais foram estabelecidas para serem adequadas ao uso pretendido em um processo de medição*" (ISO Guide 35, 2006). Um MRC *é um MR com uma ou mais propriedades especificadas caracterizadas por um procedimento metrologicamente válido, acompanhado de um certificado com o valor da propriedade especificada, a incerteza associada e a rastreabilidade metrológica declarada.*

O ISO Guide 33 (2000) recomenda que calibrações sejam feitas com no mínimo 10 MRC (preparados como as amostras), de modo a cobrir uma ampla faixa de concentrações. Mas, em rotina um menor número é geralmente utilizado. Além da calibração, os MRC são também empregados na validação de métodos analíticos, em sistemas de controle e garantia da qualidade, para estabelecer a rastreabilidade metrológica das medições e para a obtenção e manutenção da acreditação de um laboratório.

Limitações surgem devido ao pequeno número de MRC litogeoquímicos já preparados e pela ausência de valores de referência para muitos constituintes nos MR em uso. Isto ocorre porque a maioria dos mais de 380 MR geoquímicos disponíveis foi caracterizada em programas interlaboratoriais, e a sua certificação não ocorreu ou pode estar em desacordo com as recomendações vigentes (ISO Guide 35, 2006; Kane *et al*. 2003). Por isso, o uso de MR para calibração nem sempre é adequado (Dulski 2001). Adicionalmente, dada a caracterização insuficiente de muitos dos MR sua aplicabilidade é limitada, em especial no que se refere aos elementos-traço cuja determinação somente se tornou rotineira após a disseminação de técnicas instrumentais de alta sensibilidade, como a ICP-MS.

Observações como estas motivaram diversos autores a sugerirem que os valores dos MR sejam periodicamente revisados à medida que instrumentos e métodos analíticos são

aperfeiçoados. Por exemplo, Velasco-Tapia *et al*. (2001) compararam os valores recomendados de 5 MR de rochas preparados pelo USGS nas décadas de 80 e 90, (basalto BHVO-1, andesito AGV-1, riolito RGM-1 e diabásio W-1 e W-2) com novos dados disponíveis. Velasco-Tapia *et al*. (2001) observaram que 53% dos valores recomendados estavam em acordo com os valores re-calculados, 32% apresentavam diferenças de 1 a 5%, e que os demais diferiam em até 50%. Kent *et al*. (2004) compilaram valores para os lantanídeos (Ln) obtidos por espectrometria de massas com diluição isotópica (ID-MS) em diversos MR e propuseram a revisão dos valores recomendados de Er e Lu em AGV-1 e AGV-2, uma vez que apresentavam diferenças superiores a 10%. Resultados semelhantes já haviam sido apresentados por Razcek *et al*. (2001). Pretorius *et al*. (2006) propõem que valores de diversos elementos (e.g. Li, Hf, Zr, Ta, Rb, Sr, Ba, Y e Cu) em dois MR (granodiorito GSP-2 e granito G-2) sejam revistos. Weyer *et al*. (2002) utilizaram a ID-MS para investigar os valores de Zr, Hf, Nb e Ta em quatro MR de basaltos (BHVO-2, BCR-2, BE-N e BIR-1) e demonstraram que as incertezas associadas com os valores de referência poderiam ser significativamente reduzidas.

As conclusões destes trabalhos evidenciam a necessidade de certificar os valores dos MR mais usados em geoquímica analítica. Adicionalmente, estes trabalhos mostram que os métodos analíticos baseados na ID-MS são os mais apropriados para a determinação de elementos-traço em MR. Em contraste com técnicas comparativas de análise, como a calibração externa, a ID-MS permite realizar medidas consideradas absolutas, isto é, a concentração de um elemento pode ser determinada sem se recorrer a calibrações externas. Portanto, além de potencialmente permitir obtenção dados da mais alta exatidão com pequenas incertezas (Heumann 2004), a ID-MS também possibilita a obtenção de resultados diretamente rastreáveis às unidades do Sistema Internacional-SI (Lamberty *et al*. 1994). Quando a diluição isotópica é combinada com ICP-MS (*i.e.* ID-ICP-MS) essas vantagens são estendidas a uma ampla faixa de elementos que podem ser determinados numa mesma medida, como demonstrado por Willbold *et al*. (2003) e Willbold e Jochum (2005). Isto faz com que a ID-ICP-MS seja um dos métodos mais adequados para caracterizar MR.

2.3 Contextualização dos métodos desenvolvidos

A ICP-MS é amplamente utilizada na determinação de metais e metalóides presentes em águas doces a fim de avaliar a qualidade dos recursos hídricos para o consumo humano (WHO 2006). Investigações com interesse hidrogeoquímico e ambiental também recorrem a esta técnica para determinar teores totais ou para especiação de elementos-traço em águas e efluentes. Com estes objetivos, uma série de variantes do método sugerido pela EPA (200.8) já foram propostos (Fernández *et al*. 2000, Fiket *et al*. 2007, Mahar *et al*. 2008). Nesses trabalhos o foco está essencialmente nos constituintes cujos níveis máximos são regulamentados. Além destes, outros constituintes presentes em baixas concentrações, como os lantanídeos, têm se mostrado eficientes como traçadores de fontes de contaminação (Möller *et al*. 2000) e de processos de mistura de águas subterrâneas (Johannesson *et al*. 1997, Dia *et al*. 2000). Portanto, a sua determinação em águas é também desejável.

O método desenvolvido neste trabalho para determinar elementos-traço sujeitos a regulamentação em águas encontra-se no Anexo I, e uma variante dele foi desenvolvida para incluir os lantanídeos, Anexo II. A aplicabilidade do método para determinação dos lantanídeos é reforçada em resultados complementares.

Estudos da geoquímica de rochas são multielementares por natureza (Potts 1987, Hall e Plant 1992). Muitos dos constituintes de interesse são encontrados em níveis de traço e sub-traço, isto é, em concentrações inferiores a 1000 e 1 mg kg^{-1}, respectivamente. Nesse caso, a ICP-MS é considerada a técnica analítica ideal por oferecer limites de detecção apropriados sem a necessidade de procedimentos complexos de preparação das amostras, como o que ocorre quando os lantanídeos são determinados por espectrometria ótica de emissão (ICP-OES), a qual requer uma etapa de separação/concentração (Linge 2007). Em geral, as determinações de elementos-traço por ICP-MS complementam as determinações de elementos maiores e menores e de alguns traço realizadas por ICP-OES ou por fluorescência de raios X (XRF). Contudo, dada a natureza heterogênea dos materiais geológicos, uma massa mínima representativa da amostra original deve ser analisada. Além disso, a introdução de soluções por nebulização implica que as amostras sólidas devem ser previamente dissolvidas.

A digestão completa de materiais geológicos é obtida mediante a destruição dos minerais constituintes. Os ataques multiácidos que incluem HF são os mais empregados para a dissolução

de silicatos (Yu *et al.* 2001). A dissolução de amostras de rochas para finalidades analíticas é realizada com sucesso há muito tempo, mas os elementos determinados não incluíam suítes tão amplas como as medidas atualmente por ICP-MS e ICP-OES. Por isso, problemas diversos foram e continuam a ser encontornados quando estes procedimentos são testados (Jarvis *et al.* 1992). As principais dificuldades já encontradas estão relacionadas à complexidade das amostras e às variáveis que controlam o processo de dissolução, em especial no que se refere à estabilização dos analitos em solução e a precipitação de fluoretos insolúveis, as quais ainda não são bem entendidas (Takei *et al.* 2001, Zhaochu *et al.* 2010). Portanto, a verificação da eficácia dos procedimentos clássicos de digestão para determinações multielementares é ainda necessária.

A dissolução ácida de fases minerais refratárias é acelerada mediante aquecimento (Potts 1987). Em sistemas convencionais com frascos de politetrafluoretileno (PTFE) a temperatura máxima é limitada a 200 ºC e as pressões alcançadas raramente superam 1 MPa (Jackwerth e Gomiscek 1984). Como consequência, a dissolução total de certos tipos de amostras só é obtida após vários dias (Pretorius *et al.* 2006, Navarro *et al.* 2008). Uma alternativa para reduzir o tempo de digestão é usar temperaturas e pressões mais elevadas obtidas com equipamentos específicos como o *High Pressure Asher-System* (HPA-S fabricado pela Anton Paar, Austria). Neste equipamento a digestão com HF é realizada em tubos de carbono vítreo, em temperaturas de até 260 ºC a pressão de 13 MPa.

Alternativas às digestões ácidas são a fusão e a sinterização das amostras com fundentes apropriados. A sinterização com Na_2O_2 foi descrita em alguns trabalhos e permite medir os ETR, e outros traço, a depender do procedimento adotado após a dissolução do sinterizado (Yu *et al.* 2001, Meisel *et al.* 2002). Diversos procedimentos de dissolução completa de rochas para a determinação de elemento-traço por ICP-MS são revisados no Anexo III.

Como exposto anteriormente muitos MR de rochas em uso apresentam uma caracterização insuficiente frente às possibilidades analíticas atuais. Por exemplo, alguns elementos como Cr, Ni, Cu, Zn, Sr e Sn, ainda não possuem valores de referência, ou apenas valores informativos foram propostos. Com o intuito de contribuir com a caracterização de alguns RM (em uso e em preparação) a técnica de ID-ICP-MS foi aplicada para a determinação destes elementos. Tais resultados são apresentados no Anexo IV, um manuscrito em preparação.

Um elemento que recebeu especial atenção nessa investigação foi o Cr no MRC BRP-1. Dúvidas sobre a adequação do valor de referência deste elemento surgiram a partir de dados

obtidos numa rodada do teste de proficiência GeoPT25 (2009), no qual BRP-1 foi utilizado como amostra teste. Diferentemente dos demais elementos certificados, a média dos valores reportados para o Cr, $10,7\pm0,5$ mg kg^{-1} ($\pm$desvio-padrão do valor provisório calculado), não coincide com o valor certificado, $12,4\pm0,8$ mg kg^{-1} ($\pm$ sua incerteza expandida ao nível de 95%). Análises realizadas neste trabalho (Anexo III) produziram um valor médio de $11,4\pm0,7$ mg kg^{-1} (±1 desvio padrão), que é, intermediário ao valor de referência e o indicado pelo teste de proficiência GeoPT25 (2009). Portanto, espera-se que com a aplicação da ID-ICP-MS, a qual é capaz de gerar resultados com pequenas incertezas associadas, se consiga avaliar se o valor certificado precisa ou não de revisão.

3. OBJETIVOS

Os objetivos desta pesquisa são:

1) Estudar, desenvolver e aprimorar métodos analíticos para determinação de elementos-traço em amostras de águas e rochas usando a ICP-QMS como técnica de medição.

2) Avaliar as condições de operação do ICP-QMS, sua otimização, calibração e, quando necessário, a aplicação de correções matemáticas para a determinação dos analitos de interesse.

3) Investigar a aplicabilidade e as limitações da CC para atenuar interferentes poliatômicos, bem como avaliar a veracidade e as incertezas dos resultados obtidos para os MR de águas e rochas analisados.

4) Aplicar e aperfeiçoar procedimentos de decomposição total de rochas silicáticas. Além de testar os procedimentos clássicos de dissolução (com HF/HNO$_3$ em frascos de PFA e bombas de PTFE), pretende-se investigar alternativas, como o uso do HPA-S, para o estabelecimento de procedimentos mais rápidos de dissolução. Avaliar alternativas para expandir a suíte de elementos determináveis após a sinterização da amostra.

5) Aplicar a ID-ICP-MS para obtenção de resultados que contribuam para a caracterização de elementos-traço em alguns MR de rocha em uso e em preparação.

4. CONCLUSÕES

Métodos analíticos para a determinação de amplas suítes de elementos-traço de interesse em hidrogeoquímica e litogeoquímica foram investigados e aprimorados no âmbito deste projeto. Estes métodos se mostram capazes de gerar resultados com incertezas apropriadas para analises em questão.

A utilização da CC possibilitou uma simplificação dos métodos desenvolvidos, uma vez que um número menor de correções matemáticas para subtração de interferentes poliatômicos precisam ser aplicadas e permitiu melhorar os limites de detecção para elementos tradicionalmente considerados de difícil determinação, possibilitando sua medição em níveis sub $\mu g\ l^{-1}$. Neste caso, a análise dos isótopos sujeitos a interferências é realizada empregando-se uma única condição instrumental, cujos parâmetros (vazão da mistura H_2/He e KED) não precisam ser otimizados individualmente, o que simplifica e agiliza a otimização diária do instrumento.

A determinação direta dos lantanídeos (Ln), em modo padrão, é aplicável para a análise de águas doces cobrindo uma ampla faixa de ΣLn, uma vez que a operação em modo de cela não elimina a necessidade por correções matemáticas.

O novo procedimento de digestão ácida proposto (HPA-S 4b) permite dissoluções totais e mais rápidas do que as realizadas por técnicas convencionais. A capacidade de aplicar técnicas independentes de decomposição de amostras como a digestão ácida (em sistemas convencionais de PFA e PTFE) e a sinterização possibilitou testar de maneira mais precisa a eficiência deste novo procedimento, uma vez que nem todos os 41 elementos-traço medidos possuem valores de referência disponíveis. A inclusão de uma etapa de aquecimento da dispersão do sinterizado possibilitou expandir o número de analitos determinados com a sinterização, dada a maior eficiência do processo de co-precipitação.

A aplicação da técnica de ID-ICP-MS possibilitou a obtenção de resultados com pequenas incertezas, os quais contribuem para a caracterização de MR em uso e em preparação. Estes resultados são especialmente valiosos para aqueles elementos ainda sem valores de referência estabelecidos e espera-se que eles contribuam para que os MR analisados alcancem o status de materiais certificados e/ou na revisão dos valores conhecidos.

5. REFERÊNCIAS

Becker JS (2007) Inorganic Mass spectrometry: Principles and Applications. Wiley (Chichester, England). 496p.

Cotta AJB e Enzweler J (2009) Quantification of major and trace elements in water samples by ICP-MS and collision cell to attenuate Ar and Cl-based polyatomic íons. Journal of Analytical and Atomic Spectrometry, 24, 1406-1413.

Dia A, Gruau G, Olivié-Lauquet G, Riou C, Moléenat J e Curmi P (2000) The distribution of rare earth elements in groundwaters: Assessing the role of source-rock composition, redox changes and colloidal particles. Geochimica et Cosmochimica Acta, 64: 4131-4151.

Dufailly V, Noël L e Guérin T (2008) Optimisation and critical evaluation of a collision cell technology ICP-MS system for the determination of arsenic in foodstuffs of animal origin. Analytica Chimica Acta, 611: 134-142.

Dulski P (2001) Reference materials for geochemical studies: New analytical data by ICP-MS and critical discussion of reference values. Geostandards Newsletter: The Journal of Geostandards and Geoanalysis, 25: 87-125.

Du ZY e Houk RS (2000) Attenuation of metal oxide ions in inductively coupled plasma mass spectrometry with hydrogen in a hexapole collision cell. Journal of Analytical Atomic Spectrometry, 15: 383-388.

EPA Method 200.8 Determination of trace elements in waters and wastes by inductively coupled plasma mass spectrometry, Revision 5.4, 57p.
(http://www.epa.gov/waterscience/methods/method/files/200_8.pdf)

Feldmann I, Jakubowski N e Stuewer D (1999) Application of a hexapole collision and reaction cell in ICP-MS Part I: Instrumental aspects and operational optimization. Fresenius' Journal of Analytical Chemistry, 365: 415-421.

Fernández JL, Lorens JL, López-Vera F, Gómez-Artola C, Morell I e Gimeno D (2000) Strategy for water analysis using ICP-MS. Fresenius' Journal of Analytical Chemistry, 368: 601-606.

Fiket Z, Roje V, Mikac N e Kniewald G (2007) Determination of arsenic and other trace elements in bottled waters by high resolution inductively coupled plasma mass spectrometry. Croatian Chemical Society, 80: 91-100.

GeoPT25 (2009) An international proficiency test for analytical geochemistry laboratories - report on round 25 (Basalt, HTB-1), 30p. (http://www.geoanalyst.org/geopt/GeoPT25Report.pdf)

Guia 32 (1994) Linear calibration using reference materials. International Organization for Standardization, Geneva, Switzerland.

ISO Guide 35 (2006) Reference materials - General and statistical principles for certification. International Organization for Standardization, Geneva, Switzerland, 64 p.

Hall GEW e Plant JA (1992) Analytical errors in the determination of high field strength elements and their implications in tectonic studies. Chemical Geology, 95: 141-156.

Heumann KG (2004) Isotope-dilution ICP–MS for trace element determination and speciation: from a reference method to a routine method?. Analytical and Bioanalytical Chemistry, 378:318-329.

Houk RS, Fassel VA, Flesch GD e Svec HJ (1980) Inductively coupled argon plasma as an ion source for mass spectrometry. Applied Spectroscopy, 40: 434-445.

Hutton RC e Eaton AN (1987) Role of aerosol water vapour loading in inductively coupled plasma mass spectrometry. Journal of Analytical Atomic Spectrometry, 2:595-598.

Jarvis KE, Gray AL e Houk RS (1992) Handbook of inductively coupled plasma-mass spectrometry, Blackie (London). 380p.

Jackwerth E e Gomiscek S (1984) Acid pressure decomposition in trace element analysis. Pure and Applied Chemistry, 56: 479-489.

Johannesson KH, Farnham IM, GUO C e Stetzenbach KJ (1999) Rare earth element fractionation and concentration variations along a groundwater flow path within a shallow, basin-fill aquifer, southern Nevada, USA. Geochimica et Cosmochimica Acta, 63: 2697-2708.

Johannesson KH, Stetzenbach KJ, e Hodge VF (1997) Rare earth elements as geochemical tracers of regional groundwater mixing. Geochimica et Cosmochimica Acta, 61: 3605-3618.

Kamber BS, Greig A e Collerson KD (2005) A new estimate for the composition of weathered young upper continental crust from alluvial sediments, Queensland, Australia. Geochimica et Cosmochimica Acta, 69: 1041-1058.

Kane JS, Potts PJ, Wiedenbeck M, Carignan J e Wilson S (2003) International Association of Geoanalysts' protocol for the certification of geological and environmental reference materials. Geostandards Newsletter: The Journal of Geostandards and Geoanalysis, 27: 227-244.

Kent AJR, Jacobsen B, Peate DW, Waight TE e Baker JA (2004) Isotope dilution MC-ICP-MS rare element analysis of geochemical reference materials NIST SRM610, NIST SRM612, NIST SRM614, BHVO-2G, BHVO-2, BCR-2G, JB-2, WS-E, W-2, AGV-1 and AGV-2. Geostandards Newsletter: The Journal of Geostandards and Geoanalysis, 28: 417-429.

Lamberty A, De Bièvre P e Moody JR (1994) The IRMM - International Measurement Evaluation Programme (IMEP): realization of traceability to the SI system by field laboratories. Atomic Spectroscopy, 15: 107-108.

Lawrence MG e Kamber BS (2007) Rare Earth Element Concentrations in the Natural Water Reference Materials (NRCC) NASS-5, CASS-4 and SLEW-3. Geostandard and Geoanalytical Reserch, 31: 95-103.

Lawrence MG, Greig A, Collerson KD e Kamber BS (2006) Rare Earth Element and Yttrium Variability in South East Queensland Waterways. Aquatic Geochemistry, 12: 39-72.

Linge KL (2007) Recent Developments in Trace Element Analysis by ICP-AES and ICP-MS with Particular Reference to Geological and Environmental Samples. Geostandard and Geoanalytical Reserch, 29: 7-22.

Mahar M, Tyson JF, Neubauerb K e Grosserb Z (2008) High throughput sample introduction system for the analysis of drinking waters and wastewaters by ICP-MS. Journal of Analytical and Atomic Spectrometry, 23: 1204-1213.

May TW e Wiedmeyer RH (1998) A Table of Polyatomic Interferences in ICP-MS. Atomic Spectroscopy 19: 150-155.

McCurdy E e Woods G (2004) The application of collision/reaction cell inductively coupled plasma mass spectrometry to multi-element analysis in variable sample matrices, using He as a non-reactive cell gas. Journal of Analytical and Atomic Spectrometry, 19: 607-615.

Möller P, Dulski P, Bau M, Knappe A, Pekdeger G e Jarmersted CS (2000) Anthropogenic gadolinium as a conservative tracer in hydrology. Journal of Geochemical Exploration, 70: 409-414.

Navarro MS, Andrade S, Ulbrich H, Gomes CB e Girardi VAV. (2008) The Direct Determination of Rare Earth Elements in Basaltic and Related Rocks using ICP-MS: Testing the Efficiency of Microwave Oven Sample Decomposition Procedures. Geostandard and Geoanalytical Reserch, 32: 167-180.

Nelms S (2005) Inductively coupled mass spectrometry handbook. Blackwell Publishing (Oxford, UK). 485p.

Potts PJ (1987) A handbook of silicate rock analysis. Blackie, Chapman and Hall (Glasgow, New York). 622p.

Pretorius W, Weis D, Williams G, Hanano D, Kieffer B e Scoates J. (2006) Complete trace element characterization of granitoid (USGS G-2, GSP-2) reference materials by high resolution inductively coupled plasma-mass spectrometry. Geostandard and Geoanalytical Reserch, 30: 39-54.

Raczek I, Stoll B, Hofmann AW e Jochum KP. (2001) High-precision trace element data for the USGS reference materials BCR-1, BCR-2, BHVO-1, BHVO-2, AGV-1, AGV-2, DTS-1, DTS-2, GSP-1 and GSP-2 by ID-TIMS and MIC-SSMS. Geostandards Newsletter: The Journal of Geostandards and Geoanalysis 25: 77-86.

Raut NM, Huang L, Aggarwal SK e Lin K (2003) Determination of lanthanides in rock samples by inductively coupled plasma mass spectrometry using thorium as oxide and hydroxide correction standard. Spectrochimica Acta, Part B, 58: 809-822.

Raut NM, Huang L, Lin K e Aggarwal SK (2005) Uncertainty propagation through correction methodology for the determination of rare earth elements by quadrupole based inductively coupled plasma mass spectrometry. Analytica Chimica Acta, 530: 91-103.

Takei H, Yokoyama T, Makishima A e Nakamura E. (2001) Formation and suppression of A1F$_3$ during HF digestion of rock samples in Teflon bomb for precise trace element analyses by ICP-MS and ID-TIMS. Proceeding Japan Academy, 77: 13-17.

Tanner SD, Baranov VI, Bandura DR (2002) Reaction cells and collision cells for ICP-MS: A tutorial review. Spectrochimica Acta, Part B, 57: 1361-1452.

Taylor HE. (2001) Inductively coupled plasma-mass spectrometry: practices and techniques, Academic Press, (London). 179p.

Thompson JJ e Houk RS (1987) A Study of Internal Standardization in Inductively Coupled Plasma-Mass Spectrometry. Applied Spectroscopy, 41:801-806.

US Environmental Protection Agency, national primary drinking water regulations, Maximum Contaminant Level (MCL). (http://www.epa.gov/ogwdw/contaminants/index.html).

Vanhaecke F, Vanhoe H, Dams R e Vandecasteele C (1992) The use of internal standards in ICP-MS. Talanta, 39: 737-742.

Vaughan MA e Horlick G (1986) Oxide, hydroxide, and doubly charged analyte species in inductively coupled plasma/mass spectrometry. Applied Spectroscopy, 40: 434-445.

Velasco-Tapia F, Guevara M e Verma SP. (2001) Evaluation of concentration data in geochemical reference materials. Chemie der Erde-Geochemistry, 61: 69-91.

Weyer S, Munker C, Rehkamper M e Mezger K (2002) Determination of ultra-low Nb, Ta, Zr and Hf concentrations and the chondritic Zr/Hf and Nb/Ta ratios by isotope dilution analyses with multiple collector ICP-MS. Chemical Geology, 187: 295-313.

WHO (World Health Organization), Guidelines for Drinking Water Quality, Geneva, Switzerland, 3nd edn, 2006, (ch. 8), pp. 145–196. (http://www.who.int/water_sanitation_health/dwq/gdwq3rev).

Willbold M, Jochum KP, Raczek I, Amini MA, Stoll B e Hofmann AW (2003) Validation of multi-element isotope dilution ICPMS for the analysis of basalts. Analytical and Bioanalytical Chemistry, 377: 117-125.

Willbold M e Jochum KP (2005) Multi-element isotope dilution sector field ICP-MS: A precise technique for the analysis of geological materials and its application to geological reference materials. Geostandards and Geoanalytical Research, 29: 63-82.

Yu Z, Robinson P e McGorlick P (2001) An Evaluation of Methods for the Chemical Decomposition of Geological Materials for Trace Element Determination using ICP-MS. Geostandards Newsletter: The Journal of Geostandards and Geoanalysis, 25: 199-217.

Yeghicheyan D, Carignan J, Valladon M, Bouhnik M, Le Cornec F, Castrec-Rouelle M, *et al*. (2001) A compilation of silicon and thirty one trace elements measured in the natural river water reference material SLRS-4 (NRC-CNRC). Geostandards Newsletter: The Journal of Geostandards and Geoanalysis, 25: 465-474.

Zhaochu H, Gao S, Liu Y, Hu S, Zhao L, Li Y e Wang Q (2010) NH_4F assisted high pressure digestion of geological samples for multi-element analysis by ICP-MS. Journal of Analytical and Atomic Spectrometry, 25, 408-413.

LISTA DE ANEXOS

ANEXO I

Artigo publicado: Cotta AJB e Enzweler J. (2009)

Quantification of major and trace elements in water samples by ICP-MS and collision cell to attenuate Ar and Cl-based polyatomic íons. *Journal of Analytical and Atomic Spectrometry*, 24, 1406-1413.

ANEXO II

Resumo expandido: Cotta AJB e Enzweler J.

Determinação direta de lantanídeos e outros 28 elementos em águas por ICP-MS. Apresentado no XII Congresso Brasileiro Geoquímica, Ouro Preto - MG, 18-22/Out. de 2009.

Seguido de resultados complementares.

ANEXO III

Artigo submetido: Cotta AJB e Enzweler J.

Classical and new procedures of whole rock dissolution for trace elements analysis by ICP-MS.

Aceito para publicação no periodico *Geostandard and Geoanalytical Research*.

ANEXO IV

Artigo submetido: Cotta AJB e Enzweler J.

Determination of Cr, Ni, Cu, Zn, Sr and Sn in geochemical reference materials by isotope dilution inductively coupled plasma mass spectrometry.

ANEXO I

Artigo: Cotta AJB e Enzweler J. (2009)

Quantification of major and trace elements in water samples by ICP-MS and collision cell to attenuate Ar and Cl-based polyatomic íons. *Journal of Analytical and Atomic Spectrometry*, 24, 1406-1413. (DOI: 10.1039/B901644A)

(http://pubs.rsc.org/en/Content/ArticleLanding/2009/JA/b901644a)

Quantification of major and trace elements in water samples by ICP-MS and collision cell to attenuate Ar and Cl-based polyatomic ions

Aloísio José Bueno Cotta and Jacinta Enzweiler*

Inductively coupled plasma mass spectrometry (ICP-MS) is the best fitted analytical technique for multi-element analysis of waters, because of its low detection limits. One limitation is the polyatomic interferences produced in the plasma and in the interface (e.g., $^{35}Cl^{16}O^+$ on $^{51}V^+$, $^{40}Ar^{16}O^+$ on $^{56}Fe^+$, $^{40}Ar^{35}Cl^+$ on $^{75}As^+$ and $^{40}Ar^{38}Ar^+$ on $^{78}Se^+$). These polyatomic ions can be significantly reduced by ion molecule interactions in a collision cell (CC). Several experiments done in a ICP-MS equipped with a CC pressurized by premixed H_2 7% in He, under optimized gas flow rates, demonstrate the beneficial effect of KED to suppress Ar and Cl-based interferences. These results are opposed to reports where the role of KED was denied. Under such conditions the background equivalent concentration of ^{51}V, ^{52}Cr, ^{56}Fe, ^{63}Cu, ^{75}As and ^{78}Se were improved by two orders of magnitude, allowing the quantification of these elements at low ng L^{-1} level, without the need for mathematical corrections. Moreover, we present results obtained with a multi-mode method of analysis for twenty eight elements in two water certified reference materials (CRM). In this method isotopes free from polyatomic interferences are measured in standard mode and interfered ones using CC mode. The certified and reference values were used to evaluate the analytical trueness, which was better than 5%, with all z-scores within the recommended limit. Intermediate precision was mostly better than 6% and method detection limits are fit for hydrogeochemical studies and to monitor regulated toxic trace elements in waters.

1. Introduction

The increasing exploration of surface and groundwater water resources demands compliant assessment and monitoring, which comprises several constituents including trace elements.[1–4] Most regulated trace elements can be properly measured by inductively coupled plasma mass spectrometry (ICP-MS), because this multi-element technique is able to provide the appropriate detection limits, at the sub-microgram per litre concentration range.[5–10]

During analysis, when the sample is in the ICP for analyte ionization and during the extraction process, many side reactions between the plasma gas and sample matrix produce polyatomic ions that overlap several isotopes. As a consequence, the quantification of some elements becomes difficult, especially for isotopes within the mass range of 40 to 80 a.m.u.[11–15] Background ions caused by plasma gas ($^{40}Ar^{16}O^+$ and $^{78,80}Ar_2^+$) are produced at high levels and they mainly hamper the determination of elements by increasing their detection limits ($^{56}Fe^+$ and $^{78,80}Se^+$, respectively). In addition, matrix-based ions cause sample dependent interferences (e.g. $^{35}Cl^{15}O^+$ on $^{51}V^+$, $^{35}Cl^{15}O^1H^+$ on $^{52}Cr^+$, $^{40}Ar^{23}Na^+$ on $^{63}Cu^+$, $^{40}Ar^{35}Cl^+$ on $^{75}As^+$, among others) that produce inaccurate results if not avoided or corrected.

The possibilities to deal with such interferences were expanded and improved since ICP-MS instruments equipped with collision cell (CC) or reaction cell (RC) became available.[16–19] A distinction between CC and RC based on the thermal characteristics of

the cell was proposed by Tanner et al.[20] Instead of the non trivial set up and update of mathematical correction equations[9,21–24] or time consuming matrix removal methods,[6,25–27] interactions between sampled ions and gases in a cell provide simple and effective elimination of undesired polyatomic ions.

Eiden et al.[18,19] originally recognized the unique capabilities of H_2 as a reactive gas for collision cell ICP-MS. Since then, several papers report the successful application of H_2 either alone or mixed with He at different proportions to attenuate ArX^+ and other polyatomic ions, in several matrices.[28–42] In such applications He is used as a collision gas to enhance ions transmission through collisional focusing.[20] Such collisions also decrease the mean kinetic energy of ions and likely favor reactions between ArX^+ and H_2 within the cell.[30]

The use of H_2 to solve ArX^+ interferences is well known.[30] Iglesias et al.[31] investigated the effects of different gases (H_2, He, NH_3 and N_2O) to alleviate ArO^+ and Ar_2^+ in a hexapole collision cell. They observed that given the low reactivity of H_2 with most analyte ions, mixtures of H_2/He can be effectively used in multi-element analyses. However the same is not true for highly reactive gases, as NH_3 and N_2O, which produce adducts with analyte ions (e.g. $[As(NH_3)NH_2^+]$) and complete (La, As) or partial (Fe, Se, V) shift to the respective oxide.[31]

Optimum gas flow or ideal H_2/He ratio seems to be strongly dependent on the cell design and operating conditions. For instance, even when identical instruments are used, differences in the operation conditions result in different set up of optimum gas flow rates and H_2/He ratios. This is exemplified in studies on the influence of hexapole bias (V_H) to the attenuate the signal of $^{40}Ar^{16}O^+$ and of $^{80}Ar_2^+$ with H_2 and He either alone and in mixtures.[30,33,35] Boulyga and Becker[35] were able to suppress

Institute of Geosciences, University of Campinas – UNICAMP, Campinas, SP, Brazil, P.O. Box 6152, CEP 13083-970. E-mail: jacinta@ige.unicamp.br; Fax: +55 19 3289 1562

ArX$^+$ ions at three to five orders of magnitude, using V_H bias between 0 to +1.6 V and H$_2$/He = 2/4 (2 and 4 mL/min, respectively). Feldmann et al.[30,33] obtained similar interference attenuation, but using V_H bias between −1,5 to −4 V and H$_2$/He = 5/3.

In general, efficient removal of ArX$^+$ occurs with gas flow rates between 4 to 7 mL/min with low, but variable, H$_2$/He ratios. Niemelä et al.[37] reported that isotope ratios (^{57}Fe/^{56}Fe and ^{77}Se/^{78}Se), were more accurate with premixed 7% H$_2$ in He (7.5 mL/min) as cell gas, than those obtained with H$_2$ alone. This improvement was attributed to the beneficial effect of helium as a collision gas when hydrogen is used as a reactive gas. Niemelä et al.[37] also, reported that addition of more H$_2$ to the premixed gases no further reduces ArX$^+$ (X = Ar, O and Cl) signal. Many investigations focused in the alleviation of interferences of a limited number of elements, mostly Fe, As and Se, and reports regarding the attenuation of other problematic interferences likely to occur during water analyses, as ^{35}Cl^{15}O$^+$ on ^{51}V$^+$ or ^{35}Cl^{15}O^{1}H$^+$ on ^{52}Cr$^+$ are rarer.[44]

Chrastný et al.[42] compared the use of H$_2$/He and NH$_3$/He in a hexapole CC-ICP-MS to attenuate ^{35}Cl^{16}O$^+$ and ^{40}Ar^{35}Cl$^+$ polyatomic interferences on ^{51}V$^+$ and ^{75}As$^+$, respectively. Their results[42] indicate that both gas mixtures effectively eliminate ArCl$^+$, but observed that H$_2$/He is not the ideal gas to attenuate ClO$^+$ in samples with high Cl content, and suggest the use of NH$_3$/He in such cases.

Additionally to the attenuation that can be obtained when the cell is pressurized with a reactive gas, a kinetic energy discrimination (KED) barrier potential can be established between the cell and mass analyzer to provide extra attenuation of polyatomic interferences.[38] Since polyatomic ions have larger collision cross sections (higher polarizability compared to elemental ions and eventually a dipole moment) they experience more collisions inside the cell volume and greater loss of kinetic energy.[43] Therefore a potential barrier after the cell can be used to prevent them to reach the detector.

McCurdy and Woods[44] demonstrated that polyatomic ions produced by Ar, C, S and Cl, can be attenuated over 5 orders of magnitude using KED in an octapole CC filled only with an inert gas (He). Although the well documented[28,36,38,42–44] beneficial role of KED to reduce polyatomic interferences, frequently it is not used.[37,39,41,45,46]

In this paper we present results from experiments that support the beneficial effect of KED to attenuate both reactive (ArX$^+$)[47,48] and non-reactive polyatomic interferences (ClO$^+$)[47] in a H$_2$/He cell. The combined effect of H$_2$ ion-molecule chemistry and KED to solve spectral interferences originated both from the plasma gas and from sample matrix were investigated and used to establish a simple and fast method to the determination of 28 elements, in water samples. The accuracy of the method was assessed by analysis of two water certified reference materials (NIST SRM 1640 and 1643e) during a period of few months.

2. Experimental

A quadrupole ICP-MS Xseries^{II} (Thermo, Germany) equipped with a hexapole collision cell (CC) was used. The instrument software allows the rapid switch between standard mode (no gas, cell vented to mass analyzer chamber) to CC mode, whilst continuously aspirating the sample. The pre-mixed gases H$_2$ (7%) in He (H$_2$O and other impurities <5 ppm) were admitted into CC under flow control through stainless steel lines. The measurements were made with nickel sampler and skimmer cones (1.0 mm and 0.7 mm diameter orifices) and conical nebulizer. A glass impact bead spray chamber cooled to 4 °C by a Peltier cooler and a shielded Fassel torch was used to minimize the plasma potential and thereby obtain a low and narrow initial ion energy distribution. Plasma parameters are listed in Table 1.

The daily optimization procedure involved the xyz alignment of the torch, determination of the optimum nebulizer gas flow rate and the ion lens voltage to maximize ^{115}In$^+$ signal and obtain low oxide (^{140}Ce^{16}O$^+$/^{140}Ce$^+$) and double charged ions (^{137}Ba^{++}/^{137}Ba$^+$). The detector was operated in dual mode and cross-calibration was performed weakly. Sample was introduced via peristaltic pump (orange-yellow tubing) with uptake rate of 0.8 mL min^{-1}. All measurements were made with preconditioned cones, i.e., by aspirating tap water spiked with 300 mg L^{-1} of CaCl$_2$. Occasionally, when optimum extraction voltage exceeded −150 V, sampler and skimmer cones were cleaned by sonication in deionized water for 10–15 minutes. Before measurements, cleaned cones were again conditioned for 5 minutes. This procedure reduces instrumental drift efficiently. Unconditioned cones usually show drift in the first set of analysis, due to material deposition on the cones tips.

In the established multi-mode method of analysis, the isotopes susceptible to polyatomic interferences during water analyses were measured in CC mode using specific gas flow rates, as indicated in Table 1. Here sulfur-based polyatomics were not investigated since its major interferences,[13,45] mainly ^{32}S^{16}O$^+$, ^{34}S^{16}O$^+$ and ^{32}S^{16}O$_2^+$, do not overlap the isotopes used in this

Table 1 Typical settings of the ICP-MS

Incident power	1400 W
Extraction	−210 to −160 V
Plasma gas flow	13 L min^{-1}
Nebulizer flow	0.81 to 0.85 L min^{-1}
Dwell time	10–30 ms
Measurements	3 × 30 scans
Conditions	^{140}Ce^{16}O$^+$/^{140}Ce$^+$ <2% and ^{137}Ba^{++}/^{137}Ba$^+$ <3%
CC mode	
Isotopes and gas flow	6 mL/min for ^{51}V
	4 mL/min for ^{39}K, ^{52}Cr, ^{54,56}Fe, ^{55}Mn, ^{59}Co, ^{60}Ni, ^{63}Cu, ^{66}Zn, ^{75}As, ^{78}Se
Hexapole bias	−17 V
Quadrupole bias	−14 V
Differential Aperture (DA)	−26 V
Signal	^{115}In (1 μg L^{-1}) >20 kcps and ^{78}Ar$_2$ <10 cps
Standard mode	
Isotopes	^{7}Li, ^{9}Be, ^{11}B, ^{23}Na, ^{25}Mg, ^{27}Al, ^{29}Si, ^{43}Ca, ^{85}Rb, ^{88}Sr, ^{95}Mo, ^{107}Ag, ^{111}Cd, ^{121}Sb, ^{137}Ba, ^{205}Tl, ^{206,207,208}Pb
Hexapole bias	−4 V
Quadrupole bias	0.5 V
DA	−36 V
Signal	^{115}In (1 μg L^{-1}) > 40 kcps

This journal is © The Royal Society of Chemistry 2009

J. Anal. At. Spectrom., 2009, 24, 1406–1413 | 1407

32

method. Attenuation of chlorine-based interferences was investigated because $^{35}Cl^{16}O^+$ and $^{35}Cl^{16}O^1H^+$ overlap $^{51}V^+$ and $^{52}Cr^+$, used to quantify the respective analytes.

The sample analysis starts in CC mode with 6 mL/min H_2/He for $^{51}V^+$ measurement, followed by reduction of gas flow to 4 mL/min to measure ^{39}K, ^{52}Cr, $^{54,56}Fe$, ^{55}Mn, ^{59}Co, ^{60}Ni, ^{63}Cu, ^{66}Zn, ^{75}As, ^{78}Se. After this is finished the instrument configuration switches to standard mode to measure the remaining elements. Each change is automatically performed by the instrument software and followed by a short stabilization delay of 10 seconds (user defined). The gas flow rates were set up to overcome polyatomic overlaps considering typical samples matrixes, after the optimization experiments, which are presented below. It is worth noting that the above gas flow rates may be modified according to interference attenuation requirements. Some limitations of the method are also discussed.

Two intermediate calibration solutions were used. The first was made up by the matrix elements Na, Mg, Al, K, Ca, Si, Fe, Mn, Sr and Ba in concentrations ranging from 50 to 1.5 mg L^{-1} (prepared from 1000 mg L^{-1} Merck standard solutions). The other contains the trace elements Li, Be, B, V, Cr, Fe, Co, Ni, Cu, Zn, As, Se, Rb, Mo, Ag, Sb, Tl and Pb at concentrations in the range of 600 to 25 μg L^{-1} (prepared from High-Purity Standards of 10 mg L^{-1}). All standard solutions were prepared gravimetrically in polypropylene bottles and made up with 1% HNO_3 (v/v).

The working calibration solutions were prepared separately, by diluting each intermediate calibration solution 200, 30 and 5 fold. As matrix and trace elements are calibrated separately, there is no matrix matching between samples and calibration standards. Hence, complete removal of polyatomic interference is crucial to achieve accurate results. This calibration strategy, using two sets of calibration solutions, is more flexible than to combine all elements in a single solution. It was adopted to accommodate the wide range of elemental concentrations and different sample matrixes analyzed together with NIST SRM 1640 (Trace Elements in Natural Water) and SRM 1643e (Trace Elements in Water) certified reference materials (CRM). The results for both CRM have been collected during more than 5 months at different measurement runs.

Usually samples were analyzed in groups of 5–10, bracketed by one CRM to monitor possible signal drift. Recalibration was performed when drift becomes significant (> 20%).

To overcome problems with matrix effects[49–51] five internal standards (IS) were used. Sc, Y, In, Re and Bi were combined in one solution at concentrations of 350, 100, 100, 80 and 50 μg L^{-1}, respectively. They were added using a Dispensette® (Brand). In general, 100 μl of this solution was combined with the sample aliquot and diluted to a final mass of 10,0 g with HNO_3 1%. $^{45}Sc^+$ was measured in CC mode and used as IS for the elements measured in this mode. The signals of $^{89}Y^+$, $^{115}In^+$, $^{185}Re^+$ and $^{209}Bi^+$ were interpolated to correct drift of the remaining analytes. For SRM 1643e only Sc, Y and In were used since this material contains measurable trace amounts of Re and Bi.

Prior determination, SRM 1640 and 1643e were 10 fold diluted. With this dilution factor, the concentrations of all elements in these samples are bellow the Maximum Contaminant Level (MCLs) for the contaminants specified in the National Primary Drinking Water Regulation (NPDWRs) of U.S.

Environmental Protection Agency (US EPA)[52] allowing to assess the method accuracy at this level.

Ultrapure water was obtained by Milli-Q system (Millipore) with a resistivity >18.2 M Ω.cm. Nitric acid, 37% (Merck, p.a.) was purified by sub-ebullition in a quartz device (Milestone, Germany) and hydrochloric acid, 30.9% (Merck, Suprapur) was used without further purification. All used bottles were previously overnight cleaned with 10% HNO_3 and double rinsed with ultrapure water prior use. 1% HNO_3 was frequently analyzed to determine instrumental blank and possible memory effects, which were typically <0.01 μg L^{-1} for most trace analytes. NaCl, $CaCl_2 \cdot 2H_2O$ (Merck, p.a.) and ^{50}Cr spike solution (Alfa Aesar) were used in complementary tests. All acidified solutions were made by dilution on a v/v basis.

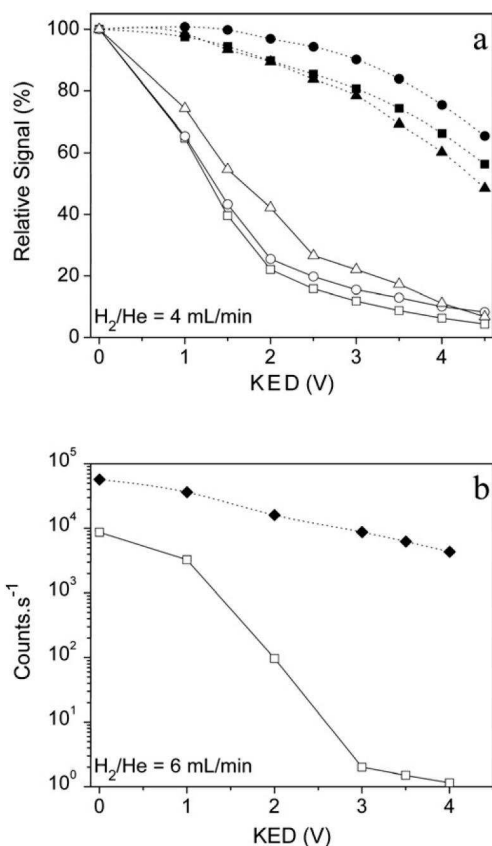## 3. Results and discussion

3.1 Assessment of CC tuning

Prior to each set of measurements the instrument is tuned in the standard and CC modes, following manufacturer recommendations. In CC mode, the hexapole bias (V_H) is set to −17 V, because it corresponds to the optimum ion transmission potential when the cell is pressurized, and the quadrupole bias (V_Q) is set to −14 V, to yield a kinetic energy discrimination of 3 V (KED = V_Q − V_H = 3V). After that, the flow of the gas mixture (7% H_2 in He) is adjusted to provide less than 10 cps at m/z 78. This is typically obtained with gas flow close to 4 mL/min, and then lenses and focus are tuned for maximum ^{115}In signal (>20 kcps ppb^{-1}).

With this instrument KED can also be applied by biasing the differential aperture (DA), however DA potential was kept more negative than the hexapole, meaning that the applied KED corresponds to the difference between V_Q and V_H. This is not usually informed in papers regarding the use of collision cells, and the lack of this information can cause some misunderstanding in relation to the actual use or not of KED.

The preferential removal of polyatomic interfering ions $^{35}Cl^{16}O^+$, $^{35}Cl^{16}O^1H^+$ and $^{40}Ar^{35}Cl^+$ from the analytes $^{51}V^+$, $^{50,52}Cr^+$ and $^{75}As^+$ by changing the KED barrier is shown in Fig. 1 (a) and (b). In Fig 1 (a) analytes, in 1% HNO_3, and Cl-based interferences produced by 1% HCl were measured separately using the same gas flow rate. The high intensity signal of interferences produced by 1% HCl cannot be completely attenuated using a gas flow rate of 4 ml/min, but the analyte/polyatomic ions ratio is improved by increasing the KED.

In Fig. 1(b) the preferential attenuation of $^{35}Cl^{16}O^+$, interfering on $^{51}V^+$, is highlighted in relation to the chromium isotope at nominal mass 50, using gas flow rate of 6 mL/min and typical Cl level of natural waters. As $^{50}Cr^+$ is not interfered by Cl-based polyatomics and there is no Cr at mass 51, both masses could be monitored together in the same solution (Cr in 1% HNO_3 spiked with and 200 mg L^{-1} of Cl, using NaCl). The signal of $^{35}Cl^{16}O^+$ was attenuated over 4 orders of magnitude until reaching background levels (<2 count.s^{-1}). But a simultaneous decrease in analyte signal was observed, almost of one tenth. The net effect is an improvement close to 3 orders of magnitude. Data of Fig 1 (a and b) show that after the multiple collisions with the cell gas, polyatomic ions possess lower axial kinetic energy than

1408 | J. Anal. At. Spectrom., 2009, 24, 1406–1413

This journal is © The Royal Society of Chemistry 2009

33

Fig. 1 Preferential attenuation of polyatomic ions signal by increasing the KED barrier at constant gas flow (7% H_2 in He). a) $^{51}V^+$ (■), $^{52}Cr^+$ (●) and $^{75}As^+$ (▲) in 1% HNO_3. $^{35}Cl^{16}O^+$ (□), $^{35}Cl^{16}O^1H^+$ (○) and $^{40}Ar^{35}Cl^+$ (△) in 1% HCl; b) $^{50}Cr^+$ (◆) and $^{35}Cl^{16}O^+$ (□), measured together in 1% HNO_3 spiked with 200 mg L^{-1} of Cl. Notice that ordinate units of the two panels are different.

monatomic ions, and thus are effectively attenuated by KED of 3V, which provides satisfactory decrease of polyatomic ions signal and improved analyte/interference ratios.

A KED value equal to zero was obtained by setting the quadrupole bias equal to the hexapole bias ($V_Q = V_H = -17V$). The V_Q was scanned to produce a KED potential of 4.5 V. This approach was adopted because it provides a fixed ion kinetic energy within the CC, since the V_H was held constant. If the hexapole bias had been scanned, the KED efficiency could be underestimated.[43]

The progressive removal of Ar and Cl-based interferences, occurring at nominal masses 51, 52, 56, 75, 78 and 80, with the increase of the gas flow rate into CC is presented in Fig. 2. The investigated polyatomic ions can be attenuated up to 4 to 5 orders of magnitude, however sensitivity is severely affected at high gas flow rates.

The increase in signal intensity of analyte and polyatomic ions (Fig. 2), with gas flow up to 2 mL/min is related to collisional focusing.[20] Once the pressure is increased the ions migrate to the axis of the hexapole resulting in better ion transmission. The detected signal thus increases until scattering losses dominate and/or the axial kinetic energy of the ion becomes smaller than KED. The small improvement in the ion signal here

observed is attributed to the use of a shielded torch, which reduces the capacity of the cell to perform focusing as a result of ion energy reduction.[44] And as pointed by Leonhard et al.,[28] if the ion beam is already well focused, collisional focusing does not necessarily lead to a substantial improvement in ion transmission efficiency.

It is also evident that if gas flow rate is used in excess, compared to the demand for polyatomic interference attenuation, a deteriorated BEC is obtained. This can be visualized in Fig 2 (d and e) where $ArCl^+$ and Ar_2^+ were totally attenuated with gas flow rates of 5-6 mL/min and further gas addition only diminished the analyte sensitivity unnecessarily.

The following discussion is centered in optimizing the conditions of gas flow rates capable to reduce the contribution of polyatomic ions to an insignificant level during real water samples analyzes, while trying to keep sensitivity as high as possible. Therefore, minimal flow rates were selected. To define the necessary gas flow the background equivalent concentration (BEC) was employed. BEC was estimated as:

$$BEC\left(\mu g\ L^{-1}\right) = \frac{counts.s^{-1}_{polyatomic\ ions} \times conc._{analyte}}{counts.s^{-1}_{analyte\ 10\mu g\ L^{-1}}}$$

In the above equation, the intensity (counts.s^{-1}) of a polyatomic ion is divided by intensity obtained from a solution containing the interfered element (conc $_{analyte}$) at 10 $\mu g\ L^{-1}$. For selenium and iron isotopes the BEC was estimated after subtracting the background ion signal from the intensity of the analyte signal.

The signals of the Cl-based interferences $^{35}Cl^{16}O^+$, $^{35}Cl^{16}O^1H^+$ and $^{40}Ar^{35}Cl^+$, Fig. 2 (a, b and d), were obtained when 1% HCl (approx. 4200 mg L^{-1} chlorine) was aspirated. This high chlorine concentration does not reflect the composition of most water samples, but was used just to exploit the CC efficiency in removing those interfering polyatomic species.

In ordinary water samples analyzed in our laboratory (drinking, river and groundwater), the chlorine content is measured by ion chromatography before ICP-MS analysis. Most samples have Cl concentration below 200 mg L^{-1}. At this chlorine level, BEC values of $^{51}V^+$, $^{52}Cr^+$ and $^{75}As^+$ in CC mode using H_2/He at 4 mL/min are 0.1, 0.005 and 0.003 $\mu g\ L^{-1}$, respectively. While BEC values for $^{52}Cr^+$ and $^{75}As^+$ are low enough for accurate determination of these elements in water samples at the sub $\mu g\ L^{-1}$ (ppb) level, for $^{51}V^+$ it is still relatively high, and could produce inaccurate results. To reduce the interference of $^{35}Cl^{16}O^+$ on $^{51}V^+$ to a negligible level, a gas flow of 6 mL/min must be used. This yields a BEC of 0.004 $\mu g\ L^{-1}$, meaning an overall improvement of 530 times, when the gas flow is changed from 0 to 6 mL/min.

The effective removal of the interfering polyatomic ions on $^{51}V^+$ and $^{75}As^+$ is visualized in Fig. 3. When the measurements are made without gas or at low gas flow the $ArCl^+$ contribution to $^{75}As^+$ is about 10% and the signal of V^+ is fully hidden by the ClO^+. With standard ICP-MS conditions that contribution, indicated by the (x), is even greater. With proper gas flows these interferences are reduced to less than 2 count.s^{-1}.

The data in Fig. 2 and 3 can be used to estimate of the necessary gas flow rate to account for a specific chlorine level. For instance, when samples with 500 mg L^{-1} of Cl are analyzed, the BEC values of $^{51}V^+$, $^{51}Cr^+$ and $^{75}As^+$ can be kept below 0.005 $\mu g\ L^{-1}$, if the gas flows indicated above are

This journal is © The Royal Society of Chemistry 2009

34

J. Anal. At. Spectrom., 2009, **24**, 1406–1413 | 1409
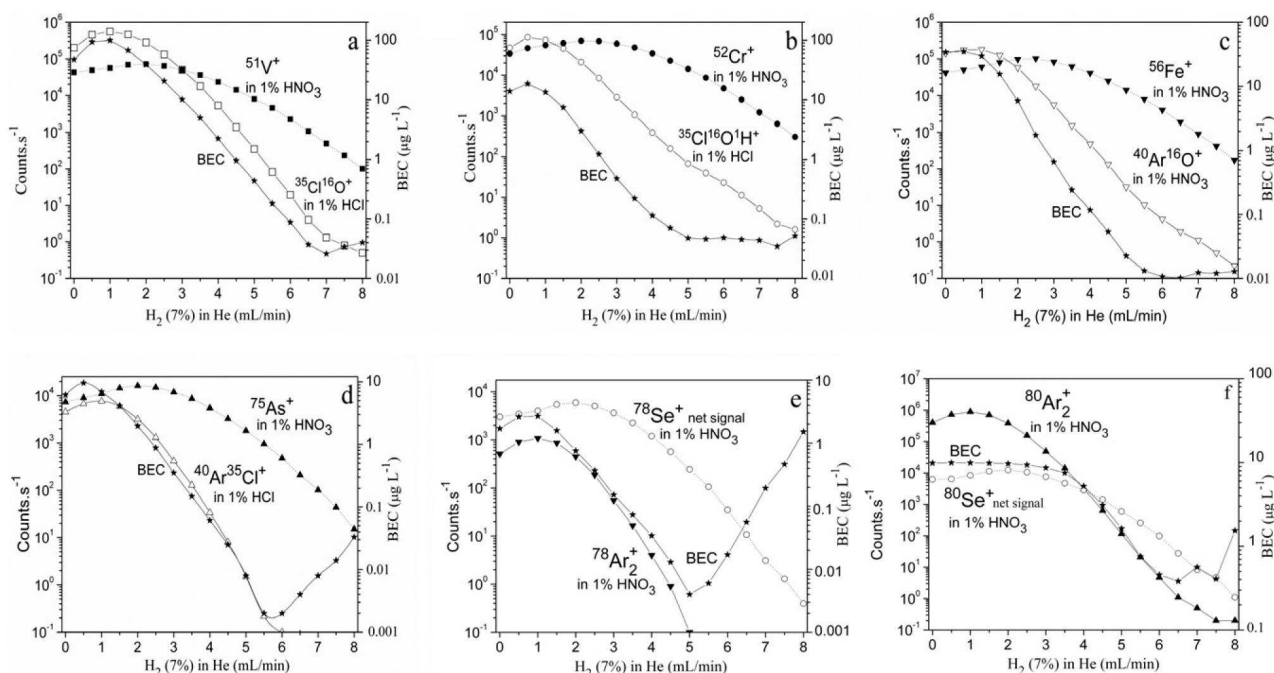
Fig. 2 Effect of the increase of the gas flow rate in polyatomic interferences attenuation, analyte ion signal (10 μg L^{-1}) and background equivalent concentration (BEC), with KED = 3V. Symbols: BEC (*); a) $^{51}V^+$ (■) and $^{35}Cl^{16}O^+$ (□); b) $^{52}Cr^+$ (●) and $^{35}Cl^{16}O^1H^+$ (○); c) $^{56}Fe^+$ (▼) and $^{40}Ar^{16}O^+$ (▽); d) $^{75}As^+$ (▲) and $^{40}Ar^{35}Cl^+$ (△); e) $^{78}Se^+$ (○) and $^{78}Ar_2^+$ (▼); f) $^{80}Se^+$ (○) and $^{80}Ar_2^+$ (▲). The net signals for iron and selenium isotopes correspond to the total counts at the specific mass after background subtraction: $^{78}Se^+$ (10 μg L^{-1} solution) = total counts at m/z 78 − $^{78}Ar_2^+$ (in 1% HNO$_3$).

increased by 0.5 mL/min. Thus, the method may be easily adapted to samples with different Cl content. But, above that Cl level, the use of higher gas flow rates implies in significant loss in sensitivity and specifically turns $^{51}V^+$ measurement difficult. In such case, a reactive gas (1% NH$_3$ in He), as recommended by Chrastný et al.,[42] is more effective to accomplish the removal of ClO$^+$.

The attenuation of the chlorine hydroxide ($^{35}Cl^{16}O^1H^+$) that hampers the quantification of Cr with its most abundant isotope $^{52}Cr^+$ (83.8%), is shown in Fig. 2 (b). The overall improvement of $^{52}Cr^+$ BEC surpasses 120 times when the gas flow increases from 0 to 4 mL/min. The subsequent change in the slope of the $^{35}Cl^{16}O^1H^+$ line when gas flow reaches 5 mL/min, indicates a possible contamination of Cr in the 1% HCl (suggested since the lines of $^{35}Cl^{16}O^1H^+$ and $^{52}Cr^+$ take the same slop), hence further improvement in BEC was not possible. In a similar way, the measurement of $^{40}Ar^{16}O^+$ (Fig. 2 c) at high gas flows (> 6 mL/min) seems to be affected due the presence of Fe in the blank.

The occurrence of $^{40}Ar^{23}Na^+$ was investigated by introducing a solution with 500 mg L^{-1} of Na. The results (not presented) showed significant formation of ArNa$^+$ and consequently serious interference on $^{63}Cu^+$ when no gas was added to CC. This interference was fully removed by adding a gas flow of 4 mL/min.

For quantification purposes, the isotope $^{78}Se^+$ was preferred instead of $^{80}Se^+$, as the former has a BEC 150 times smaller than the last, at 4 mL/min (Fig. 2 e and f). With this gas flow rate the BEC of $^{78}Se^+$ and $^{56}Fe^+$ are 0.03 and 0.12 μg L^{-1}, respectively, and are appropriate to the intended application. If desired, those BEC can be reduced to 0.004 and 0.02 μg L^{-1} using 5 mL/min. However, 4 mL/min was preferred to measure $^{78}Se^+$ and $^{56}Fe^+$,

because it is the same gas flow established for $^{75}As^+$, $^{63}Cu^+$ and $^{52}Cr^+$. This simplifies the instrument tuning and implies in higher speed of analysis.

The signals of selenium isotopes present the most severe loss in intensity with gas flow increase, possibly due to hydride formation as pointed out by Boulyga and Becker.[35] Sloth and Larsen[53] also reported the formation of SeH$^+$, but with methane as reaction gas. The quantification of Se in CC mode with H$_2$/He mixture is a good example of chemical mitigation of undesired ions, where polyatomic ($^{78,80}Ar_2^+$) and analyte ions react with the gas, but the reaction is faster with the former, leading to an improvement in the value of Se$^+$ BEC.

3.2 Trueness

The assessment of trueness requires the comparison of averaged measurement results with a reference value (RV). Ideally it should be tested at three concentration levels in order to check if any observed difference is a function of the analyte content.[54] However, few water certified reference materials are available. Thus our method validation was limited to two NIST reference materials (SRM 1640 and 1643e) that possess certified or reference values with low uncertainties for a wide trace element suite. These certified reference materials contain different matrix and levels of trace elements. SRM 1640 contains higher sodium and lower trace elements level than SRM 1643e, while the opposite occurs for calcium concentration.

Bias, uncertainty of bias, as defined by Linsinger,[55] and z-score were evaluated by analysis of the two CRM during a period of few months, characterizing intermediate precision. The mean

35
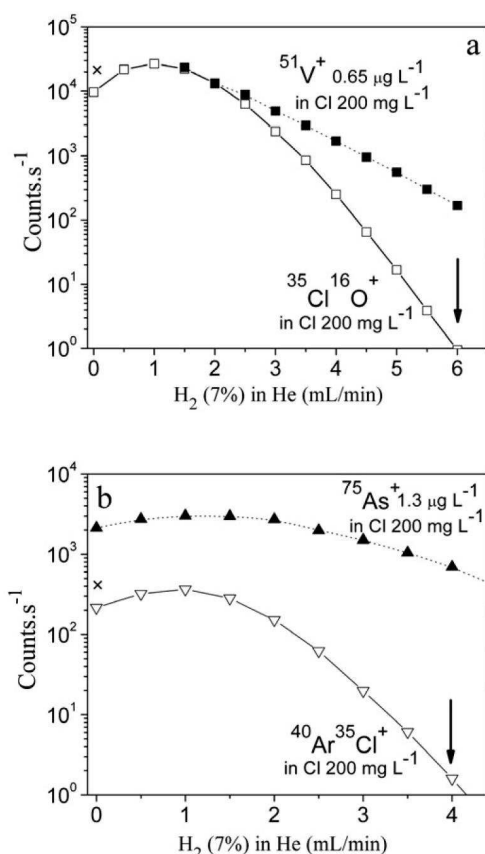
Fig. 3 Attenuation of Cl-based interferences corresponding to a sample with high chlorine content in 20-fold diluted NIST SRM 1640 spiked with 200 mg L^{-1} of Cl. KED = 3V. a) $^{35}Cl^{16}O^+$ ($\square$) and $^{51}V^+$ ($\blacksquare$); b) $^{40}Ar^{35}Cl^+$ ($\triangle$) and $^{75}As^+$ ($\blacktriangle$). The arrows indicate the recommended gas flow rate and (x) at the y-axis corresponds the production of polyatomic ion in standard mode.

results and respective standard deviation (s) obtained for 10-fold diluted aliquots are presented in Tables 2 and 3 and are compared with respective certified or reference value (*RV*) and uncertainties (U_{CRM}). The next columns include bias, calculated as the relative difference (%) between the mean of results for each analyte and the respective RV, followed by uncertainty of bias and z-score in the last two columns.

Uncertainty of bias (u_b), was obtained by combining standard uncertainty of the mean value ($u = s/\sqrt{n}$, where s is the standard deviation of the number n of available results) and the standard uncertainty of the certified/reference value (U_{CRM}/k, where k is the coverage factor), as shown:

$$u_b = \sqrt{\frac{s^2}{n} + \frac{U_{CRM}^2}{k}}$$

The certificate of the SRM 1643e informs the values of the coverage factor used to expand the uncertainty of each certified value, while in the certificate of SRM1640 that information is absent, so k = 2 was adopted to calculate the uncertainty of bias for SRM1640. The uncertainty in the concentration of the commercial standard solutions (0.5%) used to prepare the

Table 2 Results (µg L^{-1}) for 10-fold diluted SRM 1640, certified/reference values (RV), bias, uncertainty of bias (u_b) and z-score

Analyte	Mean ± 1s (n = 8)	RV ± U$_{SRM}$	bias (%)	u$_b$	z-score
Li	50.3 ± 3.4	50.8 ± 1.4	−1.0	1.4	−0.4
Be	36.20 ± 2.32	34.99 ± 0.41	3.5	0.84	1.4
B	295.7 ± 18.0	301.6 ± 6.1	−2.0	7.1	−0.8
Na	28366 ± 1588	29394 ± 310	−3.5	582	−1.8
Mg	5661 ± 357	5828 ± 56	−2.9	129	−1.3
Al	55.1 ± 8.4	52.1 ± 1.5	5.8	3.1	1.0
Si	4863 ± 374	4737 ± 120	2.7	145	0.9
K	995 ± 142	995 ± 27	0.0	52	0.0
Ca	7073 ± 368	7056 ± 89	0.2	138	0.1
V	13.28 ± 0.85	13.01 ± 0.37	2.1	0.35	0.8
Cr	39.3 ± 2.0	38.7 ± 1.6	1.6	1.1	0.6
Mn	123.6 ± 6.1	121.7 ± 1.1	1.6	2.2	0.9
Fe	35.1 ± 2.7	34.4 ± 1.6	2.0	1.2	0.6
Co	21.00 ± 0.94	20.31 ± 0.31	3.4	0.37	1.9
Ni	28.1 ± 1.8	27.4 ± 0.8	2.6	0.8	0.9
Cu	87.4 ± 3.2	85.3 ± 1.2	2.5	1.3	1.6
Zn	56.9 ± 5.6	53.3 ± 1.1	6.8	2.1	1.8
As	27.61 ± 1.85	26.71 ± 0.41	3.4	0.69	1.3
Se	23.00 ± 1.36	21.99 ± 0.51	4.6	0.54	1.9
Rb	2.16 ± 0.26	2.00 ± 0.02	8.0	0.09	1.7
Sr	125.1 ± 5.8	124.4 ± 0.7	0.6	2.1	0.3
Mo	47.17 ± 1.78	46.82 ± 0.26	0.7	0.64	0.5
Ag	7.60 ± 0.42	7.63 ± 0.25	−0.4	0.19	−0.2
Cd	23.64 ± 0.82	22.82 ± 0.96	3.6	0.56	1.5
Sb	13.78 ± 0.50	13.81 ± 0.42	−0.2	0.27	−0.1
Ba	150.7 ± 5.1	148.2 ± 2.2	1.7	2.1	1.2
Pb	28.70 ± 1.33	27.93 ± 0.14	2.8	0.48	1.6

Table 3 Results (µg L^{-1}) for 10-fold diluted SRM 1643e, certified/reference values (RV), bias, uncertainty of bias (u_b) and z-score

Analyte	Mean ± 1s (n = 6)	RV ± U$_{SRM}$	bias (%)	u$_b$	z-score
Li	17.4 ± 1.4	17.4 ± 1.7	0.0	0.8	0.0
Be	13.82 ± 0.74	13.98 ± 0.17	−1.1	0.31	−0.5
B	162.3 ± 17.8	157.9 ± 3.9	2.8	7.4	0.6
Na	20378 ± 988	20740 ± 260	−1.7	424	−0.9
Mg	8036 ± 365	8037 ± 98	0.0	157	0.0
Al	139.3 ± 18.3	141.8 ± 8.6	−1.8	7.9	−0.3
K	1996 ± 111	2039 ± 29	−1.9	47	−0.9
Ca	31793 ± 1110	32300 ± 1100	−1.6	600	−0.8
V	36.91 ± 1.13	37.86 ± 0.59	−2.5	0.54	−1.8
Cr	20.79 ± 1.29	20.40 ± 0.24	1.9	0.54	0.7
Mn	37.70 ± 1.88	38.97 ± 0.45	−3.3	0.80	−1.6
Fe	99.7 ± 5.2	98.1 ± 1.4	1.6	2.24	0.7
Co	26.70 ± 1.14	27.06 ± 0.32	−1.3	0.49	−0.7
Ni	60.91 ± 2.36	62.41 ± 0.69	−2.4	1.02	−1.5
Cu	22.48 ± 0.97	22.76 ± 0.31	−1.2	0.42	−0.7
Zn	76.5 ± 5.1	78.5 ± 2.2	−2.2	2.2	−0.9
As	59.14 ± 3.13	60.45 ± 0.72	−2.2	1.33	−1.0
Se	11.78 ± 1.37	11.97 ± 0.14	−1.6	0.56	−0.3
Rb	14.14 ± 0.71	14.14 ± 0.18	0.0	0.30	0.0
Sr	331.2 ± 22.5	323.1 ± 3.6	2.5	9.4	0.9
Mo	121.7 ± 5.6	121.4 ± 1.3	0.2	2.4	0.1
Ag	1.02 ± 0.04	1.062 ± 0.075	−4.0	0.029	−1.5
Cd	6.45 ± 0.34	6.568 ± 0.073	−1.8	0.14	−0.8
Sb	58.17 ± 2.08	58.30 ± 0.61	−0.2	0.90	−0.2
Ba	543.2 ± 14.4	544.2 ± 5.8	−0.2	6.6	−0.2
Tl	7.44 ± 0.28	7.445 ± 0.096	−0.1	0.12	0.0
Pb	19.59 ± 0.70	19.63 ± 0.21	−0.2	0.30	−0.1

calibration solutions was not included in the combined uncertainty, as it is negligible in comparison with the other components considered.

This journal is © The Royal Society of Chemistry 2009

J. Anal. At. Spectrom., 2009, **24**, 1406–1413 | 1411

36

The handbook for calculation of measurement uncertainty in environmental laboratories[54] requires that if CRM are used to estimate the bias, these should be analyzed in at least 5 different analytical series before the values are used. This requirement was obeyed because data from more than 6 different runs were used. The averaged relative standard deviation for all analytes is 6.5% for SRM 1640 and 5.6% for SRM1643e. And no difference in precision was observed between elements measured in standard and CC mode.

All elements were determined with relative bias smaller than 8% and mostly show opposite deviation from RV for the two reference materials. In general, the agreement between results and reference values is better for SRM 1643e than SRM 1640. The largest deviations from RV were observed for Al, Zn and Rb measured in SRM 1640. However the results of these trace elements in SRM 1643e are in good agreement with RV. The difference observed in SRM 1640 may be associated to environmental contamination because dilutions were not made in clean-room conditions and the certificates of these water standard reference materials recommend their manipulation in a Class-100 clean hood. Despite that, the bias of the vast majority of elements is <5%.

To assess if the difference between mean values and RV is significant from an uncertainty point of view, the z-score was also calculated.[56] In simple terms, the z-score is absolute bias divided by the uncertainty of the bias:

$$z\text{-score} = \frac{(\text{Mean} - \text{RV})}{u_b}$$

Significant bias is defined as z-score >|2|.[56] Most z-score values (56% for SRM 1640 and 85% for SRM 1643e) lie within the −1 to +1 range, reflecting the close agreement between mean and RV, and all other elements present z-score within ± 2. So these results are free of significant bias.

The high quality data obtained for these two CRM indicates that the proposed method is fit for trace elements determination in common water matrices.

In additional tests, other 10-fold diluted aliquots of both CRM were spiked with 200 mg L^{-1} of Cl (using NaCl). The relative deviation of V, Cr, Cu and As results from un-spiked samples were negligible (<0.2%), and totally insignificant considering the method precision, showing that polyatomic species are being properly attenuated. Results of other elements measured in CC mode, like Fe and Se, were also in agreement with RV, indicating that the interference attenuation is not affected in an enriched matrix.

The interference on the nominal mass of As$^+$ due to formation of ^{40}Ca^{35}Cl$^+$ in CC mode operating with KED of 3V and H$_2$/He at 4 mL/min was investigated introducing a solution with 100 mg L^{-1} of Ca, prepared from CaCl$_2$·2H$_2$O. At this Ca level, none interference was detected, corroborating findings of other authors.[41]

Method detection limits, Table 4, are given as three times the standard deviation (3s) of eight measurements in 1% HNO$_3$ solution spiked with analytes at concentrations corresponding 3 to 5 times the instrumental detection limit.[21]

Method detection limits are below typical trace elements concentrations found in uncontaminated water samples, and are

Table 4 Method detection limits (MDL) in μg L^{-1}

Isotope	Mode	MDL	Isotope	Mode	MDL
^{7}Li	Standard	0.012	^{60}Ni	CC	0.014
^{9}Be	Standard	0.008	^{63}Cu	CC	0.009
^{11}B	Standard	0.054	^{66}Zn	CC	0.006
^{23}Na	Standard	7.1	^{75}As	CC	0.007
^{25}Mg	Standard	3.0	^{78}Se	CC	0.010
^{27}Al	Standard	0.1	^{85}Rb	Standard	0.002
^{29}Si	Standard	50	^{88}Sr	Standard	0.001
^{39}K	CC	5.0	^{95}Mo	Standard	0.003
^{43}Ca	Standard	30	^{107}Ag	Standard	0.003
^{51}V	CC	0.008	^{111}Cd	Standard	0.004
^{52}Cr	CC	0.005	^{121}Sb	Standard	0.004
^{54}Fe	CC	0.13	^{137}Ba	Standard	0.004
^{55}Mn	CC	0.01	^{205}Tl	Standard	0.001
^{56}Fe	CC	0.07	^{206,7,8}Pb	Standard	0.003
^{59}Co	CC	0.003			

generally 10 to 100 times lower than the MCLs for contaminants specified in official regulations.[3,53]

4. Conclusions

It was demonstrated that H$_2$ ion-molecule chemistry and KED in a hexapole CC is efficient to improve the BEC of ^{51}V$^+$, ^{52}Cr$^+$, ^{56}Fe$^+$, ^{75}As$^+$ and ^{78}Se$^+$ isotopes by over two orders of magnitude. As a result reliable analysis of these elements can be accomplished by CC-ICP-MS at the low ng L^{-1} level.

The accuracy of the proposed "multi-mode" method was confirmed by the analyses of two CRM. Even when 10-fold aliquots of both CRM were spiked with chlorine at levels usually found in typical samples, the results of interfered elements were not affected, confirming that the desired level of interference attenuation was accomplished. But, if more complex samples have to be analyzed and/or other polyatomic interferences are known or expected, the prescribed gas flow or KED, and in last instance the cell gas, may be adjusted to provide the demanded level of interference attenuation.

Method detection limits are appropriate for most hydrogeochemical studies. As low ng L^{-1} concentrations of Cr, As and Se can be determined using the same CC conditions for concomitant ClOH$^+$, ArCl$^+$ and Ar$_2^+$ removal, speciation of these elements may be accomplished in a single run.[57]

5. Acknowledgements

References

1 WHO (World Health Organization), *Guidelines for Drinking Water Quality*, Geneva, Switzerland, 3nd edn, 2006, (ch. 8), pp. 145–196. (http://www.who.int/water_sanitation_health/dwq/gdwq3rev).
2 EU (European Union), *Directive 98/83/EC on the Quality of Water intended for Human Consumption*, 1998, OJ, L330, pp. 32–54.(http://www.fsai.ie/legislation/food/eu_docs/Water/Dir%2098.83.EC.pdf).
3 CONAMA (Conselho Nacional do Meio Ambiente) Resolution No 357, 2005, 24 pp.(http://www.mma.gov.br/port/conama/res/res05/res35705.pdf).

1412 | *J. Anal. At. Spectrom.*, 2009, **24**, 1406–1413

This journal is © The Royal Society of Chemistry 2009

37

4 CONAMA (Conselho Nacional do Meio Ambiente) Resolution No 396, 2008 11 pp.(http://www.mma.gov.br/port/conama/legiabre.cfm?codlegi = 562).
5 D. Beauchemin, J. W. McLaren, A. P. Mykytiuk and S. S. Berman, *Anal. Chem.*, 1987, **59**, 778–783.
6 G. E. M. Hall, J. E. Vaive and J. Pelchat, *J. Anal. At. Spectrom.*, 1996, **11**, 779–786.
7 M. Nicolaï, C. Rosin, N. Tousset and Y. Nicolai, *Talanta*, 1999, **50**, 433–444.
8 J. L. Fernández-Turiel, J. F. Llorens, F. López-Vera, C. Gómez-Artola, I. Morell and D. Gimeno, *Fresenius J. Anal. Chem.*, 2000, **368**, 601–606.
9 P. Jitaru, K. Tirez and N. De Brucker, *At. Spectrosc.*, 2003, **24**, 1–10.
10 M. Mahar, J. F. Tyson, K. Neubauer and Z. Grosser, *J. Anal. At. Spectrom.*, 2008, **23**, 1204–1213.
11 E. H. Evans and J. J. Giglio, *J. Anal. At. Spectrom.*, 1993, **8**, 1–18.
12 T. W. May and R. H. Wiedmeyer, *At. Spectrosc.*, 1998, **19**, 150–155.
13 V. N. Epov, D. Lariviere., E. N. Epova and R. D. Evans, *Geostand. Geoanal. Res.*, 2004, **28**, 213–224.
14 J. W. Olesik and D. R. Jones, *J. Anal. At. Spectrom.*, 2006, **21**, 141–159.
15 S. Wilbur, *Spectroscopy*, 2008, **23**, 18–23.
16 D. J. Douglas, *Can. J. Spectrosc.*, 1989, **34**, 38–49.
17 J. T. Howan and R. S. Houk, *Appl. Spectrosc.*, 1989, **43**, 976–980.
18 G. C. Eiden, C. J. Barinaga and D. W. Koppenaal, *J. Anal. At. Spectrom.*, 1996, **11**, 317–322.
19 G. C. Eiden, C. J. Barinaga and D. W. Koppenaal, *Rapid Commun. Mass Spectrom.*, 1997, **11**, 37–42.
20 S. D. Tanner, V. I. Baranov and D. R. Bandura, *Spectrochim. Acta, Part B*, 2002, **57**, 1361–1452.
21 US Environmental Protection Agency, *USEPA Method 6020A, Revision 5.4*, US EPA, USA, 1994(http://www.epa.gov/SW-846/pdfs/6020a.pdf).
22 V. N. Epov, I. E. Vasil'eva, V. I. Lozhkin, E. N. Epova, L. F. Paradina and A. N. Suturin, *J. Anal. Chem.*, 1999, **54**, 837–842.
23 J. L. M. de Boer, *J. Anal. At. Spectrom.*, 2000, **15**, 1157–1160.
24 D. A. Polya, P. R. Lythgoe, F. Abou-Shakra, A. G. Gault, J. R. Brydie, J. G. Webster, K. L. Brown, M. K. Nimfopoulos and K. M. Michailidis, *Mineral. Mag.*, 2003, **67**, 247–261.
25 J. W. McLaren, A. P. Mykytiuk, S. N. Willie and S. S. Berman, *Anal. Chem.*, 1985, **57**, 2907–2911.
26 E. M. Heithmar, T. A. Hinners, J. T. Rowan and J. M. Riviello, *Anal. Chem.*, 1990, **62**, 857–684.
27 M. Satyanarayanan, V. Balaram, T. G. Rao, B. Dasaram, S. L. Ramesh, R. Mathur and R. K. Drolia, *Indian J. Mar. Sci.*, 2007, **36**, 71–75.
28 P. Leonhard, R. Pepelnik, A. Prange, N. Yamada and T. Yamada, *J. Anal. At. Spectrom.*, 2002, **17**, 189–196.
29 J. Darrouzès, M. Bueno, G. Lespès, M. Holeman and M. Potin-Gautier, *Talanta*, 2007, **71**, 2080–2084.
30 I. Feldmann, N. Jakubowski and D. Stuewer, *Fresenius J. Anal. Chem.*, 1999, **365**, 415–421.
31 M. Iglesias, N. Gilon, E. Poussel and J. M. Mermet, *J. Anal. At. Spectrom.*, 2002, **17**, 1240–1247.
32 C. J. Barinaga and D. W. Koppenaal, *Rapid Commun. Mass Spectrom.*, 1994, **8**, 71–76.
33 I. Feldmann, N. Jakubowski, C. Thomas and D. Stuewer, *Fresenius J. Anal. Chem.*, 1999, **365**, 422–428.
34 C. P. Ingle, P. K. Appelblad, M. A. Dexter, H. J. Reida and B. L. Sharp, *J. Anal. At. Spectrom.*, 2001, **16**, 1076–1084.
35 S. F. Boulyga and J. S. Becker, *Fresenius J. Anal. Chem.*, 2001, **370**, 618–623.
36 M. A. Dexter, H. J. Reid and B. L. Sharp, *J. Anal. At. Spectrom.*, 2002, **17**, 676–681.
37 M. Niemelä, P. Perämäki, H. Kola and J. Piispanen, *Anal. Chim. Acta*, 2003, **493**, 3–12.
38 N. Yamada, J. Takahashi and K. Sakata, *J. Anal. At. Spectrom.*, 2002, **17**, 1213–1222.
39 S. J. Christopher, R. D. Day, C. E. Bryana and G. C. Turk, *J. Anal. At. Spectrom.*, 2005, **20**, 1035–1043.
40 H. Chu, Y. Yip, K. Chan and W. Sham, *J. Anal. At. Spectrom.*, 2006, **21**, 1068–1071.
41 V. Dufailly, L. Noël and T. Guérin, *Anal. Chim. Acta*, 2008, **611**, 134–142.
42 V. Chrastný, M. Komárek, M. Mihaljevič and J. Štíchová, *Anal. Bioanal. Chem.*, 2006, **385**, 962–970.
43 B. Hattendorf and D. Günther, *J. Anal. At. Spectrom.*, 2004, **19**, 600–606.
44 E. McCurdy and G. Woods, *J. Anal. At. Spectrom.*, 2004, **19**, 607–615.
45 S. Mazan, N. Gilon, G. Crétier, J. L. Rocca and J. M. Mermet, *J. Anal. At. Spectrom.*, 2002, **17**, 366–370.
46 T. Arnold, J. N. Harvey and D. J. Weiss, *Spectrochim. Acta, Part B*, 2008, **63**, 666–672.
47 G. K. Koyanagi, V. V. Lavrov, V. Baranov, D. Bandura, S. Tanner, J. W. McLaren and D. K. Bohme, *Int. J. Mass Spectrom.*, 2000, **194**, L1–L5.
48 V. G. Anicich, *Astrophys. J. Suppl.*, 1993, **84**, 215–315.
49 F. Vanhaecke, H. Vanhoe, R. Dams and C. Vandecasteele, *Talanta*, 1992, **39**, 737–742.
50 I. Rodushkin, T. Ruth and D. Klockare, *J. Anal. At. Spectrom.*, 1998, **13**, 159–166.
51 J. J. Thompson and R. S. Houk, *Appl. Spectrosc.*, 1987, **41**, 801–806.
52 US Environmental Protection Agency, *National Primary Drinking Water Regulations, Maximum Contaminant Level (MCL)*. (http://www.epa.gov/ogwdw/contaminants/index.html).
53 J. J. Sloth and E. H. Larsen, *J. Anal. At. Spectrom.*, 2000, **15**, 669–672.
54 NORDTEST, *Handbook for Calculation of Measurement Uncertainty in Environmental Laboratories*, Nordest, Finland, Version 1.3, 2nd edn, October 2003, 52 pp. (http://www.nordtest.org/register/techn/tlibrary/tec537.pdf).
55 T. P. J. Linsinger, *TrAC, Trends Anal. Chem.*, 2008, **27**, 916–923.
56 I. Taverniers, M. De Loose and E. V. Bockstaele, *TrAC, Trends Anal. Chem.*, 2004, **23**, 535–552.
57 K. R. Neubauer, P. A. Perrone, W. M. Reuterand and R. Thomas, Spectroscopy, 2006, **May Spec. Issue**, 20–32.

J. Anal. At. Spectrom., 2009, **24**, 1406–1413 | 1413

38

ANEXO II

Resumo expandido: Cotta AJB e Enzweler J.

Determinação direta de lantanídeos e outros 28 elementos em águas por ICP-MS.

Apresentado no XII Congresso Brasileiro Geoquímica, Ouro Preto - MG, 18-22/Out. de 2009.

Nesta versão a denominação "lantanídeos (Ln)" substitui o nome "elementos terra raras (ETR)", o qual aparece na versão original do resumo, para melhor descrever os elementos determinados.

Seguido de resultados complementares.

DETERMINAÇÃO DIRETA DE LANTANÍDEOS E OUTROS 28 ELEMENTOS EM ÁGUAS POR ICP-MS

Cotta A.J.B.[1] e Enzweiler J.[2]

[1] Departamento de Geologia e Recursos Naturais- DGRN, UNICAMP, aloisio@ige.unicamp.br [2] Departamento de Geologia e Recursos Naturais- DGRN, UNICAMP, jacinta@ige.unicamp.br

RESUMO

Este trabalho demonstra que a determinação direta de lantanídeos (Ln) por ICP-MS em águas pode ser realizada concomitantemente à quantificação de outros 28 elementos. No método descrito, interferências poliatômicas do tipo ArX^+, ClO^+ e $ClOH^+$ são eficientemente atenuadas com o uso de cela de colisão. Para as interferências nos Ln este recurso não é eficaz e correções matemáticas foram utilizadas. A exatidão do método é demonstrada pela análise de materiais de referência de águas e rochas. Nas amostras de água analisadas os Ln puderam ser quantificados em níveis comparáveis ao encontrados em ambientes costeiros, caracterizados pela baixa abundância destes elementos.

PALAVRAS CHAVE: ICP-MS, lantanídeos, cela de colisão, águas

INTRODUÇÃO

A espectrometria de massas com plasma de argônio indutivamente acoplado (ICP-MS) é a técnica ideal para quantificar metais e metalóides em águas superficiais e subterrâneas. A elevada sensibilidade da técnica proporciona limites de detecção (LD) e, por conseguinte, a precisão e a exatidão requeridas para diversas aplicações. O método US EPA 6020A descreve a determinação de um conjunto de analitos, entre eles Al, Cd, Cr, As, Tl que são potencialmente nocivos e que devem ter suas concentrações monitoradas para assegurar a qualidade/adequação dos recursos hídricos aos seus diversos usos (Conama 396). Por outro lado, avanços na instrumentação permitem aprimorar e expandir a capacidade analítica dos métodos já descritos. O objetivo deste trabalho é avaliar a possibilidade de incluir os lantanídeos (Ln) num método no qual são quantificados 28 analitos (Cotta e Enzweiler 2009). Como na geoquímica de rochas, os padrões de Ln em águas são usados para investigar e identificar processos hidrogeoquímicos e a presença e magnitude da contribuição antrópica.

Em águas não contaminadas os Ln são encontrados em concentrações que variam de algumas centenas de ppt (i.e. ng L^{-1}) a níveis sub ppt decrescendo de La para Lu. A baixa concentração dos Ln em águas implica num desafio analítico, mesmo para uma técnica sensível como o ICP-MS. A pré-concentração dos Ln em resinas de troca iônica é uma opção, porém este procedimento é demorado, complexo, encarece a análise e limita o número de elementos determinados, uma vez que nem todos analitos de interesse são quantitativamente concentrados (Hall *et al*. 1996). A determinação direta de Ln em águas foi reportada por Lawrence *et al*. (2006) utilizando um instrumento similar ao empregado neste trabalho, porém sem incluir outros

elementos. Assim sendo, é desejável desenvolver um único método que permita a determinação direta dos Ln em águas, junto com outros analitos.

MATERIAIS E MÉTODOS

O instrumento utilizado é um ICP-MS quadrupolar, equipado com cela de colisão, CC-ICP-MS (Thermo, *Xseries^{II}*). A cela de colisão é usada sob condições específicas, para medir os analitos interferidos por íons poliatômicos, como $^{35}Cl^{16}O^+$ em $^{51}V^+$, $^{35}Cl^{16}O^1H^+$ em $^{52}Cr^+$, $^{23}Na^{40}Ar^+$ em $^{63}Cu^+$, $^{40}Ar^{16}O^+$ em $^{56}Fe^+$, $^{40}Ar^{35}Cl^+$ em $^{75}As^+$ e $^{40}Ar^{38}Ar^+$ em $^{78}Se^+$ sem a necessidade de correções matemáticas. Com este recurso, os LD destes analitos podem ser melhorados em duas ordens de magnitude, se comparados a valores obtidos sem a pressurização da cela. A Tabela 1 contém as condições instrumentais utilizadas e os isótopos medidos.

Tabela 1. Parâmetros instrumentais e isótopos medidos

Potência do plasma	1400 W
Extração	-210 to -160 V
Tempo de integração	10 – 20 ms *(10 - 40 ms)***
Medidas	3 x 30 scans *(3 x 60 scans)***
Condições	$^{140}Ce^{16}O^+/^{140}Ce^+ < 2\%$ e $^{137}Ba^{++}/^{137}Ba^+ < 3\%$
Modo CC	
Isótopos e fluxo de gás	6 mL/min para ^{51}V
	4 mL/min para ^{39}K, $^{52,53}Cr$, $^{54,56}Fe$, ^{55}Mn, ^{59}Co, ^{60}Ni, ^{63}Cu, ^{66}Zn, ^{75}As, ^{78}Se, $^{115}In*$
Potencial da cela	-17 V
Potencial do quadrupolo	-14 V
Sinal	^{115}In (1 µg L^{-1}) >20.000 cps e $^{78}Ar_2$ <10 cps
Modo padrão	
Isótopos	^7Li, ^9Be, ^{11}B, ^{23}Na, ^{25}Mg, ^{27}Al, ^{29}Si, ^{43}Ca, ^{85}Rb, ^{88}Sr, ^{89}Y, ^{95}Mo, ^{107}Ag, ^{111}Cd, ^{121}Sb, ^{137}Ba, ^{139}La, ^{140}Ce, ^{141}Pr, ^{143}Nd, ^{147}Sm, ^{151}Eu, $^{157,160}Gd$, ^{165}Ho, ^{166}Er, ^{169}Tm, ^{172}Yb, ^{175}Lu, $^{185}Re*$, ^{205}Tl, $^{206,207,208}Pb$, ^{232}Th, ^{238}U
Potencial da cela	-4 V
Potencial do quadrupolo	0.5 V
Signal	^{115}In (1 µg L^{-1}) > 40.000 cps

* padrão interno. ** modificações implementas na versão final do método.

A formação de óxidos e hidróxidos de Ba e Ln leves interfere na determinação dos Ln médios e pesados. A correção de tais interferências foi efetuada com equações matemáticas conforme proposto por Raut *et al.* (2003). A calibração do instrumento foi realizada como descrito em Cotta e Enzweiler (2009), mas com adição dos Ln a partir de soluções-padrão High Purity Standards de 10 mg L^{-1}.$^{115}In^+$ e $^{185}Re^+$ foram utilizados como padrão interno para correção de *drift* instrumental. A validação do método foi efetuada pela análise de 2 materiais de referência certificados (MRC) de águas, NIST SRM 1640 e SRM 1643e, e para os Ln, de 4 MR de basaltos (BRP-1, BCR-2, BHVO-2 e BIR-1), dissolvidos com HF/HNO$_3$ e diluídos 20.000 vezes.

RESULTADOS

Os resultados de 28 elementos obtidos nos 2 MRC de águas e para os Ln nos 4 MR de rochas encontram-se nas Fig. 1 e Fig. 2, respectivamente. A concordância entre os valores obtidos de Ln e os valores de referência mostra que as interferências foram corrigidas independentemente do grau de fracionamento das amostras. Os dados dos demais elementos determinados nos 2 MRC (SRM 1640 e 1643e) indicam que o método produz resultados exatos para todos os analitos.
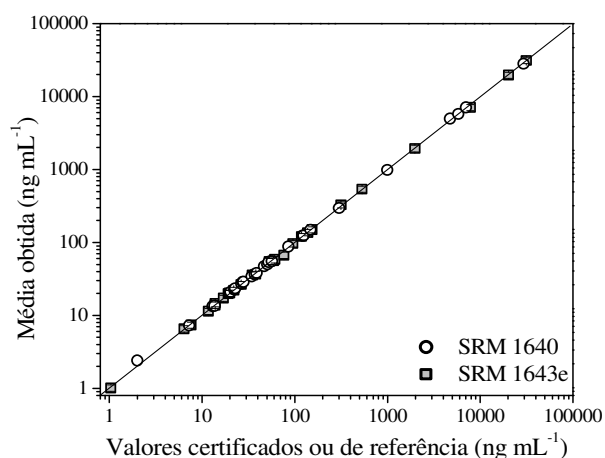
Figura 1. Comparação entre resultados obtidos para 28 elementos e valores de referência em MRC, Ln não incluídos dada a ausência de valores de referência.
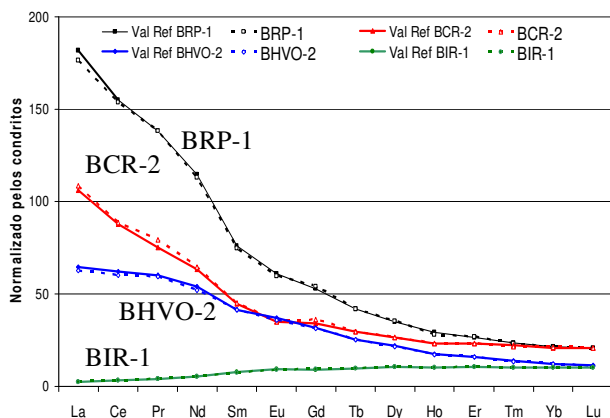
Figura 2. Valores de referência (Val Ref, linha cheia) e dados obtidos (pontilhada) para Ln normalizados (Anders e Grevesse, 1989).

Os resultados de Ln em SRM 1640 e em 5 amostras de águas superficiais coletadas em drenagens da Mata Santa Genebra (Campinas, SP), encontram-se na Fig. 3. A maioria das águas das drenagens apresenta um padrão plano com anomalias de Ce e Eu e pequeno fracionamento em relação ao MUQ. O MUQ é definido pela média de 25 sedimentos australianos (Kamber *et al*. 2005). A amostra CS 8 apresenta os mais baixos valores determinados (ΣLn= 0,07 ppb), sendo estes semelhantes aos tipicamente observados em águas de estuários (ΣLn= 0,10 ppb).

A amostra CS 8 apresenta uma anomalia positiva de Gd, que pode estar associada ao lançamento de efluentes que contêm compostos usados para contraste em exames de ressonância magnética, no qual Gd-DTPA é ministrado aos pacientes. O SRM 1640 apresenta um padrão suave de Ln com as maiores concentrações totais (ΣLn= 1,62 ppb) e relativo enriquecimento de Ln leves, mas uma anomalia negativa de Ce.
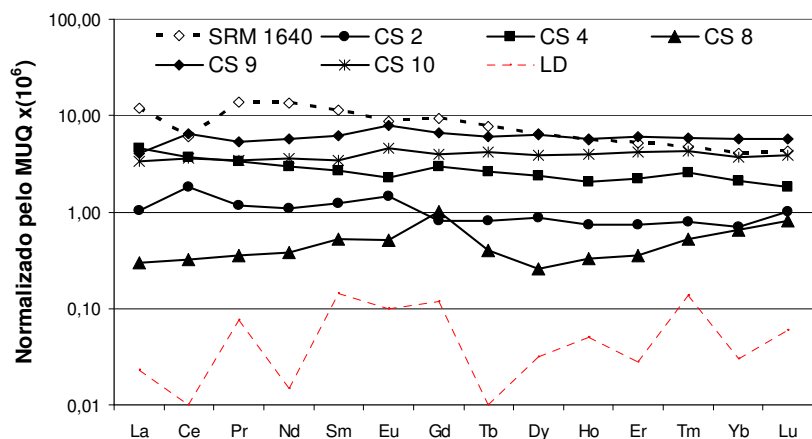
Figura 3. Diagrama de Ln de águas superficiais (CS 02 a 10), do material de referência SRM 1640 e limites de detecção (LD) normalizados ao MUQ.

As concentrações encontradas próximos ao LD, explicam a baixa precisão dos dados, entre 10 e 20 %. Esta pode ser melhorada empregando-se maiores tempos de integração (p. ex., 40 ms ao invés de 20 ms) e um maior número varreduras por medida. Nas condições usadas, o LD é de aproximadamente 1 ppt para La e Ce e decresce até 0,05 ppt para Yb e Lu.

CONCLUSÕES

No atual estágio de desenvolvimento deste método analítico é possível determinar todos os elementos-traço, aqui referidos, com limites de detecção apropriados para estudos hidrogeoquímicos e ambientais.

REFERÊNCIAS

Anders E. e Grevesse N. 1989. Abundances of the elements: Meteoritic and solar. *Geochim. Cosmochim. Acta,* **53**, 197-214.

CONAMA (Conselho Nacional do Meio Ambiente) Resolução Nº 396, 2008, 11 pp.

Cotta A. J. B. e Enzweiler J. 2008. Análise de águas em ICP-MS e melhoria dos limites de detecção de ferro, arsênio e selênio com o uso de cela de colisão/reação. In: Congr. Bras. Geol., 44, Curitiba, Anais, **1**: 353-355.

Cotta A. J. B. e Enzweiler J. 2009. Quantification of major and trace elements in water samples by ICP-MS and collision cell to attenuate Ar and Cl-based polyatomic íons. *J. Anal. At. Spectrom.*, submetido.

Hall G. E. M., Vaive J. E. e Pelchat J. 1996. Performance of Inductively Coupled Plasma Mass Spectrometric Methods Used in the Determination of Trace Elements in Surface Waters in Hydrogeochemical Surveys. *J. Anal. At. Spectrom.*, **11**, 779-786.

Kamber B. S., Greig A. e Collerson K. D. 2005. A new estimate for the composition of weathered young upper continental crust from alluvial sediments, Queensland, Australia. *Geochimica et Cosmochimica Acta*, **69**, 1041-1058.

Lawrence M. G., Greig A., Collerson K. D., e Kamber B. S. 2006. Direct quantification of rare earth element concentrations in natural waters by ICP-MS. *Appl. Geochem.*, **21**, 839-848.

US Environmental Protection Agency, USEPA Method 6020A, Revision 5.4 US EPA, USA, 1994.

Aqui resultados complementares obtidos para SLRS-4 e SLWE-3 (MR de água de rio e estuário, respectivamente, preparados pelo NRCC) e algumas amostras são apresentados. Estes MR não possuem valores certificados para os lantanédeos (Ln), apenas valores propostos por Yeghicheyan *et al.* (2001) e Lawrence *et al.* (2006 e 2007) são conhecidos e foram utilizados para comparação.

As baixas concentrações nas quais os Ln são encontrados em águas não contaminadas implicam num desafio analítico, mesmo para uma técnica sensível como a ICP-MS. A semelhança do que é feito na geoquímica de rochas, os padrões normalizados dos Ln em águas podem ser usados para investigar processos hidrogeoquímicos (Johannesson *et al.* 1997, Dia *et al.* 2000, Johannesson 1999) e a magnitude da contribuição antrópica (Möller *et al.* 2000).

A formação de óxidos e hidróxidos de Ba e Ln leves interfere na determinação dos Ln médios e pesados. Inicialmente investigou-se o uso da CC na atenuação de tais interferentes, apesar do uso da cela (com fluxo de gás de 4 ml/min e KED) reduzir a taxa de óxidos, CeO^+/Ce^+ de 1,5 % para 1,0 %, isso não elimina a necessidade correções matemáticas. Por isso, optou-se por determinar os Ln em condição padrão, por oferecer maior sensibilidade.

A correção das interferências, Tabela 1, foi efetuada com equações matemáticas conforme proposto por Raut *et al.* (2003 e 2005). A subtração das contribuições de $^{135}Ba^{16}O^+$ e $^{134}Ba^{16}O^1H^+$ sobre o $^{151}Eu^+$ recebeu atenção especial, uma vez que diferentemente do encontrado em rochas, a razão Ba/Eu em águas é tipicamente maior que 1.000, o que implica em correções bastante elevadas que precisam ser estabelecidas diariamente. Para os demais Ln as correções podem alcançar 15% do sinal registrado, mas em geral estão abaixo de 10%. É mostrado na Tabela 2 que a determinação de Gd com seu isótopo de massa 160 é, no geral, menos afetada que a do isótopo 157, e que para o ^{151}Eu as interferências são bastante intensas.

Tabela 1. Lista de interferentes corrigidos matematicamente

Isótopo	Interferentes
$^{151}Eu^+$	$^{135}Ba^{16}O^+$, $^{134}Ba^{16}O^1H^+$
$^{159}Tb^+$	$^{143}Nd^{16}O^+$, $^{142}Ce^{16}O^1H^+$, $^{142}Nd^{16}O^1H^+$
$^{160}Gd^+$	$^{144}Nd^{16}O^+$, $^{144}Sm^{16}O^+$, $^{143}Nd^{16}O^1H^+$
$^{163}Dy^+$	$^{147}Sm^{16}O^+$, $^{146}Nd^{16}O^1H^+$
$^{165}Ho^+$	$^{149}Sm^{16}O^+$, $^{148}Nd^{16}O^1H$, $^{148}Sm^{16}O^1H^+$
$^{166}Er^+$	$^{150}Nd^{16}O^+$, $^{150}Sm^{16}O^+$, $^{149}Sm^{16}O^1H^+$
$^{169}Tm^+$	$^{153}Eu^{16}O^+$, $^{152}Sm^{16}O^1H^+$
$^{172}Yb^+$	$^{156}Gd^{16}O^+$, $^{155}Gd^{16}O^1H^+$
$^{175}Lu^+$	$^{159}Tb^{16}O^+$, $^{158}Gd^{16}O^1H^+$

Tabela 2. Razão entre concentrações obtidas sem e com correção dos interferentes para alguns Ln em amostras com diversas graus de fracionamento (La/Yb) e razões Ba/Eu

La/Yb	Ba / Eu	^{151}Eu	^{157}Gd	^{160}Gd	^{159}Tb	^{172}Yb
12,5	159	1,01	1,10	1,04	1,04	1,07
21,5	1.571	1,15	1,18	1,07	1,08	1,06
8,6	22.416	3,3	1,05	1,03	1,01	1,09
8,5	30.895	4,0	1,04	1,10	1,02	1,06
9,6	51.444	6,0	1,00	1,02	1,00	1,06
33,5	103.339	10,3	1,08	1,03	1,05	1,15

Na Figura 1 (a) os valores obtidos são comparados aos publicados para SLRS-4. O padrão obtido é suave e concordante (± 8 %) com valores conhecidos. A Figura 1(b) contém os padrões obtidos para o SLRS-4 sem diluição, diluído 10 e 50 vezes e os LD calculados a partir de análises do branco (HNO_3 1%). Em cada padrão também é dado o somatório das concentrações dos Ln (ΣLn). A precisão variou entre 5 e 10 %, 5-15% e 10-50% para a amostra não diluída, diluída 10 vezes e diluída 50 vezes, respectivamente. Nesta última, dada à proximidade aos LD a precisão é pobre, porém o padrão ainda pode ser reproduzido. Por isso, estabeleceu-se como limite "prático" de detecção (LPD) que resultados acima da linha 0,1 no gráfico normalizado estão acima do LPD e quando abaixo de 0,1 estes não podem ser determinados adequadamente, nas condições utilizadas.
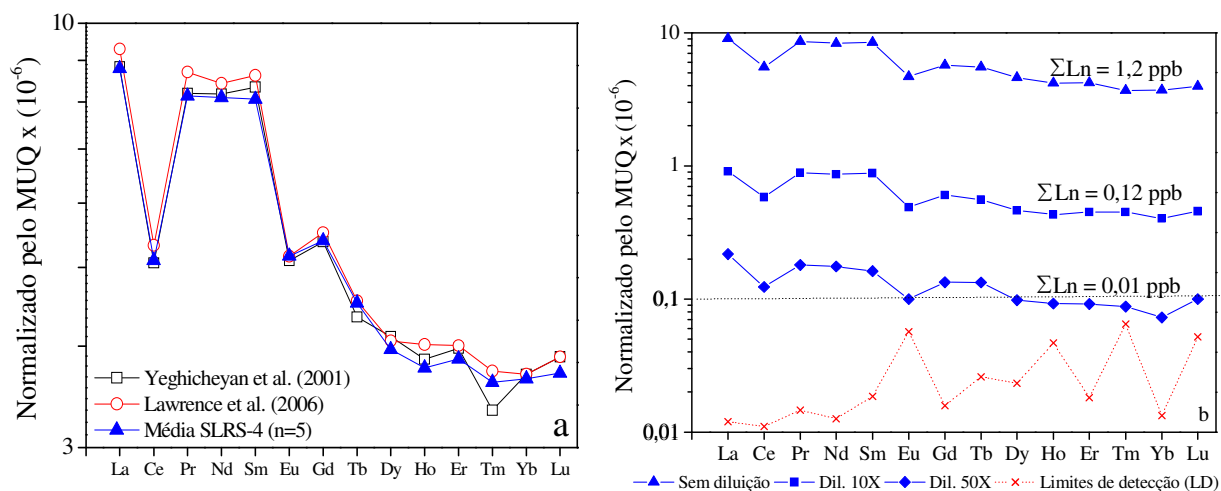
Figura 1. Comparação entre resultados obtidos e conhecidos para SLRS-4 (a) e teste de reprodução do padrão de Ln para baixas concentrações (n=3) e LD (b).

A Figura 2 (a) contém exemplos que mostram que os LPD alcançados são suficientemente baixos para a determinação dos Ln em águas diversas, como da região serrana do Rio de Janeiro (RJ), de poço da Mata Santa Genebra, Campinas/SP (Poço MSG), de drenagem após percorrer a MSG (MSG-2) e de uma torneira do Instituto de Geociências (IG), UNICAMP. As amostras apresentam padrões distintos com anomalias de Ce e Eu e pequeno fracionamento em relação ao MUQ (Kamber *et al*. 2005).

Para a amostra Poço MSG a razão Ba/Eu é de aprox. 1.500 o que implica numa interferência de 15% sobre [151]Eu e para a MSG-2 a sobreposição corresponde a 80%, esta amostra apresenta expressiva anomalia positiva de Gd (observada em ambos isótopos monitorados) que pode estar associada ao lançamento de efluentes contendo o complexo Gd-

DTPA, o qual é ministrado aos pacientes para contraste em exames de ressonância magnética. Uma anomalia menos intensa também foi observada na água do IG. O SLEW-3 foi analisado (após diluição de 3 vezes), Fig. 2 (b), para testar a eficácia das correções em amostras com elevada razão Ba/Eu, este MR não é certificado para Ln, mas valores foram publicados por Lawrence *et al*. (2007), o qual procedeu com a separação/concentração dos Ln antes das determinações por ICP-MS. Os resultados de Eu, e outros Ln pesados, são concordantes, mas La, Ce, Pr e Sm estão abaixo do LPD.
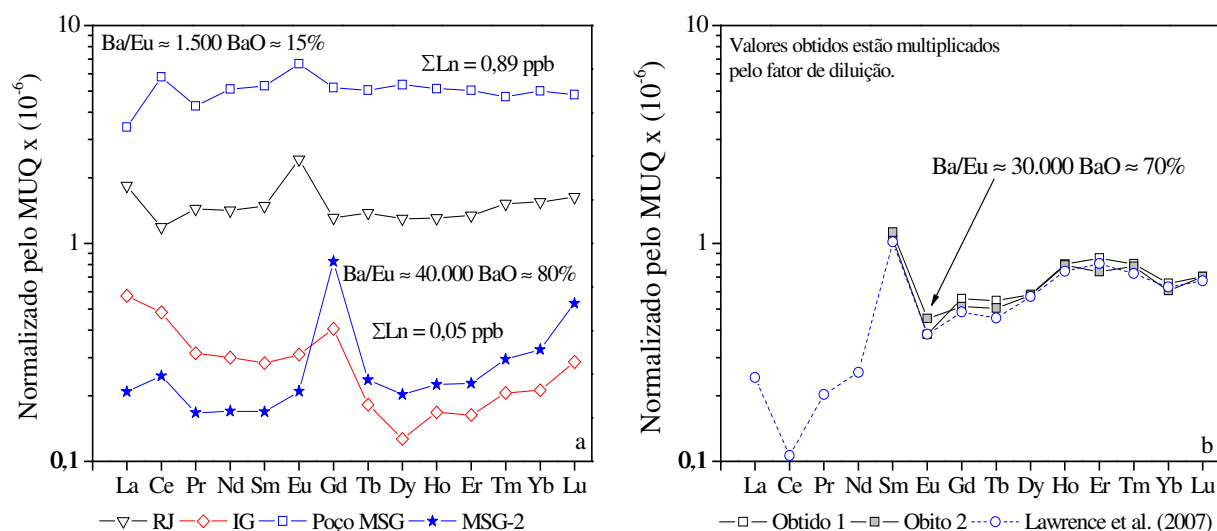
Figura 2. Padrões normalizados de Ln em águas de diversas localidades (a) e para SLEW-3 (b). As amostras foram filtradas em membrana de 0,45 µm e acidificadas com HNO₃ purificado. Segundo Lawrence *et al*. (2007), SLEW-3 foi contaminado com Sm durante a coleta.

Em síntese os baixos LPD alcançados permitem a determinação direta dos Ln em diversa águas. Com a inclusão dos Ln e com o aumento do número de varreduras por medida (de 30 para 60) o tempo de análise passou de 2 para aprox. 5 minutos/amostra. As interferências poliatômicas sobre os Ln foram devidamente corrigidas, mesmo nos casos mais difíceis. O método se mostra aplicável à análise de águas doces cobrindo uma ampla faixa de ΣLn. Para baixas concentrações (*i.e.* padrão próximo a linha 0,1 do gráfico normalizado) e/ou amostras de matriz complexa técnicas de pré-concentração/separação devem ser aplicadas, nestes casos, o método apresentado é apenas investigativo.

ANEXO III

Artigo aceito para publicação: Cotta AJB e Enzweler J.

Classical and new procedures of whole rock dissolution for trace elements analysis by ICP-MS. *Geostandard and Geoanalytical Research*.

Classical and new procedures of whole rock dissolution for trace elements determination by ICP-MS

Aloísio J.B. **Cotta** and Jacinta **Enzweiler***
Instituto de Geociências
Universidade Estadual de Campinas - UNICAMP, C.P. 6152
CEP 13083-970 Campinas, SP, Brazil
* Corresponding author. e-mail: jacinta@ige.unicamp.br

Abstract

Sample digestion is a critical stage in the process of chemical analysis of geological materials by ICP-MS. We present a new HF/HNO_3 procedure to dissolve silicate rock samples using a High Pressure Asher-System (HPA-S). The formation of insoluble AlF_3 was the major obstacle to achieve full recoveries. This was overcome by setting appropriate digestion temperature and adding Mg to the samples before digestion. The sodium peroxide sintering was also investigated and a heating step of the alkaline sinter solution improved the recoveries of thirteen elements other than lanthanides. The results of these procedures were compared with data sets generated by other common acid decomposition techniques. Forty one trace elements were determined using an ICP-QMS equipped with collision cell. Under optimum conditions of gas flow and kinetic energy discrimination, polyatomic interferences were eliminated or attenuated. The measurement bias obtained for eight reference materials (BCR-2, BHVO-2, BIR-1, BRP-1, OU-6, GSP-2, GSR-1 and RGM-1) was generally better than ±5% and intermediate precision was of the same order. The expanded measurement uncertainties estimated for common acid dissolutions was between 7 and 15%, mostly. New data sets for RM are provided, including constituents with unavailable reference values and also for the USGS candidate reference material G-3.

Introduction

Inductively coupled plasma mass spectrometry with quadrupole mass filter (ICP-QMS) is the dominant multi-element analytical technique used to determine trace and sub-trace elements in geological samples because it is able to cover most of the relevant analytes like lanthanides (Ln), high field strength elements (HFSE = Zr, Nb, Hf, Ta, Th and U), in a single run. The low detection limits, isotope ratio measurement capability, high sample throughput and relative cost-effective analysis are the main strengths of ICP-MS. However, the introduction of sample via nebulization system requires the complete dissolution of the test portion. As a result, the sample preparation step may be the main constrain in terms of time of analysis and accuracy of results. Even so, sample dissolution allows representativeness concerning the mass of the test portions, which is important due to the intrinsic heterogeneity of geological materials.

The generalized use of ICP-MS for the analysis of geological matrices brought to light many old and new aspects related to the complete recovery of analytes. As a result, the main sample digestion procedures were revisited, improved and also innovated during the last two decades.

The complete dissolution of some rock matrices is difficult when resistant minerals are present, such as garnet, sphene, spinel, zircon, rutile and chromite. Total digestion of samples containing such phases can be achieved by acid attack in sealed polytetrafluoroethylene (PTFE) bombs at high temperatures (> 160 °C) for several days (Yu *et al.* 2001, Révillon *et al.* 2009). Several acid mixtures have already been tested, like HF/HNO$_3$ (Eggins *et al.* 1997, Robinson *et al.* 1999, Liang *et al.* 2000, Jain *et al.* 2001, Takei *et al.* 2001, Raut *et al.* 2003), HF/HClO$_4$ (Jarvis 1990, Totland *et al.* 1992, Yokoyama *et al.* 1999, Yu *et al.* 2000, Dulski 2001, Raczek *et*

al. 2001, Makishima and Nakamura 2006, Nakamura and Chang 2007), HF/H_2SO_4 (Totland *et al.* 1992, Chao and Sanzolone 1992, Yu *et al.* 2001) and $HF/HBr/HNO_3$ (Makishima and Nakamura 2001, Makishima *et al.* 2002). In order to avoid the use of HF, Hu *et al.* (2010) demonstrated that a combination of NH_4F and HNO_3 is effective to dissolve granite samples. The use of H_2SO_4 is generally unadvisable because it prolongs the evaporation time, tends to precipitate Sr, Ba and Pb sulfates and may cause the hydrolysis of Th, Ta and Nb (Münker 1998, Yu *et al.* 2001). Pretorius *et al.* (2006) and Révillon *et al.* (2009) advocated that the tri-acid mixtures $HF/HNO_3/HClO_4$ dissolve granitoid and sediment samples more efficiently than HF/HNO_3, but Pretorius *et al.* (2006) reported that recoveries were higher for some elements (e.g. Sn, Ga, Rb and Zr) when perchloric acid is absent in the digestion mixture. The addition of $HClO_4$ produces a more efficient attack of refractory minerals, like those of the spinel group, and improves the removal of fluorides (Kato *et al.* 1998, Robinson *et al.* 1999, Yokoyama *et al.* 1999). However, the complete elimination of HF can induce the polymerization and hydrolysis some of the HFSE, if they are not stabilized in solution as F^- or Cl^- complexes. Therefore, Münker (1998) suggested the stabilization of HFSE using HCl after the evaporations stages with $HClO_4$.

In addition to difficulties related to the dissolution of resistant minerals and the stabilization of the elements in the solution, the formation of insoluble fluorides, which incorporate large proportions of trace elements, represent another drawback of acid digestions (Yokoyama *et al.* 1999). Takei *et al.* (2001) observed that the precipitation of fluorides, during HF/HNO_3 sample dissolution (205 ºC, 2 days), is controlled by the relative proportions of Al:Mg:Ca, in particular the $[(Mg+Ca)/Al]_M$ ratio of the sample. In further tests, Takei *et al.* (2001) demonstrated that AlF_3 is the most resistant fluoride formed during high-T digestion of andesites and rhyolites and that, unlike other decomposable fluorides (as MgF_2, $CaAlF_5$ and ralstonite: $CaMg_2Al_2F_{12}$), it persists even after two evaporation steps with $HClO_4$. According to

Takei *et al.* (2001), the addition of Mg to the sample to produce $[(Mg+Ca)/Al]_M \approx 1$ suppresses the formation of AlF_3. That ratio of major alkaline earth elements to aluminum favors the formation of decomposable fluorides, e.g., ralstonite, which consumes the dissolved Al preventing the precipitation of AlF_3. Alternatively, Navarro *et al.* (2008) and Hu *et al.* (2010) reported that the formation of such insoluble phases is avoided when small quantities of sample (40 and 50 mg, respectively) are dissolved and the digestion mixture is not allowed to dry completely during evaporations. However, Takei *et al.* (2001) reported the formation of AlF_3 during the decomposition of test portions as small as 20 mg. Additionally, the use of very small test portions is not recommended, because few reference materials (RM) have their homogeneity tested at the milligram scale (Cotta *et al.* 2007) and real samples are not expected to be more homogeneous than RM.

The formation of insoluble fluorides and the coprecipitation of trace elements when small test portions (8-40 mg) are dissolved were also investigated by Makishima *et al.* (2002). These authors explained the selective retention of Cu, Cr, Ni and Zn based on similarities of charge, ionic radius and preferential co-ordination number in Mg and Al fluorides. The dissolution of basaltic rock samples is generally non-affected by the formation of AlF_3 because they naturally contain favorable $[(Ca+Mg)/Al]_M$ (Robinson *et al.* 1999, Takei *et al.* 2001). Additionally, the absence of refractory phases exempts the use of very high temperatures and pressures.

Microwave-assisted dissolution procedures of geological samples are insufficiently energetic to digest refractory phases, resulting in incomplete recoveries of associated trace elements (Totland *et al.* 1992 and 1995, Sen Gupta and Bertrand 1995, Wu *et al.* 1996, Yang *et al.* 1998, Yu *et al.* 2001, Makishima *et al.* 2002). Thereby its applicability seems restricted to dissolve basalts (Navarro *et al.* 2008) or in some environmental applications, where fast dissolutions are aimed and complete recovery is not required.

Acid digestion using drastic conditions (up to 320 ºC and at 130 bar) can be safely performed with a commercial apparatus (High Pressure Asher System, HPA-S, from Anton Paar, Austria). The application of HNO_3 or HCl/HNO_3 mixtures with HPA-S to decompose biological materials and for the dissolution of platinum group elements (PGE) in geological samples is well documented (Amarasiriwardena *et al.* 1994, Müller and Heumann 2000, Meisel *et al.* 2001, Paliulionyte *et al.* 2006). The use of such high pressure system to fully dissolve rock samples, with HF and ultimately to quantify REE and HFSE has not been reported yet. Here, we describe the development of a digestion procedure using HPA-S that enables faster dissolution of samples containing refractory phases, which otherwise require several days to digest in PTFE bombs.

Alternatives to the acid dissolution are fusion and sintering procedures. These are frequently applied to samples containing resistant minerals. Fusion of silicate samples with $LiBO_2/Li_2B_4O_7$ results in the formation of a glass readily soluble in dilute nitric and hydrochloric acids (Cremer and Schlocker 1976, Feldman 1983). The presence of Si and the large amount of flux demand a high dilution factor to keep the total content of dissolved solids of the final solution below the ICP-MS instrument requirements. Si and B can be partially eliminated as volatile SiF_4 and HBF_4 during evaporations with HF (Yu *et al.* 2001, Panteeva *et al.* 2003, Awaji *et al.* 2006). To circumvent matrix effects during analysis in the ICP-MS, external calibration is better performed with matched certified reference materials (CRM) (Balaram *et al.* 1995, Awaji *et al.* 2006, Madinabeitia *et al.* 2008). The main drawbacks of the fusion are severe polyatomic interferences on several isotopes (e.g. $^{28}Si^{16}O^1H^+$ and $^{29}Si^{16}O^+$ on $^{45}Sc^+$ and also B-based oxides, Wu *et al.* 1996), partial loss of volatile elements, as Pb, Sb, Sn, Zn and Cs (Totland *et al.* 1992) and contamination of the ICP-MS with Li and B (Münker 1998, Roy *et al.* 2007).

The sintering or fusion with sodium peroxide offers some advantages over the fusion with lithium borate compounds. For instance, the lower temperature minimizes losses by

volatilization, Na_2O_2 decomposes to $NaOH$ and H_2O_2 and does not introduce elements that cause significant instrument memory effects (Meisel *et al.* 2002). The sinter is readily dissolved in water, which leads to the precipitation of Fe and Ti hydroxides and to the co-precipitation of many traces elements (Ln and others). This allows their separation from solution matrix with high sodium and silica contents (Robinson *et al.* 1986, Longerich *et al.* 1990, Kleinhanns *et al.* 2002). With this procedure, most geological samples can be completely decomposed providing fast analysis for Ln, Sc and Y, but the HFSE cannot be measured due to incomplete co-precipitation (Yu *et al.* 2001). To circumvent this problem, Duan *et al.* (2002) proposed the addition of small amount of Ti and Fe to the test portion before fusion with Na_2O_2 and $NaOH$, and after cooling, the melt is dissolved in water and the solution is heated to boiling to decompose H_2O_2. This heating step favors the complete precipitation of $Ti(OH)_4$ and $Fe(OH)_3$, and hence improves the co-precipitation of the HFSE. However, Bayon *et al.* (2009) reported incomplete recovery for Nb and Ta with this procedure. Differently from the above, Meisel *et al.* (2002) mixed the solution obtained through acid dissolution of hydroxides with the supernatant and so was able to measure the Ln, HFSE and other elements.

Although ICP-QMS instruments have experienced significant improvements, like the incorporation of the collision cells (Turner *et al.* 1997) and the development of new skimmer cones (Nelms 2005), the sample dissolution procedures did not evolve at the same pace. The aim of this work is to explore the high temperature and pressure provided by the HPA-S to develop a new, fast and effective digestion procedure for rock samples, especially for granites, for which the classical acid dissolution is very time consuming. The sintering procedure was investigated and modified, after Duan *et al.* (2002), aiming to improve the co-precipitation of trace elements. For comparison with the developed procedures, the HF/HNO_3 acid digestion (in closed PFA vessels and PTFE bombs) was also used for the determination of forty-one trace elements by

ICP-QMS equipped with a collision cell (CC). The benefit of measuring Sc, V, Cr, Co, Ni, Cu, Zn and Sr in CC mode is investigated. Results obtained for eight RM are compared with the reference values and the measurement uncertainty calculated for two CRM materials, following the `top-down' approach of NORDTEST (2004).

Experimental

Reagents and apparatus

Hydrofluoric (48% m/m, reagent A.C.S., Merck) and perchloric acids (70% m/m, reagent A.C.S., Merck) were distilled in a PFA sub-boiling (Savillex) system, while nitric (65% m/m, reagent A.C.S., Merck) and hydrochloric acids (37% m/m, reagent A.C.S., Merck) were distilled in a quartz sub-boiling distillation system (DuoPur, Milestone, Italy). Water used was always ultra pure obtained using Elix and Milli-Q systems in tandem (Millipore, USA). Granular Na_2O_2 ($\geq$ 95% m/m, pure, Fluka, France) was pulverized in an agate ball jar and used for sample sintering in glassy carbon crucibles (Sigradur, Germany). Single element standard solutions, (10.00 ± 0.03 $\mu g\ ml^{-1}$, High Purity Standards, USA) were gravimetrically combined to prepare two multi-element solutions, Cal-1 and Cal-2, in FEP bottles. The constituents of each solution were defined based on element stability and their concentrations were designed to mimic crustal abundance. Cal-1 contains elements stabilized in 2% HNO_3 while Cal-2 contains the elements (Zr, Nb, Mo, Sn, Sb, Hf, Ta and W) that demand the addition of trace amount of HF ($\approx 0.01\%$) in 2% HNO_3 for stabilization. In and Re solutions (High Purity Standards), were used as internal standards. TiO_2 (99.995%) and Fe_2O_3 (99.998%, Puratronic, Alfa Aesar, USA), were used in complementary tests in the sintering procedure. About 500 mg of MgO (99.998%, Puratronic, Alfa Aesar, USA), was dissolved in 15 ml of 10% HNO_3 and used for HPA-S digestions. In other

tests the solid MgO was used directly. Plastic containers, pipette tips and tubes were cleaned with a mixture of 8% HNO_3 + 2% HCl and rinsed with water. All weighing were performed with an analytical balance (Sartorius, Germany). The static electricity of the PFA and PTFE vessels was removed using an antistatic gun (Zerostat[®], SPI Supplies, USA).

Reference materials

Six RM from USGS (basalts: BCR-2, BHVO-2, BIR-1, rhyolite: RGM-1, granodiorite: GSP-2 and the candidate granite RM G-3), a granite (GSR-1) from Institute of Geophysical and Geochemical Exploration (IGGE, China) and the CRM produced by IAG (slate: OU-6, Kane (2004)) and by a joint project between Brazilian institutions and the USGS (basalt: BRP-1, Cotta and Enzweiler (2008)), were analyzed in this study. The effectiveness of the HPA-S for rapid dissolution of rocks was tested using granitic RM (GSR-1 and GSP-2). BCR-2 and BRP-1 were also analyzed to test the influence of basaltic composition in the formation of the insoluble phases.

Several terms (e.g. certified, uncertified, consensus, accepted, recommended, informative, and preferred) have been used to describe the concentration values of CRM or RM. ISO Guide 30 (1992) is under revision and is expected to contain definitions for the first three referred terms. In present work we will use a general "reference value" (VIM 2008), but will maintain the original term used by the RM producer or calculated in compilations, in the notes of the tables. In the absence of an assigned value, some published data were used for comparison.

Sample decomposition

Different decomposition procedures were tested and applied to the reference materials. Before use, the RM were homogenized by inverting and rolling each container. Small portions were taken and dried at 110 °C for 2 hours and results are expressed on dry basis.

Sintering

For sintering, 100 mg of sample and 500 mg of pulverized Na_2O_2 were weighed in glassy carbon crucibles, thoroughly mixed and heated for 30 minutes at 480 ºC. Upon cooling, water was added drop-wise until the vigorous reaction ceased. The solution with the (Fe,Ti)-hydroxide precipitate was carefully transferred to a centrifuge tube, centrifuged (at 4.000 rpm for 10 minutes) and the supernatant discharged to remove soluble components, mainly sodium and silicon. The precipitate was dissolved by adding first 10 ml of water and then 2 ml of HNO_3 plus 1 drop of HF and completed to 20.0 g with water. With this procedure some analytes of interest (e.g. HFSE) were not quantitatively co-precipitated. Therefore a heating step (1 hour at ~130 ºC) after the dissolution of the sinter with water and the addition of Fe and Ti to the sample, by spiking the Na_2O_2 (2 mg of each/500 mg of Na_2O_2), as reported by Duan *et al.* (2002), were investigated in order to achieve quantitative co-precipitation of extra analytes. The differences among the sintering procedures are outlined in Figure 1.
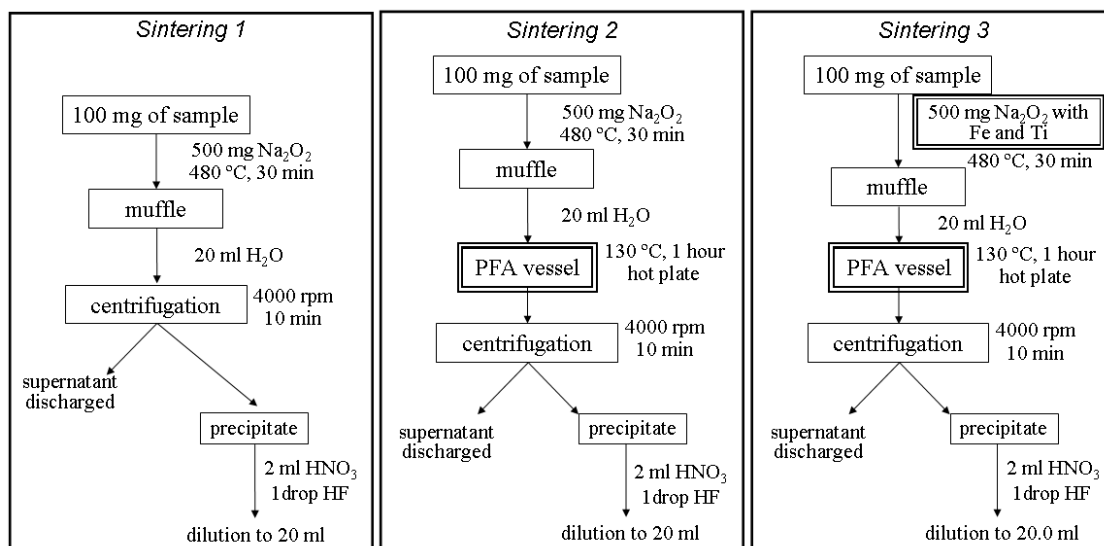
Figure 1. Flow charts illustrating the tested sintering procedures. The double border boxes highlight the differences among the procedures.

Acid decomposition

Three different acid decomposition procedures were used in this study. In all cases, the test portions of each RM were directly weighed in the digestion containers, and attacked with a mixture of 0.5 ml HNO_3 and 2 ml of HF.

Table-top procedure

One hundred milligrams of basaltic RM were dissolved using PFA vessels of 60 ml (Savillex, PN: 301-060-01-058-04). The vessels with the test portion and the HF/HNO_3 mixture were closed using the spanner wrench set and heated on hot plate at 130 °C for at least 2 hours. After digestion, the solution was evaporated to near dryness and two aliquots of 1 ml of HNO_3 were sequentially added and evaporated. Nitric acid (2 ml) and water (2 ml) were used to take up the residue. The vessels were closed again and heated for 1 hour to obtain a clear solution. After cooling, the solution was gravimetrically diluted with water to 20.0 g in a clean LPDE centrifuge tube.

Bomb procedure

To dissolve samples other than basalts acid digestions bombs with 23 ml PTFE cups (Parr Instrument Company, USA) were used. The test portion (100 mg) was weighed and the HF/HNO_3 mixture was added to the PTFE cup. The cup and its cover were sealed with PTFE tape. The set was inserted in a stainless steal "jacket", closed and heated on a hot plate for 4 days at 180 ºC. Upon cooling, $HClO_4$ (0.5 ml) was added to the solution and evaporated at 150 ºC to
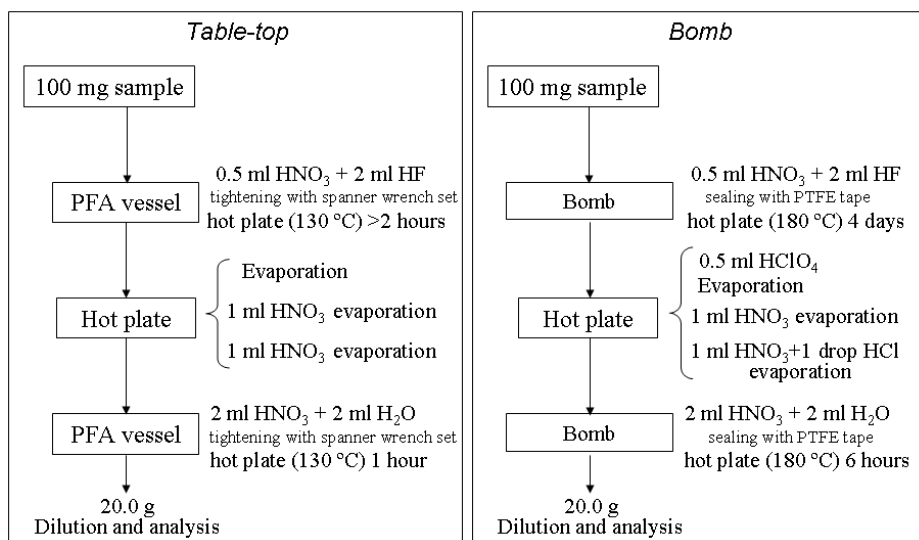
near dryness (about 4 hours). Portions of 1 ml of HNO_3 and 1 ml of HNO_3 plus a 1 drop of HCl were sequentially added and evaporated at 130 ºC. The use of HCl was intended to improve the stabilization of HFSE, Sb, Sn and Cs and other elements after $HClO_4$ evaporation (Münker 1998, Yu *et al.* 2000, Duslki 2001), the final amount of chloride was intentionally maintained at a low level to minimize the formation of Cl-based polyatomic interferences. In order to obtain a clear solution, the residue was taken up in 2 ml of HNO_3 and 2 ml of water, the lid sealed again with tape, the bomb assembled and additionally heated for at least 6 hours at 180 ºC. Liang *et al.* (2000) demonstrated that this second stage of heating is essential to obtain full recoveries of trace elements that otherwise may be retained as persistent fluorides. Sample solutions were subsequently diluted with water to 20.0 g. The Table-top and Bomb procedures are schematized in Figure 2.

Figure 2. Flow chart illustrating the Table-top and Bomb procedures.

HPA-S procedures

For the dissolution using the HPA-S, test portions were weighed directly into glassy carbon tubes and digested using the HF/HNO_3 mixture for 3 hours at 130 bar. Three different digestion temperatures combined with four processing schemes were tested in order to obtain complete recoveries (Table 1). The modifications in the processing involved the acids used to drive off the HF during the evaporation stage and the addition of Mg before digestion.

After decomposition in HPA-S, the sample solution was transferred to a PFA vessel, the digestion tube was rinsed with few milliliters of water, which were added to the PFA vessel content. In procedure HPA-S 1 the sample processing scheme followed the Table-top procedure, using only HNO_3. However, even with an extended taking up time and increasing the hot plate temperature to 180 ℃, a white precipitate was not entirely dissolved.

Table 1.Details of the sample processing scheme after dissolution in HPA-S

Identification and conditions	Evaporation scheme	Test portion mass (mg)	Addition of Mg	Occurrence of precipitates
HPA-S 1 (260 ℃, 3 h)	Two aliquots of 1 ml of HNO_3	100	No	Yes
HPA-S 2 (260 ℃, 3 h)	One aliquot of 0.5 ml of $HClO_4$, followed by 1 ml HNO_3, and 1 ml HNO_3 + 1 drop of HCl	100	No	Yes
HPA-S 3 (260 ℃, 3 h)	Two aliquots of 0.5 ml of $HClO_4$, followed by 1 ml HNO_3 + 1 drop of HCl	100 and 50	Yes*, to obtain $[(Mg+Ca)/Al]_M \approx 2$	No
HPA-S 4a (200 ℃, 3h) HPA-S 4b (220 ℃, 3 h)	One aliquot of 0.5 ml of $HClO_4$, followed by 1 ml HNO_3, and 1 ml HNO_3 + 1 drop of HCl	50	Yes**, to obtain $[(Mg+Ca)/Al]_M \approx$ 1.1-1.5	No

* Mg was added to the test portion using a solution of 20.1 mg /l^{-1}, followed by drying on hot plate, before digestion.
** About 6-7 mg of high purity MgO was added directly to the test portion to avoid the drying step.

Given the difficulties in dissolving the precipitate, incomplete recoveries of many analytes (discussed bellow) were observed with procedure HPA-S 1. HPA-S 2 used an evaporation scheme similar to that described in the Bomb method, which includes $HClO_4$. Basaltic samples were also digested to check if the sample composition had any effect over the formation of

insoluble phases. After the evaporation step, the four samples (GSP-2, GSR-1, BRP-1 and BCR-2) presented white precipitates that remained even after the take up step. These residues were separated by centrifugation and analyzed by scanning electron microscopy (SEM) and X-ray diffraction (XRD). The solutions were analyzed even though.

In procedure HPA-S 3 magnesium was added to the samples (GSP-2 and GSR-1) before digestion to produce $[(Mg+Ca)/Al]_M \approx 2$, according Table 1. Test portions of 100 and 50 mg were evaluated. In the following experiments (HPA-S 4), the digestions were performed at 200 ºC (HPA-S 4a) and 220 ºC (HPA-S 4b). Test portions of 50 mg were used and required 6-7 mg of MgO. After the uptake step, the sample solution was diluted to 10.0 g with water.

Attenuation of polyatomic interferences with collision cell

The overlap of polyatomic ions over isotopes of target analytes imposes serious restrictions on some trace elements analyses by ICP-QMS (Tan and Horlick 1986, Epov *et al.* 2004). The incorporation of the collision cell (CC) technology by ICP-QMS instruments allows effective attenuation of several interfering ions, in particular those corresponding to the first line of transition elements (Leonhard *et al.* 2002, McCurdy and Woods 2004, Cotta and Enzweiler 2009). A collision cell consists of an enclosed multipole located before the mass analyzer that is pressurized to promote collisions between the added gas and the ions sampled from the plasma. Pure H_2, which is virtually non-reactive with most analytes (Eiden *et al.* 1996), and mixtures with He are the preferred gases used in CC because the generation of in-cell formed interferences and scattering are minimized (Feldmann *et al.* 1999, Dexter *et al.* 2002, Yamada *et al.* 2002, Niemelä *et al.* 2003). Du and Houk (2000) demonstrated that mixtures He/H_2 are also useful to attenuate MO^+ without forming the corresponding MOH^+. The selective removal of molecular species in a CC occurs because polyatomic ions have larger collision cross-section than single analyte ions and, hence, experience a larger number of collisions with the cell gas. Consequently, polyatomic species loose more kinetic energy than analyte ions and, therefore, can be discriminated with the placement of a potential barrier downstream the cell (e.g. by setting the quadrupole bias voltage at a potential more positive than the cell pole bias potential). This approach is known as kinetic energy discrimination (KED). Besides KED, other process can also contribute to remove interferences, one of them is the collision induced dissociation (Bandura *et al.* 2001, Tanner *et al.* 2002), but this is restricted to weakly bonded polyatomic ions.

Instrumental analysis

Measurements were performed using an ICP-QMS equipped with CC technology (*Xseries^{II}*, Thermo, Germany). The instrument settings are outlined in Table 2. The effect of cleaning and conditioning the nickel sample and skimmer cones is crucial to minimize instrumental drift and a detailed description of the instrument set up, including CC optimization is described in Cotta and Enzweiler (2009). Briefly, the instrument is first optimized in standard mode using a 1 µg l^{-1} tuning solution containing Li, Co, In, Ba, Ce, Th and U to obtain maximum signal intensity for ^{7}Li and ^{235}U with minimum formation of oxides and double charge species. When operating in CC mode the gas flow rate added to the cell is adjusted to provide less then 20 counts s^{-1} for ^{78}Ar$_2^+$ and maximum sensitivity for ^{59}Co$^+$ and ^{115}In$^+$. The decrease in the ^{78}Ar$_2^+$/^{115}In$^+$, versus the gas flow added to the cell, is also used to define the gas flow rate required to achieve the desired degree of interference attenuation.

Table 2. Typical settings of the ICP-MS and isotopes used for quantification

Incident power	1400 W
Extraction	-210 to -160 V
Plasma gas flow	13 l min^{-1}
Nebulizer flow	0.81 to 0.85 l min^{-1}
Dwell time	10 – 30 ms
Measurements	3 x 30 scans
Conditions	^{140}Ce^{16}O$^+$/^{140}Ce$^+$ < 2% and ^{137}Ba^{++}/^{137}Ba$^+$ < 3%
CC mode	
Isotopes	^{29}Si*, ^{49}Ti*, ^{45}Sc, ^{51}V, $^{52,\,(53)}$Cr, ^{59}Co, ^{60}Ni, ^{63}Cu, ^{66}Zn, ^{88}Sr, ^{115}In**
Hexapole bias	-17 V
Quadrupole bias	-14 V
7% H$_2$ in He	3.7 to 4.0 ml min^{-1}
Signal	^{115}In (1 µg l^{-1}) >20.000 cps and ^{78}Ar$_2$ < 20 cps
Standard mode	
Delay	20 seconds for pressure stabilization
Isotopes	^{7}Li, ^{9}Be, ^{71}Ga, ^{85}Rb, ^{89}Y, ^{90}Zr, ^{93}Nb, ^{95}Mo, ^{111}Cd, $^{118,\,(120)}$Sn, ^{121}Sb, ^{133}Cs, ^{137}Ba, ^{139}La, ^{140}Ce, ^{141}Pr, ^{143}Nd, ^{147}Sm, ^{151}Eu, $^{(157),160}$Gd, ^{159}Tb, ^{163}Dy, ^{165}Ho, ^{166}Er, ^{169}Tm, $^{172,\,(174)}$Yb, ^{175}Lu, ^{178}Hf, ^{181}Ta, ^{182}W, ^{185}Re**, ^{206,207,208}Pb, ^{232}Th, ^{238}U
Hexapole bias	-2 V
Quadrupole bias	0.3 V
Signal	^{115}In (1 µg l^{-1}) > 40.000 cps and ^{238}U (1 µg l^{-1}) > 80.000 cps

* used in mathematical corrections; ** internal standard; qualifier isotopes are indicated within parentheses.

In the established multi-mode method of analysis, isotopes susceptible to polyatomic interferences originating from sample matrix elements and argon (e.g. $^{40}Ar^{23}Na^+$ on $^{63}Cu^+$, $^{40}Ar^{48}Ti^+$ on $^{88}Sr^+$), acids ($^{35}Cl^{16}O^+$ on $^{51}V^+$, $^{35}Cl^{16}O^1H^+$ on $^{52}Cr^+$, $^{40}Ar^{19}F^+$ on $^{59}Co^+$) and/or affected by background ions are measured in CC mode employing pre-mixed 7% H_2 in He to attenuate such overlaps. The remaining analytes were measured in standard mode (Table 2). The change from CC to standard mode is automatically performed by the ICP-QMS software, and a short delay of 20 seconds was implemented after the measurements in CC mode to assure the stabilization of the pressure before analysis in standard mode.

After decomposition, one aliquot of the obtained solution was gravimetrically diluted with 1% HNO_3 within 24 hours before analysis. Internal standards (In and Re at 2 ng g^{-1}, in 1% HNO_3), to compensate for instrumental drift and matrix effects were added on-line using a Y connector. Sample and internal standards flows were adjusted to provide equal admission rates. The overall dilution factor of test portions was 5000 fold. The precision of the measured signal for internal standards in a single run was generally better than 1%. A rinse solution of 2% HNO_3 with trace amount of HF was aspirated between samples (McGinnis *et al.* 1997). The calibration of the instrument was performed using three standard solutions prepared from serial dilution (50, 10 and 3 times) of Cal-1 and Cal-2, which covers the expected range of concentrations in the investigated samples.

Correction of interferences

It has been well known that the oxides (and to a lesser extent hydroxides) of Ba and the light lanthanides (Ln) can cause interference problems with the heavier Ln (Jarvis 1990, Dulski 1994, Robinson *et al.* 1999). Generally, the most expressive interference occurs on Eu isotopes

due to typical high ratio Ba/Eu found in geological materials. For quantification the less abundant isotope ^{151}Eu was preferred over ^{153}Eu, because the interference of BaO and BaOH is less intense (Dulski 1994, Olive *et al.* 2000). Oxide and hydroxide interferences on Ln were subtracted according Raut *et al.* (2003). This procedure, which uses the rates of ThO$^+$/Th$^+$ and ThOH$^+$/Th$^+$ to normalize the previously determined production rate of Ba and Ln oxides and hydroxides, could be implemented because the rates in which such interferences form and behave are similar under the used instrumental conditions. Prior analyses, the CeO$^+$/Ce$^+$ was adjusted within 1.2 to 1.5% and it varied less than 10% during a whole analytical run. The mean rates of ThO$^+$/Th$^+$ and ThOH$^+$/Th$^+$, measured for calibration standards and samples, were used to recalculate the interference correction factors. These factors were converted in a mathematical correction and introduced in the software of the ICP-MS to subtract the interferences. The uncertainties associated to these corrections were minimized by the use of isotopes indicated by Raut *et al.* (2005). A similar correction procedure was applied to account for possible interference on ^{178}Hf, ^{181}Ta, ^{182}W and ^{185}Re originating from Dy, Ho Er and Tm oxides, but these corrections had a minor impact since such overlaps, generally, correspond to less than 2% of the analytes signal. Although the operation of CC has proven effective to eliminate Ar-based polyatomics (e.g. ^{40}Ar^{23}Na), mathematical corrections were implemented for ^{45}Sc, ^{63}Cu and ^{66}Zn isotopes measured in CC mode, to account for interferences coming from oxides and hydroxides of Si (^{29}Si^{16}O and ^{28}Si^{16}O^{1}H) and of Ti (^{47,50}Ti^{16}O and ^{46,49}Ti^{16}O^{1}H), which were only partially attenuated in the CC measuring mode. The overlap of ^{141}Pr^{2+} and ^{142}Ce^{2+} over ^{71}Ga was also mathematically subtracted. The overlap of ^{115}Sn on the ^{115}In was subtracted mathematically using the signal of ^{118}Sn.

Internal and external standardization

Selecting a suitable set of internal standards for routine analysis of geological samples, which are not present in the sample, do not suffer from interference and efficiently correct analyte signal for drift and matrix effects, is often difficult, specially when numerous analytes are measured. Therefore the options for internal standardization are restricted to few elements. Robinson (1999) and Yu *et al.* (2000) compared the use of just one against four internal standards (^{84}Sr, ^{115}In, ^{185}Re, ^{209}Bi) and concluded that a single internal standard (^{115}In) is sufficient for accurate trace elements using a HR-ICP-MS. However, Eggins *et al.* (1997) found that one internal standard is unsatisfactory for rock analysis using an ICP-QMS instrument, and proposed a combination of internal and external standardization procedures. An external standardization technique, as reported by Eggins *et al.* (1997), was applied to correct for element specific drift. This correction involves the systematic measurement of a solution after the calibration and again every 5-10 samples. A RM, identified as monitor solution, was spiked using Cal-1 and Cal-2 to assure sufficient signal to all isotopes, and used for external standardization. A RM was preferred over a synthetic solution containing trace elements in 1% HNO_3, to better match real samples.

In this study a dual-mode method of analysis was employed with a single internal standard used for a group of analytes. The internal standards were selected in order to be close to the masses of the isotopes used for quantification. For middle mass elements (*m/z* from 45 to 88) measured in CC mode, ^{115}In was used as internal standard, while for the heavier isotopes measured in standard mode, ^{185}Re was used. Occasionally, low masses analytes (^{7}Li and ^{9}Be measured in standard mode) present sharper drift than ^{185}Re, and are only effectively corrected when internal and external standardization procedures are employed together.

Measurement uncertainty and bias assessment

The measurement uncertainty (U) was calculated following NORDTEST (2004). This approach specifies that uncertainties must be calculated using data obtained for CRM. The results of BRP-1 and OU-6, digested using Table-top and Bomb procedures, respectively, were used to calculate U. The uncertainty of bias (u_{bias}), and the precision of the method, given by the relative standard measurement uncertainty, RSD, are combined and expanded according U (%) = $k*(u^2_{bias}+ RSD^2)^{1/2}$, where a coverage factor k = 2, approximates the confidence level of 95%.

Apart, the significance of the bias was tested using the expression $|MV - RV| \leq k(SD^2_{MV} + SD^2_{RV})^{1/2}$, Eq. (1), where MV and RV are the mean of results and reference values, SD^2_{MV} and SD^2_{RV} are the variances associated to the MV and RV, respectively.

Method Detection limits

Detection limits (DL) are influenced by instrumental sensitivity, memory effects, polyatomic interferences and contamination from analytical reagents and environment. The method detection limits (MDL) were estimated as the mean of the procedural blank plus three times the standard deviation of at least 7 measurements of a procedural blank solution spiked with analytes at concentration corresponding to 3 to 5 times the instrumental DL, determined using pure 1% HNO_3. For Table-top and bomb procedures blanks and MDL were similar and are presented together. The addition of Mg to the samples in procedures HPA-S 3 and HPA-S 4b rose the MDL for some elements, such as V, Cr, Co, Ni, Mo, Rb and Ba. For Sintering 1 and 2 procedures the concentration of the blank and MDL were determined analyzing the procedural blank without the centrifugation step, i.e. dissolving the blank (sintered Na_2O_2) with the acid that would be used to dissolve the precipitate. For Sintering 3, the procedural blank could be processed as a sample,

because it had sufficient Fe and Ti to precipitate. The MDL of lanthanides in sintering procedures were similar of those obtained for the acid digestions, while higher MDL, up to one order of magnitude, were observed for Ni, Sr, Ba, Zr and Pb. Blank subtraction was generally negligible (< 2%), except for low concentration analytes (Rb, Cs, Th in BIR-1) after acid decomposition and for Ni in GSR-1 and RGM-1 by sintering, for which substantial blank corrections were applied.

Results

The results are arranged in four parts, starting by the degree of attenuation of polyatomic interferences provided by the operation in CC mode. Following, are an assessment of trace elements recoveries obtained with the three sintering procedures and the development of the decomposition scheme using HPA-S. Finally, the means of replicate measurements are graphically compared with reference values and the assessment of measurement uncertainty is presented.

Optimization of the gas flow rate in the collision cell

The attenuation of polyatomic interferences on masses (m/z = 45, 49, 51, 52, 53, 63 and 78), achieved by increasing the gas flow rate added to the CC, while aspirating an acid digestion solution of GSR-1 is presented in Figure 3, with the signal of those masses rationed against the signal recorded for [115]In. This mass was selected for normalization because it is unaffected by polyatomic interferences and GSR-1 was used as test sample because of its low concentration of elements measured in CC mode (Sc, V, Cr, Co, Ni, Cu and Zn). Before starting the measurements, a potential barrier for ions with low kinetic energy was implemented by biasing the quadrupole mass analyzer at a positive potential in relation to the cell, as indicated in Table 2. Initially, without adding gas to the cell, the signal recorded at each mass is the sum of counts

belonging to the analyte plus the signal of interfering species. With the pressurization of the CC the contribution of the interfering species to the total number of counts is reduced, while analyte ions maintain their count rates. Thereby the observed ratios decrease with the increase of the gas flow until gain stabilizes in terms of interference attenuation, indicated by a constant ratio. However, if a gas flow beyond the necessary is applied the sensitivity is compromised because analyte ions are also attenuated. Therefore, the optimum gas flow is a compromise between high sensitivity and adequate level of interference removal.
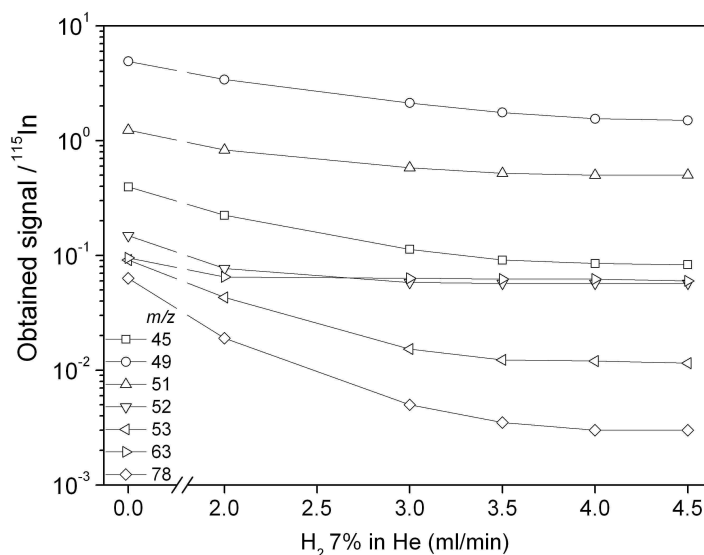
Figure 3. Attenuation of polyatomic interferences obtained by increasing the gas flow rate in the collision cell. The constant ratio indicates the optimum gas flow to attenuate interferences.

Figure 3 shows that gas flow rates between 3.5 and 4.0 ml/min efficiently remove the overlaps of $^{35}Cl^{16}O^+$ on $^{51}V^+$, $^{36}Ar^{16}O^+$ and $^{35}Cl^{16}O^1H^+$ on $^{52}Cr^+$, $^{37}Cl^{16}O^+$ on $^{53}Cr^+$, $^{35}Cl^{14}N^+$ on $^{49}Ti^+$ and $^{40}Ar^{23}Na^+$ over $^{63}Cu^+$. The attenuation of interferences over $^{53}Cr^+$ and $^{49}Ti^+$ are presented because they are used as qualifier isotope (to confirm results of $^{52}Cr^+$) and for mathematical corrections, respectively. The attenuation of $^{78}Ar_2^+$ was also included because it is used in the daily tuning as an indirect indicator of the gas flow necessary to obtain the desired level of interference attenuation. Very low levels of $^{40}Ar^{19}F^+$, $^{40}Ar^{26}Mg^+$ and $^{40}Ar^{48}Ti^+$ (which

interfere on ^{59}Co, ^{66}Zn and ^{88}Sr) were observed with GSR-1 as test solution, therefore the attenuation of such interferences are absent in Figure 3.

A significant removal of ^{29}Si^{16}O$^+$ and ^{28}Si^{16}O^{1}H$^+$ both interfering on ^{45}Sc$^+$ was achieved with a gas flow rate between 3.5 and 4 ml/min (Figure 3), but differently from the other mentioned interferences, the overlaps on ^{45}Sc$^+$ were not entirely removed with the CC and, hence, an additional mathematical correction was applied. Similar situation occurred for ^{63}Cu and ^{66}Zn, which are interfered by oxides and hydroxides of Ti. In comparison with the standard mode of operation, the use of a moderate gas flow rate (~ 4 ml/min) in the CC removed about 70-80% of the interferences caused by oxides and hydroxides on ^{45}Sc, ^{63}Cu and ^{66}Zn, reducing such interferences to less than 5% of the each mass signal.

Regarding the alleviation of interferences caused by oxides and hydroxides of lanthanides (Ln), the operation in CC mode produces only a minor effect. For instance, the ratio CeO$^+$/Ce$^+$ is only reduced from 1.5 to 1.0% with gas flow rate of ~ 4 ml/min and KED, and mathematical corrections would still be needed. Therefore, Ln were determined in standard mode taking advantage of the higher sensitivity. Du and Houk (2000) explained that the low efficiency of the CC in the attenuation of Ln^{16}O$^+$ is related to the small difference in collision cross-section between the heavy analyte (Ln$^+$) and respective interferences (Ln^{16}O$^+$).

Assessment of recoveries of trace elements after sintering

The recovery, expressed by the ratio obtained/reference value, of forty one trace elements for samples decomposed by sintering is shown in Figure 4. Using the Sintering 1 procedure the Ln, Sc, Co, Sr, Y and Ba were fully recovered, but other elements of interest display incomplete and variable recovery yields. The inclusion of a heating step after dissolving the sinter with water

improved significantly the recoveries of Ni, Zr, Nb, Cd, Sn, Sb, Hf, Pb and Th. BRP-1 contains

about three to ten times the amount of Fe and Ti, compared to GSP-2 and RGM-1, respectively.

This could explain the better results observed for BRP-1. However, adding extra Fe and Ti to the

acid rock samples did not improve the recoveries for the investigated samples.
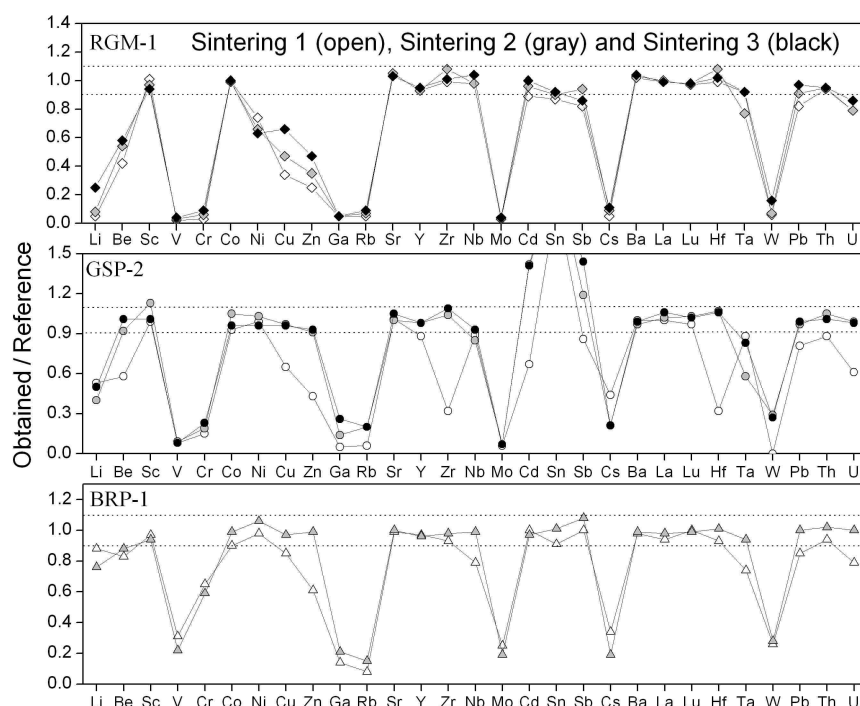
Figure 4. Recoveries of trace elements, expressed as the ratio between obtained mean value and the reference value. La and Lu summarize the behavior of lanthanides. The dotted lines delimit recoveries between 90 and 110%.

Recoveries of Ta were variable. For instance, the recoveries for the basalt samples (BRP-1, BCR-2 and BHVO-2) were near total, 94% in average, while for other samples (OU-6, GSR-1, RGM-1, GSP-2 and G-3) it was between 68 and 91%. This lack of consistency prevents the determination of Ta. Bayon *et al.* (2009) also reported incomplete recoveries for Ta using a similar procedure.

Cu, Zn and U also presented reasonable recoveries using Sintering 2 procedure, but are not consistent enough to be useful, unless the isotope dilution technique is applied to account for

partial losses (Catterick *et al.* 1998). Due to their solubility in the alkaline solution, Li, Be, V, Cr, Ga, Rb, Mo, Cs and W cannot be recovered. The recoveries of Cd, Sn and Sb in GSP-2 were calculated against published results (Pretorius *et al.* 2006), because reference values are not available for this RM. The high values were confirmed by results obtained with other dissolution techniques.

Compared to the other digestion techniques used in this work, the procedure Sintering 2 is less time consuming and can be used for the determination of a large suite of elements (Ln, Ni, Sc, Co, Sr, Y, Ba, Zr, Nb, Cd, Sn, Sb, Hf, Pb and Th). Some limitations are the variable co-precipitation efficiency of elements of great interest, such as Rb, Ta and U, and the lack of pure reagents. Averaged results for elements that were systematically fully recovered with the different sintering procedures are presented in the Table 3, together with other results.

Dissolution of granitic samples using High Pressure Asher (HPA-S)

The recovery of trace elements determined after sample decomposition with procedures HPA-S 1 and HPA-S 2 are presented in Figure 5. The major difficulty found was the precipitation of poorly soluble fluorides, which incorporated large proportions of trace elements preventing their accurate determination. With procedure HPA-S 1, involving only HNO_3 in the evaporation steps, few elements (e.g., Zr) were completely recovered, Figure 5a. These results indicate that phases which normally are difficult to digest in granites, like zircon, were decomposed, but given the inability of the HNO_3 in eliminating the formed fluorides low recoveries were observed for most analytes.
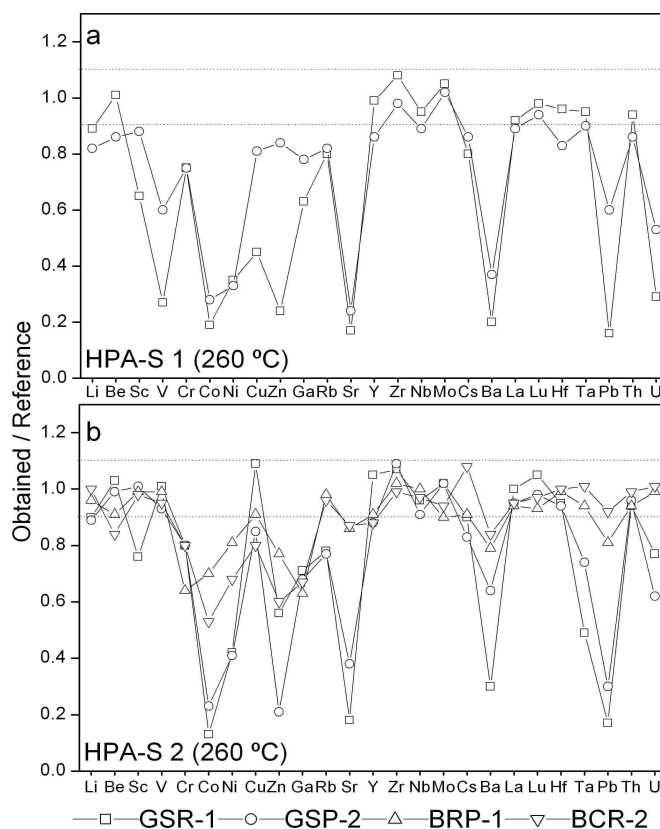
Figure 5. Recoveries, expressed as the ratio between obtained mean value and the reference value, of trace elements after dissolution in HPA-S, procedures HPA-S 1 (a) and HPA-S 2 (b). Dotted lines delimit recoveries between 90 and 110%.

In an attempt to eliminate the fluorides one aliquot (0.5 ml) of $HClO_4$ was included in the evaporation step of the procedure HPA-S 2. Besides GSR-1 and GSP-2, basalts (BCR-2 and BRP-1) were also digested to test whether the formation of fluorides is influenced by sample composition, more specifically by the $[(Mg+Ca)/Al]_M$ ratio. These samples were chosen because they encompass a wide range of $[(Mg+Ca)/Al]_M$ ratios, respectively 0.15, 0.21, 0.82 and 0.98 for GSR-1, GSP-2, BCR-2 and BRP-1.

The inclusion of $HClO_4$ in the evaporation scheme resulted in higher recoveries for most trace elements analyzed in GSP-2 and GSR-1, Figure 5b. This improvement reflects the effectiveness of $HClO_4$ in decomposing fluorides compared to HNO_3. The total recoveries of a series of elements (such as V, Zr, Hf, Nb, Mo, Th and Ln) indicate that the granitic samples were

dissolved. However, a white precipitate remained undissolved in all samples tested. These precipitates were separated and identified by scanning electron microscopy (imaging and X-ray analysis) and X-ray diffraction as constituted mainly by AlF_3. Images of fluorides collected from BRP-1 and GSP-2 are shown in Figure 6 with one typical spectrum bellow each image.

The amount of precipitate was slightly smaller for basalts samples compared to granitic ones. The precipitates also differ in particle size and shape. The occurrence of precipitates containing K is likely due to the formation of $KAlF_4$, which was observed only in GSP-2 and GSR-1, because of their higher concentration of K relative to the basalts. Iron was identified in all precipitates, and its presence may be related to the substitution of Al^{3+} by Fe^{3+} during the formation of AlF_3.
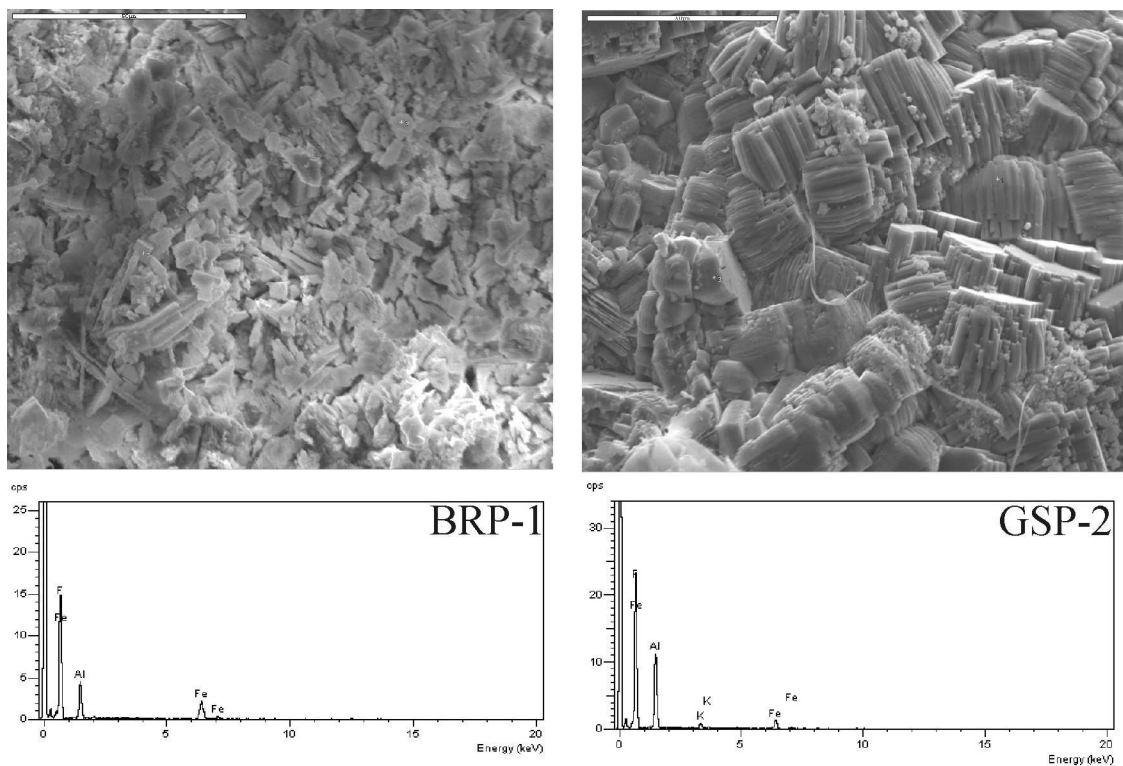
Figure 6. Backscattered SEM images of precipitates collected from BRP-1 (left) and GSP-2 (right) after dissolution with procedure HPA-S 2. Bellow each image is one spectrum (SEM-EDS) showing the composition of the precipitates as mainly aluminum fluorides, identified with XRD as AlF_3 . The scale bar corresponds to 50 µm.

Different recovery yields between basalts and granitic samples were observed with the HPA-S 2 procedure. The higher recoveries obtained for BCR-2 and BRP-1 in comparison to GSR-1 and GSP-2 may be a result of larger $[(Mg+Ca)/Al]_M$ ratios in the former compared to the granitoid samples. The larger amount of Mg and Ca can minimize the formation of AlF_3 because part of the Al available in solution is consumed in the formation of decomposable fluorides.

Takei *et al.* (2001) demonstrated that for dissolutions performed at 205 ºC in PTFE bombs, the formation of AlF_3 (which retained preferentially $Ln^{3+}>Th^{4+}>>Sr^{2+}$, Ba^{2+}) can be suppressed if Mg is added to the sample to achieve $[(Mg+Ca)/Al]_M \approx 1$. In the experiment HPA-S 2, test portions of the basalt BRP-1, which naturally possess $[(Mg+Ca)/Al]_M = 0.98$, failed in suppressing the AlF_3 precipitation. Such finding may be related to fact that digestion was performed at higher temperature and pressure than those employed by Takei *et al.* (2001). Therefore, we suggest that the higher temperatures and pressures of the HPA-S provide speed of decomposition but at the same time they also promote the formation of AlF_3 over other fluorides.

Another difference between data presented in Fig. 5b, and that of Takei *et al.* (2001) is the complete recoveries of Ln^{3+} and Th^{4+} in all samples digested with procedure HPA-S 2, even without suppressing the formation of AlF_3, and the observation that divalent ions (Co^{2+}, Zn^{2+}, Sr^{2+}, Ba^{2+} and Pb^{2+}) presented the lowest recoveries.

In HPA-S 3 an extra quantity of Mg was added to the sample to achieve $[(Mg+Ca)/Al]_M \approx$ 2, and a second evaporation step with $HClO_4$ was necessary to eliminate the extra amount of fluorides formed. Results obtained with procedure HPA-S 3 using different test portion sizes are presented in Figure 7a. In the test of procedure HPA-S 4a, the digestion temperature was diminished to 200 ºC and 50 mg GSP-2 test portions were decomposed after adding different amounts of Mg, Figure 7b. The results obtained with procedure HPA-S 3 for test portions of 50 mg were consistent with those obtained using 100 mg, Figure 7a. Therefore, to reduce the

consumption of Mg, further tests were performed with test portions of 50 mg. The incomplete

recoveries, Figure 7b, of Zr, Hf and Ln, (which in previous tests using higher temperature were

fully recovered) suggest that with procedure HPA-S 4a, the sample was only partially

decomposed. The recoveries also demonstrate a positive correlation with the amount of Mg

added, which indicates that the fluorides are still formed at 200 ºC, but can be suppressed

controlling the $[(Ca+Mg)/Al]_M$ ratio. Based on these observations, in the procedure HPA-S 4b,

the digestion was made at 220 ºC using test portions of 50 mg and with 6-7 mg of MgO. The

results obtained with procedure HPA-S 4b demonstrated satisfactory recoveries and are presented

in Table 3, in next section.
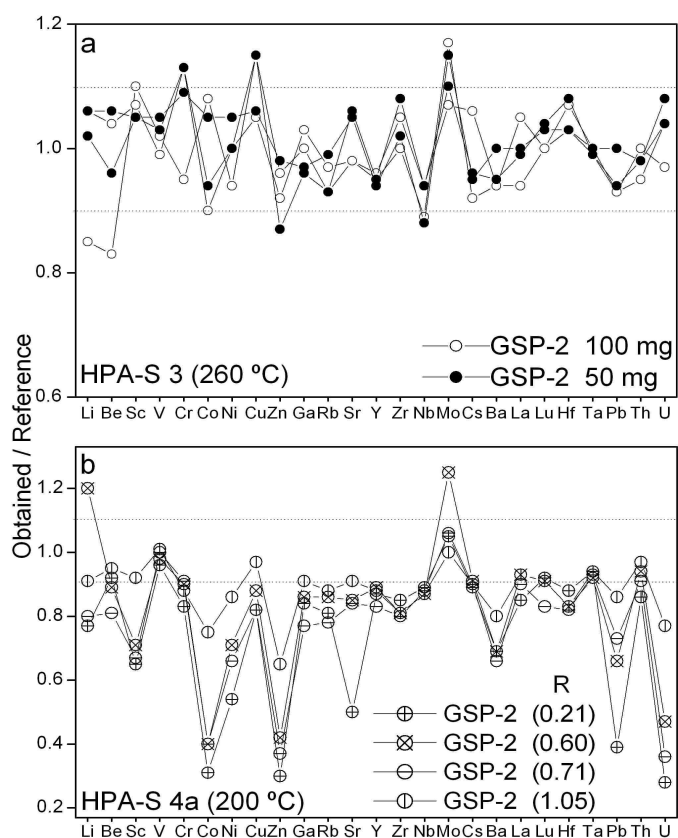
Figure 7. Recoveries, expressed as the ratio between obtained mean value and the reference
value, of trace elements in GSP-2 using procedure HPA-S 3 (a), and after dissolution of GSP-2,
without (R = 0.21) and with addition of Mg, using procedure HPA-S 4a (b), R=$[(Ca+Mg)/Al]_M$.
Dotted lines delimit recoveries between 90 and 110%.

These results demonstrate that complete recoveries is a compromise between a sufficiently high temperature to decompose the test portion and the control of the $[(Mg+Ca)/Al]_M$ to inhibit the precipitation of AlF_3.

Assessment of intermediate precision, trueness and uncertainties

Certified and other widely used RM were analyzed to demonstrate the reliability of the tested dissolution procedures. Obtained results means, standard deviation (s) and reference values are presented in Table 3, while equivalent concentration of procedural blanks and detection limits are in Table S1. The source of the reference values used for comparison is indicated at bottom of Table 3.

Reported results using Table-top, Bomb, and in some cases the Sintering 1 procedure, are mean values of at least seven separate digestions performed over more than one year and hence provide an estimate of intermediate precision for our methods. Results obtained with procedures HPA-S 3, HPA-S 4b, Sintering 2 and Sintering 3 were obtained in shorter periods and therefore contain a lower number of replicates.

In Figure 8, the ratios between the mean of each set of results and reference values for each RM are shown. The results obtained for the RM provide information on the combined effect of many sources of uncertainty covering the whole analytical method. The reported data show that the intermediate precision of the proposed procedures is generally better than 5%, except for low abundance elements like Mo, Cd, Sn, Sb, Cs and W found in basalts, Rb and Ta in BIR-1, Cd in RGM-1 and GSP-2 and Cr, Co, Ni and Zn in GSR-1.

Table 3. Mean results ± standard deviation (mg kg^{-1}) of (n) determinations and reference values (RV)

Element	BIR-1				BCR-2			BHVO-2		
	Table-top (n=7)	Sintering 2 (n=3)	Sintering 3 (n=3)	RV[#]	Table-top (n=9)	Sintering 1 (n=8)	RV[#]	Table-top (n=15)	Sintering 1 (n=3)	RV[#]
Li	3.2 ± 0.1			3.2 ± 0.2	9.1 ± 0.4		9 ± 2	4.5 ± 0.2		4.8 ± 0.2
Be	0.10 ± 0.01			0.12 ± 0.01	2.0 ± 0.2		2.3 ± 0.1[a]	1.0 ± 0.1		1 ± 0.1
Sc	43 ± 3	44 ± 1	44 ± 1	43 ± 2	32 ± 1	32 ± 3	33 ± 2	31 ± 1	31 ± 1	32 ± 1
V	329 ± 10			319 ± 18	412 ± 16		416 ± 16	324 ± 12		317 ± 11
Cr	400 ± 18			391 ± 15	16 ± 1		18 ± 2	288 ± 10		280 ± 19
Co	52 ± 1	49 ± 1	50 ± 1	52 ± 3	37 ± 2	37 ± 1	37 ± 3	45 ± 2	45 ± 1	45 ± 3
Ni	173 ± 7	163 ± 5	165 ± 7	166 ± 7	11.8 ± 0.7		18 ± 1	117 ± 5		119 ± 7
Cu	123 ± 3			119 ± 8	18.0 ± 0.9		19 ± 2	128 ± 4		127 ± 7
Zn	71 ± 5			72 ± 18	132 ± 7		127 ± 9	103 ± 6		103 ± 6
Ga	15.0 ± 1.1			15.3 ± 0.8	22.1 ± 0.8		23 ± 2	21 ± 1		22 ± 2
Rb	0.23 ± 0.04			0.20 ± 0.01	47 ± 1		46.9 ± 0.1	9.2 ± 0.4		9.11 ± 0.04
Sr	108 ± 5	108 ± 3	111 ± 2	109 ± 2	334 ± 11	339 ± 14	340 ± 3	402 ± 18	388 ± 14	396 ± 1
Y	15.4 ± 0.7	15.8 ± 0.1	15.9 ± 0.4	15.6 ± 0.9	36 ± 1	35 ± 1	37 ± 2	25.8 ± 1.2	25.5 ± 0.3	26 ± 2
Zr	14.4 ± 0.4	13.9 ± 0.2	13.1 ± 0.9	14.0 ± 0.1	182 ± 8		184 ± 1	166 ± 7		172 ± 11
Nb	0.58 ± 0.07	0.53 ± 0.02	0.57 ± 0.05	0.55 ± 0.05	11.8 ± 0.4		12.6 ± 0.4	17.5 ± 0.3		18.1 ± 1
Mo	0.07 ± 0.02			0.07	242 ± 15		250 ± 20	4.0 ± 0.3		4 ± 0.2
Cd	0.09 ± 0.01	0.08 ± 0.03	0.06 ± 0.03	0.097	-			0.08 ± 0.02		0.060 ± 0.006
Sn	0.7 ± 0.1	0.6 ± 0.1	0.6 ± 0.1	0.59 ± 0.06	2.0 ± 0.1		2.1 ± 0.1[a]	1.7 ± 0.1		1.7 ± 0.2
Sb	0.49 ± 0.02	0.50 ± 0.03	0.44 ± 0.02	0.46 ± 0.07	0.31 ± 0.03		0.4 ± 0.1[a]	0.12 ± 0.01		0.13 ± 0.04
Cs	<0.008			0.007 ± 0.003	1.2 ± 0.1		1.1 ± 0.1	0.10 ± 0.02		0.10 ± 0.01
Ba	6.7 ± 0.3	6.9 ± 0.1	7.0 ± 0.6	7.14	676 ± 10	686 ± 9	677 ± 2	129 ± 4	135 ± 3	131 ± 1
La	0.64 ± 0.04	0.64 ± 0.05	0.64 ± 0.01	0.615 ± 0.021	24.9 ± 0.5	25 ± 1	24.9 ± 0.2	15.1 ± 0.5	14.9 ± 0.5	15.2 ± 0.1
Ce	2.0 ± 0.1	1.97 ± 0.05	2.0 ± 0.1	1.92 ± 0.08	53 ± 1	53 ± 2	52.9 ± 0.2	37 ± 1	36.6 ± 0.8	37.5 ± 0.2
Pr	0.38 ± 0.02	0.39 ± 0.02	0.39 ± 0.03	0.37 ± 0.02	6.8 ± 0.2	6.8 ± 0.1	6.7 ± 0.1	5.3 ± 0.1	5.3 ± 0.1	5.35 ± 0.17
Nd	2.44 ± 0.07	2.44 ± 0.04	2.43 ± 0.07	2.38 ± 0.01	28.5 ± 0.5	28.9 ± 0.5	28.7 ± 0.1	24.2 ± 0.5	24.2 ± 0.5	24.5 ± 0.1
Sm	1.12 ± 0.03	1.13 ± 0.02	1.14 ± 0.06	1.12 ± 0.02	6.6 ± 0.1	6.6 ± 0.1	6.58 ± 0.02	6.1 ± 0.2	6.1 ± 0.1	6.07 ± 0.01
Eu	0.54 ± 0.01	0.53 ± 0.01	0.52 ± 0.02	0.53	1.97 ± 0.06	2.00 ± 0.03	1.96 ± 0.01	2.07 ± 0.05	2.10 ± 0.01	2.07 ± 0.02
Gd	1.88 ± 0.06	1.83 ± 0.04	1.84 ± 0.03	1.87 ± 0.04	6.8 ± 0.2	6.8 ± 0.1	6.75 ± 0.03	6.2 ± 0.2	6.27 ± 0.04	6.24 ± 0.03
Tb	0.36 ± 0.01	0.36 ± 0.01	0.36 ± 0.01	0.36 ± 0.03	1.05 ± 0.03	1.05 ± 0.02	1.07 ± 0.03	0.93 ± 0.02	0.91 ± 0.01	0.92 ± 0.03
Dy	2.59 ± 0.07	2.53 ± 0.03	2.56 ± 0.02	2.51	6.4 ± 0.1	6.4 ± 0.1	6.41 ± 0.03	5.3 ± 0.1	5.3 ± 0.1	5.31 ± 0.02
Ho	0.58 ± 0.02	0.57 ± 0.01	0.57 ± 0.01	0.56 ± 0.05	1.30 ± 0.04	1.30 ± 0.02	1.28 ± 0.03	0.99 ± 0.02	0.98 ± 0.01	0.98 ± 0.04
Er	1.72 ± 0.04	1.69 ± 0.04	1.72 ± 0.03	1.66	3.64 ± 0.07	3.67 ± 0.09	3.66 ± 0.01	2.53 ± 0.05	2.52 ± 0.11	2.54 ± 0.01
Tm	0.26 ± 0.01	0.24 ± 0.01	0.25 ± 0.01	0.25 ± 0.03	0.52 ± 0.01	0.53 ± 0.01	0.54 ± 0.04	0.33 ± 0.01	0.34 ± 0.01	0.33 ± 0.01
Yb	1.65 ± 0.05	1.62 ± 0.02	1.62 ± 0.01	1.65	3.34 ± 0.08	3.37 ± 0.05	3.38 ± 0.02	1.96 ± 0.04	1.99 ± 0.03	2.00 ± 0.01
Lu	0.25 ± 0.01	0.25 ± 0.01	0.25 ± 0.01	0.25 ± 0.02	0.50 ± 0.01	0.50 ± 0.01	0.503 ±0.009	0.27 ± 0.01	0.28 ± 0.01	0.274 ± 0.005
Hf	0.59 ± 0.01	0.58 ± 0.02	0.59 ± 0.05	0.582 ± 0.004	4.9 ± 0.2		4.9 ± 0.1	4.4 ± 0.2		4.36 ± 0.14
Ta	0.044 ± 0.004			0.0357 ± 0.0004	0.77 ± 0.04		0.74 ±0.02	1.16 ± 0.05		1.14 ± 0.06
W	0.05 ± 0.03			0.07	0.53 ± 0.03		0.53 ± 0.01[b]	0.25 ± 0.02		0.21 ± 0.11
Pb	3.05 ± 0.07	3.0 ± 0.1	3.1 ± 0.3	3.1 ± 0.3	10.5 ± 0.6		11 ± 1	1.6 ± 0.1		1.6 ± 0.3
Th	0.036 ± 0.003	<0.07	<0.08	0.032 ± 0.004	5.8 ± 0.1		5.7 ± 0.5	1.22 ± 0.08		1.22 ± 0.06
U	0.011 ± 0.001			0.010 ± 0.001	1.67 ± 0.04		1.69 ± 0.19	0.42 ± 0.01		0.403 ± 0.001

[#] Preferred values of GeoReM database, version 11 of 04/01/2010, (Jochum *et al.* 2005) were used for comparison. In the absence of preferred values, published results were used: [a] Mori *et al.* (2007), [b] Stoll *et al.* (2008). Results for Cd in BCR-2 are not provided because of intense interference of Mo oxides.

Table 3. (*cont.*) Mean results ± standard deviation (mg kg^{-1}), number of (n) dissolutions and reference values (RV)

Element	BRP-1 Table-top (n=15)	BRP-1 Sintering 1 (n=11)	BRP-1 Sintering 2 (n=3)	RV[#]	OU-6 Bomb (n=9)	OU-6 Sintering 1 (n=4)	OU-6 Sintering 3 (n=3)	RV[##]	RGM-1 Bomb (n=8)	RGM-1 Sintering 1 (n=7)	RGM-1 Sintering 3 (n=4)	RV[###]
Li	6.8 ± 0.4			*7.1 ± 0.3*	98 ± 6			*95.3 ± 3.8*	60 ± 2			57 ± 8
Be	1.7 ± 0.1			*1.8 ± 0.1*	2.4 ± 0.3			*2.53 ± 0.14*	2.4 ± 0.1			2.4 ± 0.2
Sc	29 ± 1	28 ± 1	27 ± 2	28.5 ± 1.2	22.4 ± 1.4	22.8 ± 0.5	22.2 ± 0.4	23.1 ± 1.6	4.5 ± 0.5	4.5 ± 0.1	4.2 ± 0.1	4.4 ± 0.3
V	405 ± 13			391 ± 10	132 ± 7			129.8 ± 5.2	12.0 ± 0.8			13 ± 2
Cr	11.4 ± 0.7			12.4 ± 0.8	79 ± 8			70.7 ± 4.1	3.3 ± 0.3			*3.7*
Co	38 ± 2	36 ± 2	37 ± 1	37.5 ± 1.8	28 ± 2	28 ± 1	28 ± 1	29.2 ± 1.4	2.0 ± 0.1	2.0 ± 0.1	2.0 ± 0.1	2.0 ± 0.2
Ni	23 ± 1		25 ± 3	23.4 ± 1.8	43 ± 3			40.2 ± 2.2	2.1 ± 0.2		2.4 ± 0.1	3.7[c]
Cu	162 ± 7			160 ± 5	43 ± 3			40.4 ± 2.9	11.3 ± 0.6			12 ± 0.4
Zn	147 ± 7			142 ± 3	108 ± 7			111.4 ± 4.6	35 ± 3			*32*
Ga	25 ± 2			24.8 ± 1.0	25 ± 1			24.17 ± 1.19	15 ± 1			15 ± 2
Rb	36 ± 1			35.4 ± 1.5	117 ± 9			121.3 ± 3.8	155 ± 7			150 ± 8
Sr	498 ± 16	492 ± 14	491 ± 32	492 ± 12	130 ± 5	133 ± 5	137 ± 1	131.7 ± 5.0	107 ± 4	110 ± 3	114 ± 2	110 ± 10
Y	42 ± 2	41 ± 1	42 ± 3	42.0 ± 2.2	26.8 ± 1	27.5 ± 0.7	28.6 ± 0.1	27.75 ± 1.18	23.2 ± 0.9	23 ± 1	23.5 ± 0.5	*25*
Zr	313 ± 12		304 ± 13	310 ± 9	172 ± 9			174.2 ± 6.1	218 ± 8		232 ± 26	220 ± 20
Nb	29 ± 1		28.9 ± 0.3	29.1 ± 1.6	13.9 ± 0.9			14.49 ± 0.78	8.4 ± 0.3		8.9 ± 0.4	8.9 ± 0.6
Mo	1.5 ± 0.2			*1.5 ± 0.1*	1.4 ± 0.4				2.6 ± 0.3			2.3 ± 0.5
Cd	0.19 ± 0.06		0.19 ± 0.02	*0.2 ± 0.1*	0.10 ± 0.02				0.08 ± 0.02		0.09 ±0.01	0.09[c]
Sn	2.6 ± 0.2		2.5 ± 0.1	*2.5 ± 0.4*	2.68 ± 0.08			2.67 ± 0.27	4.0 ± 0.3		3.7 ± 0.2	4.1 ± 0.4
Sb	0.06 ± 0.01		0.06 ± 0.01	*0.06 ± 0.01*	0.57 ± 0.04			*0.56 ± 0.06*	1.3 ± 0.1		1.2 ± 0.1	1.3 ± 0.1
Cs	0.37 ± 0.03			0.37 ± 0.02	7.9 ± 0.4			8.10 ± 0.37	10.0 ± 0.4			9.6 ± 0.6
Ba	552 ± 12	552 ± 13	549 ± 2	555 ± 15	474 ± 19	489 ± 7	489 ± 1	480 ± 14	831 ± 21	834 ± 34	832 ± 19	810 ± 46
La	41.5 ± 0.9	41.5 ± 1.5	41.9 ± 0.6	42.6 ± 1.1	33 ± 2	33 ± 1	34 ± 1	33.2 ± 1.3	23.3 ± 0.9	23.4 ± 0.6	23.8 ± 0.5	24 ± 1.1
Ce	93 ± 2	94 ± 3	92.6 ±0.5	93.3 ± 2.3	76 ± 2	77 ± 3	75 ± 13	77.1 ± 3.6	46 ± 2	46 ± 1	47 ± 2	47 ± 4
Pr	12.0 ± 0.2	12.0 ± 0.3	12.2 ± 0.3	12.3 ± 0.3	7.9 ± 0.3	8.2 ± 0.1	8.2 ± 0.3	7.91 ± 0.39	5.4 ± 0.2	5.3 ± 0.2	5.3 ± 0.1	5.32[c]
Nd	51.6 ± 0.8	51.3 ± 1.3	50.7 ± 0.4	51.9 ± 1.3	30 ± 1	31 ± 1	31 ± 1	30.2 ± 1.6	19.3 ± 0.5	19.6 ± 0.8	19.3 ± 0.4	19 ± 1
Sm	11.2 ± 0.2	11.1 ± 0.3	11.0 ± 0.2	11.2 ± 0.4	6.0 ± 0.2	6.1 ± 0.1	6.3 ± 0.2	6.01 ± 0.29	4.0 ± 0.1	4.0 ± 0.2	4.04 ± 0.05	4.3 ± 0.3
Eu	3.40 ± 0.08	3.38 ± 0.11	3.38 ± 0.05	3.42 ± 0.11	1.35 ± 0.05	1.41 ± 0.02	1.40 ± 0.03	1.36 ± 0.09	0.64 ± 0.03	0.63 ± 0.04	0.63 ± 0.02	0.66 ± 0.08
Gd	10.3 ± 0.2	10.1 ± 0.3	10.2 ± 0.1	10.4 ± 0.6	5.3 ± 0.1	5.34 ± 0.07	5.49 ± 0.08	5.30 ± 0.31	3.6 ± 0.1	3.6 ± 0.2	3.7 ± 0.1	3.7 ± 0.4
Tb	1.50 ± 0.03	1.49 ± 0.03	1.51 ± 0.01	1.52 ± 0.07	0.84 ± 0.03	0.85 ± 0.02	0.87 ± 0.01	0.86 ± 0.06	0.63 ± 0.05	0.60 ± 0.02	0.60 ± 0.01	0.605[c]
Dy	8.5 ± 0.2	8.4 ± 0.2	8.5 ± 0.1	8.5 ± 0.4	5.1 ± 0.1	5.1 ± 0.1	5.2 ± 0.1	5.06 ± 0.23	3.72 ± 0.11	3.73 ± 0.04	3.72 ± 0.02	4.1 ± 0.1
Ho	1.60 ± 0.04	1.60 ± 0.03	1.60 ± 0.02	1.62 ± 0.09	1.03 ± 0.03	1.04 ± 0.02	1.07 ± 0.02	1.04 ± 0.09	0.78 ± 0.03	0.78 ± 0.04	0.78 ± 0.01	0.769[c]
Er	4.19 ± 0.09	4.18 ± 0.08	4.17 ± 0.01	4.2 ± 0.2	3.02 ± 0.08	3.07 ± 0.07	3.03 ± 0.02	2.93 ± 0.18	2.32 ± 0.09	2.27 ± 0.02	2.28 ±0.03	2.33[c]
Tm	0.57 ± 0.01	0.57 ± 0.02	0.57 ± 0.01	0.57 ± 0.03	0.46 ± 0.03	0.45 ± 0.01	0.46 ± 0.01	*0.45 ± 0.03*	0.37 ± 0.03	0.37 ± 0.02	0.37 ± 0.01	0.36 ± 0.02[d]
Yb	3.46 ± 0.08	3.45 ± 0.08	3.44 ± 0.02	3.48 ± 0.13	3.06 ± 0.07	3.05 ± 0.08	3.08 ± 0.05	2.98 ± 0.16	2.50 ± 0.09	2.51 ± 0.09	2.51 ± 0.05	2.6 ± 0.3
Lu	0.50 ± 0.01	0.49 ± 0.01	0.50 ± 0.01	0.50 ± 0.02	0.47 ± 0.02	0.46 ± 0.01	0.47 ± 0.01	0.45 ± 0.03	0.39 ± 0.03	0.39 ± 0.02	0.39 ±0.01	0.40 ± 0.03
Hf	8.1 ± 0.3		8.1 ± 0.1	8.0 ± 0.3	4.9 ± 0.2			4.70 ± 0.36	6.2 ± 0.2		6.1 ± 0.6	5.81[c]
Ta	1.93 ± 0.08			1.96 ± 0.14	0.98 ± 0.04			1.02 ± 0.07	0.94 ± 0.04			0.95 ± 0.1
W	0.49 ± 0.05			0.48 ± 0.02[b]	1.4 ± 0.1				1.6 ± 0.1			1.5 ± 0.18
Pb	5.5 ± 0.2		5.52 ± 0.03	5.5 ± 0.4	28 ± 1			28.80 ± 1.16	24.0 ± 0.8		22.4 ± 1.2	24 ± 3
Th	3.9 ± 0.1		4.0 ± 0.1	3.97 ± 0.17	10.9 ± 1.0			11.3 ± 0.6	14.9 ± 0.7		14.3 ± 0.1	15 ± 1.3
U	0.82 ± 0.02			0.82 ± 0.03	1.9 ± 0.1			1.92 ± 0.11	5.8 ± 0.3			5.8 ± 0.5

Certified, informative (in *italic*) values and standard deviation among laboratory means (s$_L$) according the certificates: [#]Cotta and Enzweiler (2008), [##] Kane (2004). [###] Recommended and informative values provided by USGS and published results: [c] Eggins *et al.* (1997), [d] Dulski (2001).

Table 3. (*cont.*) Mean results ± standard deviation (mg kg^{-1}), number of (n) dissolutions and reference values (RV)

Element	GSP-2 HPA-S 3 (n=3)	HPA-S 4 (n=5)	Bomb (n=10)	Sintering 1 (n=9)	Sintering 3 (n=4)	RV[###]	GSR-1 HPA-S 3 (n=3)	HPA-S 4 (n=6)	Bomb (n=9)	Sintering 1 (n=3)	Sintering 3 (n=3)	RV[###]	G-3 Bomb (n=6)	Sintering 1 (n=3)	Sintering 3 (n=3)	Meisel et al. (2002)
Li	35.2 ± 4.3	34.9 ± 0.2	36.0 ± 1.7			36 ± 1	134 ± 9	137 ± 3	138 ± 7			131 ± 7	32 ± 2			
Be	1.4 ± 0.2	1.4 ± 0.1	1.4 ± 0.1			*1.5 ± 0.2*	12.0 ± 0.8	12.9 ± 0.3	12.6 ± 0.6			12.4 ± 2.1	3.9 ± 0.2			
Sc	6.5 ± 0.4	7.0 ± 0.3	6.9 ± 0.8	6.3 ± 0.1	6.4 ± 0.8	6.3 ± 0.7	5.9 ± 0.3	6.2 ± 0.2	5.8 ± 0.3	5.8 ± 0.5	5.8 ± 0.2	6.1 ± 0.6	3.6 ± 0.3	3.5 ± 0.6	3.1 ± 0.7	
V	52 ± 1	54 ± 1	52 ± 3			52 ± 4	21 ± 1	23 ± 1	21 ± 2			24 ± 3	34 ± 1			
Cr	21 ± 2	20.3 ± 0.5	21 ± 2			20 ± 6	3.0 ± 0.8	3.0 ± 0.2	2.2 ± 0.3			3.6 ± 1.1	19 ± 2			
Co	7.1 ± 0.7	7.0 ± 0.3	7.3 ± 0.5	6.9 ± 0.4	7.0 ± 0.2	7.3 ± 0.8	3.1 ± 0.8	2.8 ± 0.1	2.7 ± 0.1	2.9 ± 0.3	3.0 ± 0.1	3.4 ± 1.0	4.5 ± 0.4	4.6 ± 0.1	4.5 ± 0.2	
Ni	16.6 ± 1.1	16.7 ± 0.3	16.6 ± 0.8		16.7 ± 1.3	17 ± 2	1.8 ± 0.3	2.2 ± 0.1	1.1 ± 0.3		2.3 ± 0.1	2.3 ± 1.2	8 ± 1		8.5 ± 0.2	
Cu	47 ± 2	44 ± 2	46 ± 3			43 ± 4	2.4 ± 0.2	2.3 ± 0.1	1.6 ± 0.2			3.2 ± 1.3	16 ± 2			
Zn	113 ± 6	115 ± 6	114 ± 6			120 ± 10	27 ± 2	30 ± 6	26 ± 2			28 ± 4	81 ± 6			
Ga	22.4 ± 0.9	20.7 ± 0.2	22.8 ± 1.2			22 ± 2	19 ± 1	18.0 ± 0.4	19 ± 1			19 ± 2	24 ± 1			
Rb	234 ± 7	235 ± 2	243 ± 10			245 ± 7	444 ± 5	461 ± 11	465 ± 24			466 ± 26	156 ± 13			
Sr	235 ± 3	229 ± 2	238 ± 9	240 ± 11	241 ± 14	240 ± 10	110 ± 4	105 ± 3	107 ± 3	106 ± 5	105 ± 1	106 ± 9	440 ± 18	448 ± 10	450 ± 8	
Y	26.8 ± 0.4	26.3 ± 0.9	27.0 ± 1.6	25.6 ± 1.1	26 ± 1.45	28 ± 2	67 ± 1	67.9 ± 0.5	67 ± 4	66 ± 1	68 ± 2	62 ± 7	9.7 ± 0.4	9.7 ± 0.3	10.1 ± 0.1	10.3 ± 0.4
Zr	566 ± 19	552 ± 15	568 ± 38		599 ± 11	550 ± 30	161 ± 6	155 ± 9	159 ± 11		158 ± 7	167 ± 14	361 ± 27		355 ± 22	321 ± 46
Nb	25 ± 1	24.2 ± 0.3	25 ± 1		25.2 ± 0.3	27 ± 2	40 ± 2	40 ± 1	41 ± 1		41 ± 1	40 ± 4	12.3 ± 0.5		12.3 ± 1.2	14 ± 0.3
Mo	2.6 ± 0.2	2.2 ± 0.1	2.4 ± 0.2			*2.1 ± 0.6*	3.7 ± 0.1	3.7 ± 0.3	4.0 ± 0.5			3.5 ± 0.3	2.6 ± 0.8			
Cd	0.24 ± 0.05	0.31 ± 0.01	0.23 ± 0.10		0.28 ± 0.02	0.20 ± 0.05 [e]	0.03 ± 0.02	0.03 ± 0.01	0.02 ± 0.02		0.03 ± 0.01	0.03 ± 0.01	0.13 ± 0.07		0.17 ± 0.02	
Sn	6.0 ± 0.1	6.2 ± 0.2	5.9 ± 0.7		6.0 ± 0.5	3 ± 0.5 [e]	12.3 ± 0.4	11.9 ± 0.4	11.3 ± 1.1		11.7 ± 0.1	12.5 ± 2	2.2 ± 0.2		2.2 ± 0.1	
Sb	0.4 ± 0.1	0.43 ± 0.02	0.36 ± 0.04		0.39 ± 0.01	0.27 ± 0.08 [e]	0.23 ± 0.03	0.28 ± 0.03	0.28 ± 0.02		0.24 ± 0.01	0.21 ± 0.09	0.17 ± 0.03		0.15 ± 0.03	
Cs	1.2 ± 0.1	1.14 ± 0.03	1.16 ± 0.04			*1.2 ± 0.1*	35.4 ± 1.6	36.5 ± 0.8	37.3 ± 1.6			38.4 ± 1.5	1.5 ± 0.1			
Ba	(1259 ± 25)	1326 ± 18	1365 ± 51	1343 ± 51	1331 ± 61	1340 ± 44	(306 ± 20)	320 ± 12	326 ± 5	326 ± 6	329 ± 3	343 ± 45	1991 ± 52	2030 ± 133	1925 ± 104	
La	182 ± 12	179 ± 2	185 ± 85	184 ± 10	191 ± 10	180 ± 12	53 ± 1	52 ± 1	52 ± 2	53 ± 3	56.4 ± 0.4	54 ± 5	92 ± 2	90 ± 3	92 ± 4	92.4 ± 1.4
Ce	423 ± 16	427 ± 8	438 ± 18	424 ± 28	449 ± 15	410 ± 30	105 ± 1	105 ± 2	106 ± 4	108 ± 3	112 ± 1	108 ± 11	168 ± 7	166 ± 2	167 ± 6	171 ± 4
Pr	55 ± 3	53 ± 1	54 ± 3	55 ± 3	55 ± 2	*51 ± 5*	12.1 ± 0.5	12.1 ± 0.3	12.1 ± 0.4	12.6 ± 0.4	12.5 ± 0.2	12.7 ± 0.8	16.9 ± 0.3	16.7 ± 0.8	16.7 ± 0.9	17.4 ± 0.4
Nd	203 ± 9	200 ± 2	206 ± 6	205 ± 11	203 ± 8	200 ± 12	44 ± 1	44 ± 1	43 ± 1	45 ± 2	44.6 ± 0.7	47 ± 5	54 ± 2	54 ± 2	54 ± 2	56.8 ± 1.3
Sm	26 ± 1	25.7 ± 0.4	26.4 ± 0.9	26.4 ± 1.4	26.4 ± 0.7	27 ± 1	9.6 ± 0.2	9.6 ± 0.2	9.6 ± 0.3	9.8 ± 0.3	9.8 ± 0.2	9.7 ± 1.2	7.4 ± 0.2	7.3 ± 0.3	7.3 ± 0.4	7.69 ± 0.2
Eu	2.2 ± 0.1	2.21 ± 0.03	2.3 ± 0.1	2.3 ± 0.1	2.3 ± 0.1	2.3 ± 0.1	0.83 ± 0.02	0.82 ± 0.01	0.80 ± 0.03	0.84 ± 0.03	0.84 ± 0.02	0.85 ± 0.1	1.40 ± 0.10	1.38 ± 0.04	1.40 ± 0.06	1.50 ± 0.05
Gd	12.5 ± 0.7	11.8 ± 0.1	12.3 ± 0.5	11.6 ± 0.7	12.3 ± 0.4	*12 ± 2*	8.7 ± 0.3	8.6 ± 0.1	8.7 ± 0.2	9.0 ± 0.4	9.0 ± 0.1	9.3 ± 0.8	3.97 ± 0.08	3.9 ± 0.1	4.0 ± 0.1	4.07 ± 0.13
Tb	1.33 ± 0.01	1.25 ± 0.01	1.36 ± 0.07	1.36 ± 0.09	1.28 ± 0.03		1.56 ± 0.02	1.53 ± 0.02	1.58 ± 0.03	1.57 ± 0.02	1.61 ± 0.02	1.65 ± 0.13	0.46 ± 0.02	0.45 ± 0.01	0.47 ± 0.02	0.47 ± 0.01
Dy	5.9 ± 0.2	5.6 ± 0.1	5.9 ± 0.2	5.8 ± 0.2	5.8 ± 0.1	*6.1*	9.9 ± 0.1	9.8 ± 0.1	10.0 ± 0.2	10.0 ± 0.1	10.1 ± 0.2	10.2 ± 0.5	2.13 ± 0.05	2.13 ± 0.08	2.14 ± 0.10	2.23 ± 0.06
Ho	0.96 ± 0.05	0.93 ± 0.01	0.97 ± 0.03	0.95 ± 0.04	0.96 ± 0.02	*1.0 ± 0.1*	2.07 ± 0.03	2.05 ± 0.01	2.08 ± 0.06	2.10 ± 0.04	2.13 ± 0.04	2.05 ± 0.22	0.356 ± 0.007	0.35 ± 0.01	0.36 ± 0.01	0.37 ± 0.01
Er	2.30 ± 0.01	2.31 ± 0.03	2.37 ± 0.09	2.3 ± 0.1	2.30 ± 0.03	*2.2*	6.4 ± 0.1	6.5 ± 0.1	6.5 ± 0.1	6.5 ± 0.2	6.49 ± 0.1	6.5 ± 0.4	0.88 ± 0.02	0.88 ± 0.04	0.87 ± 0.02	0.94 ± 0.03
Tm	0.30 ± 0.01	0.28 ± 0.01	0.29 ± 0.01	0.29 ± 0.02	0.29 ± 0.01	*0.29 ± 0.02*	1.03 ± 0.02	1.04 ± 0.01	1.06 ± 0.04	1.08 ± 0.04	1.08 ± 0.01	1.06 ± 0.11	0.122 ± 0.005	0.120 ± 0.004	0.120 ± 0.005	0.123 ± 0.004
Yb	1.68 ± 0.04	1.62 ± 0.01	1.67 ± 0.07	1.64 ± 0.08	1.65 ± 0.04	1.6 ± 0.2	7.4 ± 0.2	7.4 ± 0.1	7.5 ± 0.1	7.5 ± 0.3	7.6 ± 0.1	7.4 ± 0.7	0.73 ± 0.02	0.72 ± 0.03	0.73 ± 0.03	0.74 ± 0.03
Lu	0.23 ± 0.01	0.23 ± 0.01	0.23 ± 0.01	0.23 ± 0.01	0.24 ± 0.01	*0.23 ± 0.03*	1.12 ± 0.03	1.13 ± 0.01	1.14 ± 0.03	1.10 ± 0.05	1.14 ± 0.01	1.15 ± 0.12	0.106 ± 0.004	0.104 ± 0.005	0.103 ± 0.004	0.110 ± 0.004
Hf	15.0 ± 0.3	15.2 ± 0.03	15.0 ± 0.8		14.9 ± 0.5	*14 ± 1*	5.7 ± 0.3	5.8 ± 0.3	5.7 ± 0.3		5.8 ± 0.1	6.3 ± 0.8	9.0 ± 0.4		8.8 ± 0.8	9 ± 0.7
Ta	0.90 ± 0.01	0.90 ± 0.05	0.9 ± 0.1			*0.91 ± 0.02* [f]	7.4 ± 0.05	7.3 ± 0.2	7.2 ± 0.1			7.2 ± 0.7	0.91 ± 0.04			0.89 ± 0.08
W	0.36 ± 0.02	0.36 ± 0.03	0.39 ± 0.05			0.33 ± 0.05 [e]	9.0 ± 0.3	9.1 ± 0.4	9.3 ± 0.5			8.4 ± 0.7	0.30 ± 0.04			
Pb	(39 ± 1)	41.3 ± 0.4	41 ± 2		41.7 ± 0.2	42 ± 3	(30 ± 1)	32 ± 1	32 ± 1		30 ± 3	31 ± 4	31 ± 1		32 ± 1	
Th	103 ± 3	113 ± 2	106 ± 5		106 ± 1	105 ± 8	54 ± 2	56 ± 1	54 ± 1		52.9 ± 0.5	54 ± 4	24 ± 1		24.3 ± 0.3	24.2 ± 0.1
U	2.4 ± 0.1	2.44 ± 0.02	2.5 ± 0.1			2.40 ± 0.19	18.5 ± 0.6	19.8 ± 0.6	19.0 ± 0.6			18.8 ± 2.2	2.3 ± 0.3			

[###] Recommended and informative (in *italic*) values provided by USGS and published results: [e] Pretorius *et al.* (2006), [f] Petrelli *et al.* (2007).
Results of Ba and Pb obtained with HPA-S 3 procedure (indicated within parenthesis) are subject to partial retention into AlF_3, and should not be used for further comparison, for details see text.
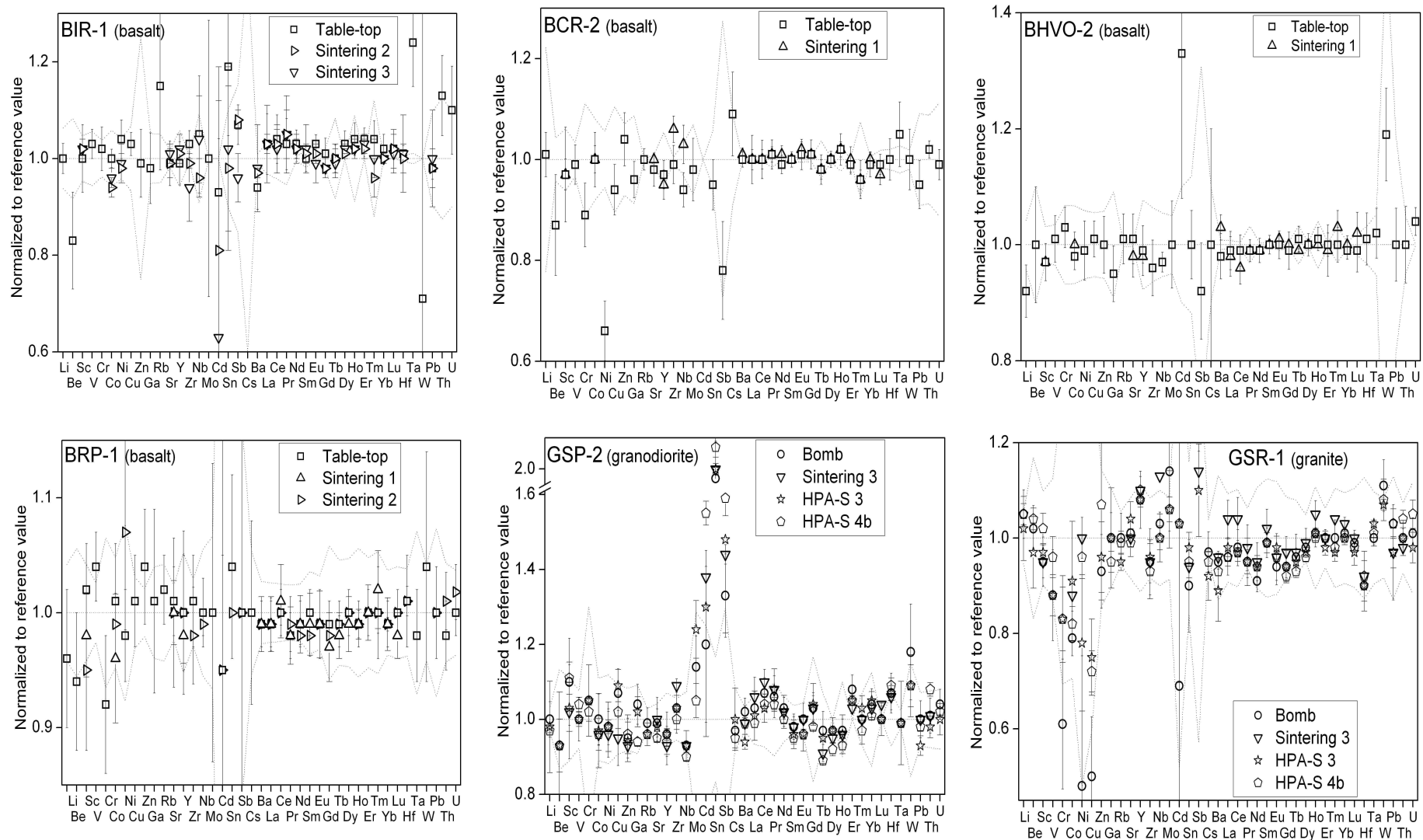
Figure 8. Mean result normalized to reference values for eight RM decomposed using different procedures. The area delimited by dotted lines represents the standard deviation (s) of the reference value. The error bar in each result represents 1s.
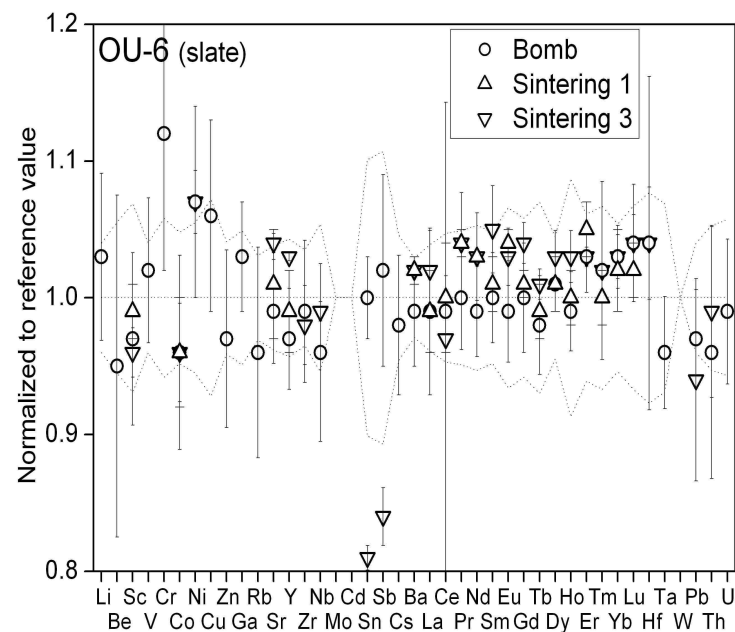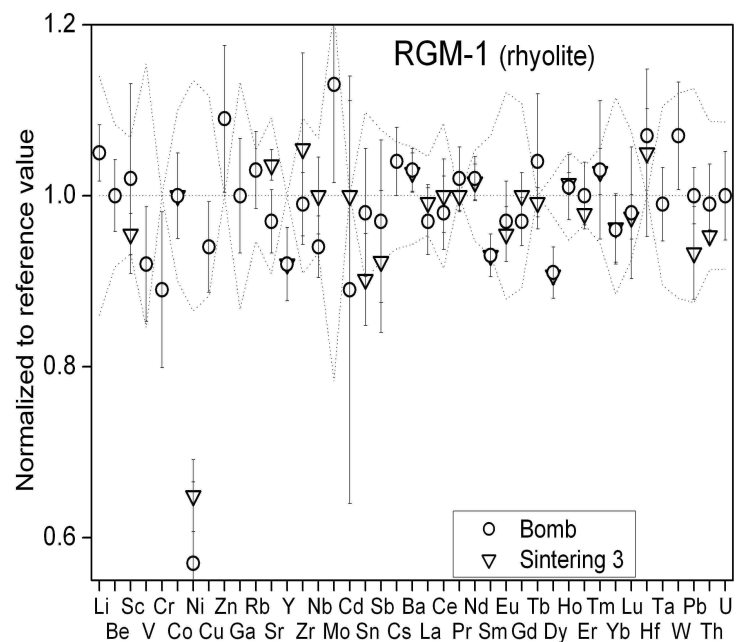
Figure 8. (*Cont.*) Mean result normalized to reference values for eight RM decomposed using different procedures. The area delimited by dotted lines represents the standard deviation (s) of the reference value. The error bar in each result represents 1s.

The different digestion techniques provided results with equivalent precision, as shown by standard deviations, in Table 3. Results obtained by acid decomposition (Table-top and Bomb and HPA-S 4b) and sintering procedures agree within their respective standard deviations, demonstrating that the applied acid decomposition was able to dissolve completely the test portions. Bias of results, estimated by (MV-RV)*100/RV, for BHVO-2, BCR-2, BIR-1, BRP-1 and OU-6, was typically within ±5%. In contrast, bias was larger for some low concentration elements in RGM-1, GSP-2 and GSR-1. However, in most cases the difference between our data and reference values are indistinguishable when the standard deviation associated to each value are considered, as shown in Figure 8.

Large differences from reference values were observed for Ni in BCR-2 and RGM-1. The mean concentration of Ni found in BCR-2, 11.8±0.7 µg g^{-1}, compared to the preferred value of 18±1 µg g^{-1} indicates a bias of -34%. However, our result agrees with ICP-MS data reported by Regnery *et al.* (2010), Liu *et al.* (2008), Mori *et al.* (2007) and Stoll *et al.* (2008), respectively 11±0.9, 11.9, 12±0.4, 12.4±1.3 µg g^{-1} and by Zheng *et al.* (2008), 12.2 µg g^{-1}, using XRF. For RGM-1, the results obtained for Ni ranged from 2.1±0.2 to 2.4±0.1 µg g^{-1}, using Table-top and sintering procedures. No recommended Ni value is available for RGM-1, and comparison was made with data published by Eggins *et al.* (1997), 3.7 µg g^{-1}. The results obtained for Ni in other RM agree with reference values within their uncertainties.

Very consistent results were obtained for Ba using Table-top, Bomb and sintering procedures. The mean results of Ba in BIR-1 are slightly below the reference value (-5%), but are similar to that reported by Willbold and Jochum (2005), 6.73±0.1 µg g^{-1}, using ID-ICP-MS. For other RM, our results for Ba deviate by less than 5% from the reference values, except in GSR-1 dissolved by HPA-S 3, which is 10% lower. Our results with the HPA-S 3 procedure for Ba and Pb in GSP-2 and for Ba in GSR-1 were lower by about 6%, compared to the values obtained with

the other dissolution techniques. However, the recoveries of Ba, Pb and other elements were complete using procedure HPA-S 4b. Comparing procedures HPA-S 3 and HPA-S 4b, the last produced complete recoveries for a wider range of elements and requires a smaller amount of Mg.

The expanded measurement uncertainty (U) for results of BRP-1 and OU-6, calculated following NORDTEST (2004) approach, are presented in Table S2. The footnote of Table S2 illustrates the calculations. U ranges from 7 to 15% for most elements. Among the exceptions of results with higher estimated uncertainties is Cr (U ≈ 20-30%), due to a non systematic bias component. When bias for these two CRM is tested with Eq. 1, the difference between means of results and reference values are not significant.

Conclusions

Classic whole rock dissolution procedures involving HF/HNO$_3$, represented by the Table-top and Bomb procedures, provided reliable results for 41 trace elements by ICP-MS. Such results were important during the establishment of the HPA-S and sintering procedures because they helped to assess the recoveries of these alternative sample decomposition schemes.

The operation of the ICP-MS in dual mode, with optimized conditions for CC and standard mode combined in a single run, allowed the determination of some elements with target isotopes interfered by polyatomic ions with minimal mathematical corrections.

The sintering with the separation of the precipitate and the heating step, as described here, provided full recovery of a large group of analytes and the final analysis of a solution with low salt content.

Among the digestion procedures tested with the HPA-S, that with intermediate temperature, addition of Mg and evaporation with $HClO_4$, was the most effective. Compared to the Bomb, the HPA-S 4b procedure is faster and particularly well suited for the determination of trace element in samples containing resistant minerals, such as granites, shortening considerably the length of the decomposition process. It may also be a promising procedure for fast dissolution of single mineral grains (e.g., zircon), as used in geochronology.

Bias of results of CRM was tested and proved none significant. In general, precision of the replicate analysis and uncertainty of bias contribute similarly to the combined uncertainty.

Acknowledgements

References

Amarasiriwardena D., Krushevska A., Argentine M. and Barnes R.M. (1994)
Vapor-phase acid digestion of micro samples of biological-material in a high-temperature, High Pressure Asher for inductively-coupled plasma-atomic emission-spectrometry. Analyst, 119, 1017-1021.

Awaji S., Nakamura K., Nozaki T. and Kato Y. (2006)
A simple method for precise determination of 23 trace elements in granitic rocks by ICP-MS after lithium tetraborate fusion. Resource Geology, 56, 471-478.

Balaram V., Ramesh S.L. and Anjaiah K.V. (1995)
Comparative study of the sample decomposition procedures in the determination of trace and rare earth elements in anorthosites and related rocks by ICP-MS. Fresenius´ Journal of Analytical Chemistry, 353, 176-182.

Bayon G., Barrat J.A., Etoubleau J., Benoit M., Bollinger C. and Revillon S. (2009)
Determination of rare earth elements, Sc, Y, Zr, Ba, Hf and Th in geological samples by ICP-MS after Tm addition and alkaline fusion. Geostandards and Geoanalytical Research, 33, 51-62.

Catterick T., Fairman B. and Harrington C. (1998)
Structured approach to achieving high accuracy measurements with isotope dilution inductively coupled plasma mass spectrometry. Journal of Analytical Atomic Spectrometry, 13, 1009-1013.

Chao T. and Sanzolone R.F. (1992)
Decomposition techniques. Journal of Geochemical Exploration, 44, 65-106.

Cotta A.J.B., Enzweiler J., Wilson S.A., Pérez C.A., Nardy A.J.R. and Larizzatti J.H. (2007)
Homogeneity of the geochemical reference material BRP-1 (Paraná Basin Basalt) and assessment of minimum mass. Geostandards and Geoanalytical Research, 31, 379-393.

Cotta A.J.B. and Enzweiler J. (2008)
Certificate of analysis of the reference material BRP-1 (Basalt Ribeirão Preto). Geostandards and Geoanalytical Research, 32, 231-235.

Cotta A.J.B. and Enzweiler J. (2009)
Quantification of major and trace elements in water samples by ICP-MS and collision cell to attenuate Ar and Cl-based polyatomic ions. Journal of Analytical Atomic Spectrometry, 24, 1406-1413.

Cremer M. and Schlocker J. (1976)
Lithium borate decomposition of rocks, minerals, and ores. American Mineralogist, 61, 318-321.

Bandura D.R., Baranov V.I., and Tanner S.D. (2001)
Reaction chemistry and collisional processes in multipole devices for resolving isobaric interferences in ICP-MS. Fresenius´ Journal of Analytical Chemistry, 370, 454-470.

Dexter M.A., Reid H.J. and Sharp B.L. (2002)
The effect of ion energy on reactivity and species selectivity in hexapole collision/reaction cell ICP-MS. Journal of Analytical Atomic Spectrometry, 17, 676-681.

Du Z., and Houk R.S. (2000)
Attenuation of metal oxide ions in inductively coupled plasma mass spectrometry with hydrogen in a hexapole collision cell. Journal of Analytical Atomic Spectrometry, 15, 393-388.

Duan D., Hangting C. and Xianjin Z. (2002)
Determination of rare and rare earth elements in soils and sediments by ICP-MS using $Ti(OH)_4$-$Fe(OH)_3$ co-precipitation preconcentration. Journal of Analytical Atomic Spectrometry, 17, 410-413.

Dulski P. (1994)
Interferences of oxide, hydroxide and chloride analyte species in the determination of rare earth elements in geological samples by inductively coupled plasma-mass spectrometry. Fresenius´ Journal of Analytical Chemistry, 350, 194-203.

Dulski P. (2001)
Reference materials for geochemical studies: New analytical data by ICP- MS and critical discussion of reference values. Geostandards Newsletter: The Journal of Geostandards and Geoanalysis, 25, 87-125.

Eggins S.M., Woodhead J.D., Kinsley L.P.J., Mortimer G.E., Sylvester P., McCulloch M.T., Hergt J.M. and Handler MR (1997)
A simple method for the precise determination of >40 trace elements in geological samples by ICPMS using enriched isotope internal standardization. Chemical Geology, 134, 311-326.

Eiden G., Barinaga C.J. and Koppenaal D.W. (1996)
Selective removal of plasma matrix ions in plasma source mass spectrometry. Journal of Analytical Atomic Spectrometry, 11, 317-322.

Epov V.N., Lariviere D., Epova E.N. and Evans R.D. (2004)
Polyatomic interferences produced by macroelements during direct multi-elemental ICP-MS hydrochemical analysis. Geostandards and Geoanalytical Research, 28, 213-224.

Feldman C. (1983)
Behavior of trace refractory minerals in the lithium metaborate fusion-acid dissolution procedure. Analytical Chemistry, 55, 2451-2453.

Feldmann I., Jakubowski N. and Stuewer D. (1999)
Application of a hexapole collision and reaction cell in ICP-MS Part I: Instrumental aspects and operational optimization. Fresenius´ Journal of Analytical Chemistry, 365, 415-421.

Hu Z., Gao S., Liu Y., Hu S., Zhao L., Lia Y. and Wang Q. (2010)
NH_4F assisted high pressure digestion of geological samples for multi-element analysis by ICP-MS. Journal of Analytical and Atomic Spectrometry, 25, 408-413.

ISO Guide 30 (1992)
Terms and definitions used in connection with reference materials (2nd edition). International Organisation for Standardisation (Geneva), 8pp.

Jain J.C., Neal C.R. and Hanchar J.M. (2001)
Problems associated with the determination of rare earth elements of a "Gem" quality zircon by inductively coupled plasma-mass spectrometry. Geostandards Newsletter: The Journal of Geostandards and Geoanalysis, 25, 229-237.

Jarvis K.E. (1990)
A critical evaluation of two sample preparation techniques for low-level determination of some geologically compatible elements by ICP-MS. Chemical Geology, 83, 89-103.

Jochum K.P., Nohl U., Herwig K., Lammel E., Stoll B. and Hofmann A.W. (2005)
GeoReM: A new geochemical database for reference materials and isotopic standards. Geostandards and Geoanalytical Research, 29, 333-338.

Kane J. (2004)
Report of the International Association of Geoanalysts on the certification of Penrhyn Slate, OU-6. Geostandards and Geoanalytical Research, 28, 53-80.

Kato Y., Ohta I., Tsunematsu T., Watanabe Y., Isozaki Y., Maruyama S. and Imai N. (1998)
Rare earth element variations in mid-Archean banded iron formations: Implications for the chemistry of ocean and continent and plate tectonics. Geochimica et Cosmochimica Acta, 62, 3475-3497.

Kleinhanns I.C., Kreissig K., Kamber B.S., Meisel T., Nagler T.F. and Kramers J.D. (2002)
Combined chemical separation of Lu, Hf, Sm, Nd, and REEs from a single sock digest: precise and accurate isotope determinations of Lu-Hf and Sm-Nd using multicollector-ICPMS. Analitycal Chemistry, 74, 67-73.

Leonhard P., Pepelnik R., Prange A., Yamada N. and Yamada T. (2002)
Analysis of diluted sea-water at the ng L^{-1} level using an ICP-MS with an octopole reaction cell. Journal Analytical and atomic Spectroscopy, 22, 189-196.

Liang Q. and Grégoire D.C. (2000)
Determination of trace elements in twenty six Chinese geological reference materials by inductively coupled plasma-mass spectrometry. Geostandards and Geoanalytical Research, 24, 51-63.

Liang Q., Jing H. and Grégoire D.C. (2000)
Determination of trace elements in granites by inductively coupled plasma-mass spectrometry. Talanta, 51, 507-513.

Liu Y.S., Zong K., Kelemen P.B. and Gao S. (2008)
Geochemistry and magmatic history of eclogites and ultramafic rocks from the Chinese continental scientific drill hole: Subduction and ultrahigh-pressure metamorphism of lower crustal cumulates. Chemical Geology, 247, 133-153.

Longerich H.P., Jenner G.A., Fryer and Jackson S.E. (1990)
Inductively coupled plasma mass spectrometric analysis of geological samples: Case studies. Chemical Geology 83, 105-118.

Madinabeitia S.G., Lorda M.E.S. and Ibarguchi J.I.G. (2008)
Simultaneous determination of major to ultratrace elements in geological samples by fusion-dissolution and inductively coupled plasma mass spectrometry techniques. Analytica Chimica Acta, 625, 117-130.

Makishima A. and Nakamura E. (2001)
Determination of total sulfur at microgram per gram levels in geological materials by oxidation of sulfur into sulfate with in situ generation of bromine using isotope dilution high resolution ICP-MS. Analytical Chemistry, 73, 2547-2553.

Makishima A. and Nakamura E. (2006)
Determination of major, minor and trace elements in silicate samples by ICP-QMS and ICP-SFMS applying isotope dilution-internal standardisation (ID-IS) and multi-stage internal standardisation. Geostandards and Geoanalytical Research, 30, 245-271.

Makishima A., Kobayashi K and Nakamura E. (2002)
Determination of chromium, nickel, copper and zinc in milligram samples of geological materials using isotope dilution high resolution inductively coupled plasma-mass spectrometry. Geostandards Newsletter: The Journal of Geostandards and Geoanalysis, 26, 41-51.

McCurdy E. and Woods G. (2004)
The application of collision/reaction cell inductively coupled plasma mass spectrometry to multi-element analysis in variable sample matrices, using He as a non-reactive cell gas. Journal of Analytical Atomic Spectrometry, 19, 607-615.

McGinnis C.E., Jain J.C. and Neal C.R. (1997)
Characterisation of memory effects and development of an effective wash protocol for the measurement of petrogenetically critical trace elements in geological samples by ICP-MS. Geostandards Newsletter: The Journal of Geostandards and Geoanalysis, 21, 289-305.

Meisel T., Moser J., Fellner N., Wegscheider W., Schoenberg R. (2001)
Simplified method for the determination of Ru, Pd, Re, Os, Ir and Pt in chromitites and other geological materials by isotope dilution ICP-MS and acid digestion. Analyst, 126, 322-328.

Meisel T., Schöner N., Paliulionyte V. and Kahr E. (2002)
Determination of rare earth elements, Y, Th, Zr, Hf, Nb and Ta in geological reference materials G-2, G-3, SCo-1 and WGB-1 by sodium peroxide sintering and inductively coupled plasma-mass spectrometry. Geostandards Newsletter: The Journal of Geostandards and Geoanalysis, 26, 53-61.

Mori L., Gómez-Tuena A., Cai Y. and Goldstein S.L. (2007)
Effects of prolonged flat subduction on the Miocene magmatic record of the central Trans-Mexican Volcanic Belt. Chemical Geology, 244, 452-473.

Muller M. and Heumann K.G. (2000)
Isotope dilution inductively coupled plasma quadrupole mass spectrometry in connection with a chromatographic separation for ultra trace determinations of platinum group elements (Pt, Pd, Ru, Ir) in environmental samples. Fresenius´ Journal of Analytical Chemistry, 368, 109-115.

Münker C. (1998)
Nb/Ta fractionation in a Cambrian arc/back arc system, New Zealand, source constraints and application of refined ICP-MS techniques. Chemical Geology, 144, 23-45.

Nakamura K. and Chang Q. (2007)
Precise determination of ultra-low (sub-ng g^{-1}) level rare earth elements in ultramafic rocks by quadrupole ICP-MS. Geostandards and Geoanalytical Research, 31, 185-197.

Navarro M.S., Andrade S., Ulbrich H., Gomes C.B. and Girardi V.A.V. (2008)
The direct determination of rare earth elements in basaltic and related rocks using ICP-MS: Testing the efficiency of microwave oven sample decomposition procedures. Geostandards and Geoanalytical Research, 32, 167-180.

Nelms S.M. (2005)
Inductively coupled plasma mass spectrometry handbook. Blackwell Publishing (Oxford, UK), 485pp.

Niemelä M., Perämäki P., Kola H. and Piispanen J. (2003)
Determination of arsenic, iron and selenium in moss samples using hexapole collision cell, inductively coupled plasma-mass spectrometry. Analytica Chimica Acta, 493, 3-12.

NORDTEST (2004)
Handbook for Calculation of Measurement Uncertainty in Environmental Laboratories. 2º ed., 52pp. (Accessed in http://www.nordtest.org/register/techn/tlibrary/tec537.pdf)

Paliulionyte V. Meisel T., Ramminger P. and Kettisch P. (2006)
High Pressure Asher digestion and an isotope dilution-ICP-MS method for the determination of platinum-group element concentrations in chromitite reference materials CHR-Bkg, GAN Pt-1 and HHH. Geostandards and Geoanalytical Research, 30, 87-96.

Panteeva S.V., Gladkochoub D.P., Donskaya T.V., Markova V.V. and Sandimirova G.P. (2003)
Determination of 24 trace elements in felsic rocks by inductively coupled plasma mass spectrometry after lithium metaborate fusion. Spectrochimica Acta Part B, 58, 341-350.

Petrelli M., Perugini D., Poli G. and Peccerillo A. (2007)
Graphite electrode lithium tetraborate fusion for trace element determination in bulk geological samples by laser ablation ICP-MS. Microchimica Acta, 158, 275-282.

Pretorius W., Weis D., Williams G., Hanano D., Kieffer B. and Scoates J. (2006)
Complete trace elemental characterization of granitoid (USGS G-2, GSP-2) reference materials by high resolution inductively coupled plasma-mass spectrometry. Geostandards and Geoanalytical Research, 30, 39-54.

Raczek I., Stoll B., Hofmann A.W., Jochum K.P. (2001)
High-precision trace element data for the USGS reference materials BCR-1, BCR-2, BHVO-1, BHVO-2, AGV-1, AGV-2, DTS-1, DTS-2, GSP-1 and GSP-2 by ID-TIMS and MIC-SSMS. Geostandards Newsletter: The Journal of Geostandards and Geoanalysis, 25, 77-86.

Raut N.M., Huang L.S., Aggarwal S.K., Lin K.C. (2003)
Determination of lanthanides in rock samples by inductively coupled plasma mass spectrometry using thorium as oxide and hydroxide correction standard. Spectrochimica Acta Part B, 58, 809-822.

Raut N.M., Huang L.S., Lin K.C. and Aggarwal S.K. (2005)
Uncertainty propagation through correction methodology for the determination of rare earth elements by quadrupole based inductively coupled plasma mass spectrometry. Analytica Chimica Acta, 530, 91-103.

Regnery J., Stoll B. and Jochum K.P. (2010)
High-resolution LA-ICP-MS for accurate determination of low abundances of K, Sc and other trace elements in geological samples. Geostandards and Geoanalytical Research, 34, 19-38.

Révillon S. and Hureau-Mazaudier D. (2009)
Improvements in digestion protocols for trace element and isotope determinations in stream and lake sediment reference materials (JSd-1, JSd-2, JSd-3, JLk-1 and LKSD-1). Geostandards and Geoanalytical Research, 33, 397-413.

Robinson P., Higgins N.C. and Jenner G.A. (1986)
Determination of rare-earth elements, yttrium and scandium in rocks by an ion exchange X-ray fluorescence technique. Chemical Geology, 55, 121-137

Robinson P., Townsend A.T., Yu Z. and Münker C. (1999)
Determination of scandium, yttrium and rare earth elements in rocks by high resolution inductively coupled plasma-mass spectrometry. Geostandards Newsletter: The Journal of Geostandards and Geoanalysis, 23, 31-46.

Roy P., Balaram V., Bhattacharaya A., Nasipuri P. and Satyanarayanan M. (2007)
Estimation of Ti, Zr, Nb, Hf, Ta, Th and U in beach placers and ferrodiorites by inductively coupled plasma-mass spectrometry using lithium metaborate fusion digestion technique. Current Science, 93, 1122-1126.

SenGupta J.G. and Bertrand N.B. (1995)
Direct ICP-MS determination of trace and ultratrace elements in geological materials after decomposition in a microwave oven .2. Quantitation of Ba, Cs, Ca, Hf, In, Mo, Nb, Pb, Rb, Sn, Sr, Ta and Tl. Talanta, 42, 947-1957.

Stoll B., Jochum K.P., Herwig K., Amini M., Flanz M., Kreuzburg B., Kuzmin D., Willbold M. and Enzweiler J. (2008)
An automated iridium-strip heater for LA-ICP-MS bulk analysis of geological samples. Geostandards and Geoanalytical Research, 32, 5-26.

Takei H., Yokoyama T., Makishima A. and Nakamura E. (2001)
Formation and suppression of AlF_3 during HF digestion of rock samples in Teflon bombs for precise trace element analyses by ICP-MS and ID-TIMS. Proceedings of the Japan Academy, Series B, 77, 13-17.

Tan S.H. and Horlick G. (1986)
Background spectral features in inductively coupled plasma-mass spectrometry. Applied Spectroscopy, 40, 445-460.

Tanner S.D., Baranov V.I. and Bandura D.R. (2002)
Reaction cells and collision cells for ICP-MS: a tutorial review. Spectrochimica Acta Part B, 57, 1361-1452.

Totland M., Jarvis I. and Jarvis K.E. (1992)
An assessment of dissolution techniques for the analysis of geological samples by plasma spectrometry. Chemical Geology, 95, 35-62.

Totland M., Jarvis I. and Jarvis K.E. (1995)
Microwave digestion and alkali fusion procedures for the determination of the platinum-group elements and gold in geological materials by ICP-MS. Chemical Geology, 124, 21-36

Turner P., Merren T., Speakman J. and Haines C (1997)
Interface studies in the ICP-mass spectrometer, in: G. Holland, S.D. Tanner (Eds.), Plasma Source Mass Spectrometry: Developments and Applications, The Royal Society of Chemistry, Cambridge, 28-34.

VIM (2008)
International vocabulary of metrology - Basic and general concepts and associated terms (VIM). 3rd edition, JCGM 200:2008, 90pp. (http://www.bipm.org/en/publications/guides/vim.html).

Weyer S., Münker C., Rehkämper M. and Mezger K. (2002)
Determination of ultra-low Nb, Ta, Zr and Hf concentrations and the chondritic Zr/Hf and Nb/Ta ratios by isotope dilution analyses with multiple collector ICP-MS. Chemical Geology, 187, 295-313.

Willbold M. and Jochum K.P. (2005)
Multi-element isotope dilution sector field ICP-MS: A precise technique for the analysis of geological materials and its application to geological reference materials. Geostandards and Geoanalytical Research, 29, 63-82.

Wu S., Zhao Y.H., Feng X.B. and Wittmeier A. (1996)
Application of inductively coupled plasma mass spectrometry for total metal determination in silicon-containing solid samples using the microwave-assisted nitric acid-hydrofluoric acid-hydrogen peroxide-boric acid digestion system. Journal of Analytical Atomic Spectrometry, 11, 287-296.

Yamada N., Takahashi J. and Sakata K. (2002)
The effects of cell-gas impurities and kinetic energy discrimination in an octopole collision cell ICP-MS under non-thermalized conditions. Journal of Analytical Atomic Spectrometry, 17, 1213-1222.

Yang L., Lam J.W.H., Sturgeon R.E., McLaren J.W. (1998)
Decomposition of marine sediments for quantitative recovery of chromium and inductively coupled plasma mass spectrometric analysis. Journal of Analytical Atomic Spectrometry, 13, 1245-1248.

Yokoyama T., Makishima A. and Nakamura E. (1999)
Evaluation of the coprecipitation of incompatible trace elements with fluoride during silicate rock dissolution by acid digestion. Chemical Geology, 157, 175-187.

Yu Z., Norman M.D. and Robinson P. (2003)
Major and trace element analysis of silicate rocks by XRF and laser ablation ICP-MS using lithium borate fused glasses: Matrix effects, instrument response and results for international reference materials. Geostandards Newsletter: The Journal of Geostandards and Geoanalysis, 27, 67-89.

Yu Z., Robinson P. and McGoldrick P. (2001)
An evaluation of methods for the chemical decomposition of geological materials for trace element determination using ICP-MS. Geostandards Newsletter: The Journal of Geostandards and Geoanalysis, 25, 199-217.

Yu Z., Robinson P., Townsend A.T., Münker C. and Crawford A.J. (2000)
Determination of high field strength elements, Rb, Sr, Mo, Sb, Cs, Tl and Bi at ng g-1 levels in geological reference materials by magnetic sector ICP-MS after HF/HClO$_4$ high pressure digestion. Geostandards Newsletter: The Journal of Geostandards and Geoanalysis, 24, 39-50.

Zheng J.P., Sun M., Griffin W.L., Zhou M.F., Zhao G.C., Robinson P., Tang H.Y. and Zhang Z.H. (2008)
Age and geochemistry of contrasting peridotite types in Dabie UHP belt, eastern China: Petrogenetic and geodynamic implications. Chemical Geology, 247, 282-304.

Supporting Information

Table S1. Procedural blanks and detection limits (DL), expressed as equivalent concentration ($\mu g\ g^{-1}$) in the sample considering a dilution factor of 5000

Element	Table-top and Bomb		HPA-S 3		HPA-S 4b		Sintering 1and 2		Sintering 3	
	Blank	DL	Blank	DL	Blank	DL	Blank	DL	Blank	DL
Li	0.06	0.09	0.10	0.12	0.03	0.05				
Be	0.01	0.01	0.01	0.02	0.01	0.02				
Sc	0.02	0.03	0.01	0.03	0.01	0.02	0.04	0.12	0.05	0.12
V	0.05	0.1	1.2	2.0	0.2	0.4				
Cr	0.2	0.2	1.5	1.8	0.9	1.0				
Co	0.03	0.04	0.2	0.3	0.1	0.2	0.05	0.11	0.06	0.16
Ni	0.2	0.3	1.0	1.2	0.8	0.9	1.8	2.0	2.0	2.2
Cu	0.3	0.3	1.0	1.1	0.2	0.2				
Zn	0.5	0.6	0.6	1.3	1.3	2.5				
Ga	0.01	0.01	0.2	0.3	0.01	0.02				
Rb	0.07	0.08	0.3	0.5	0.06	0.08				
Sr	0.2	0.2	0.8	0.9	0.3	0.5	6	8	5	7
Y	0.01	0.01	0.22	0.23	0.07	0.09	0.20	0.22	0.04	0.10
Zr	0.1	0.2	0.3	0.4	0.1	0.2	3.5	5.0	3.6	5.8
Nb	0.01	0.01	0.04	0.06	0.00	0.01	0.02	0.03	0.3	0.6
Mo	0.04	0.05	0.06	0.18	0.04	0.08				
Cd	0.01	0.03	0.02	0.03	0.01	0.03	0.03	0.05	0.04	0.1
Sn	0.02	0.03	0.04	0.07	0.01	0.05	0.12	0.15	0.08	0.2
Sb	0.01	0.01	0.1	0.2	0.1	0.1	0.01	0.02	0.01	0.03
Cs	0.005	0.008	0.01	0.03	0.01	0.02				
Ba	0.22	0.32	2.2	3.5	0.5	1.0	0.8	1.3	1.4	1.9
La	0.01	0.01	0.2	0.3	0.01	0.02	0.02	0.03	0.06	0.1
Ce	0.01	0.01	0.4	0.5	0.05	0.1	0.06	0.06	0.09	0.2
Pr	0.01	0.01	0.05	0.05	0.004	0.006	0.00	0.01	0.01	0.02
Nd	0.002	0.008	0.1	0.2	0.015	0.021	0.01	0.02	0.03	0.08
Sm	0.001	0.006	0.02	0.03	0.001	0.002	0.003	0.006	0.003	0.02
Eu	0.000	0.005	0.003	0.003	0.000	0.000	0.001	0.002	0.002	0.004
Gd	0.001	0.006	0.04	0.04	0.015	0.019	0.002	0.004	0.01	0.02
Tb	0.001	0.006	0.01	0.02	0.008	0.008	0.001	0.003	0.002	0.005
Dy	0.001	0.006	0.01	0.01	0.009	0.015	0.001	0.001	0.004	0.01
Ho	0.001	0.004	0.002	0.002	0.001	0.002	0.001	0.003	0.001	0.005
Er	0.001	0.003	0.002	0.004	0.001	0.002	0.001	0.003	0.001	0.004
Tm	0.001	0.003	0.001	0.001	0.001	0.002	0.001	0.003	0.001	0.004
Yb	0.001	0.005	0.02	0.02	0.009	0.011	0.001	0.002	0.002	0.005
Lu	0.001	0.003	0.001	0.002	0.001	0.003	0.001	0.003	0.001	0.003
Hf	0.004	0.01	0.005	0.01	0.001	0.002	0.02	0.06	0.04	0.07
Ta	0.003	0.005	0.003	0.007	0.004	0.008				
W	0.05	0.05	0.01	0.01	0.003	0.007				
Pb	0.03	0.03	0.2	0.3	0.1	0.2	0.2	0.4	0.3	0.5
Th	0.01	0.02	0.03	0.05	0.09	0.02	0.03	0.07	0.03	0.08
U	0.003	0.004	0.008	0.009	0.002	0.004				

Table S2. Bias (A), relative standard measurement uncertainty (B), expanded uncertainties of CRM divided by respective coverage factor, uncertainty of bias (u_{bias}) and expanded measurement uncertainties (U) calculated for BRP-1 and OU-6. All terms are expressed as %.

	BRP-1 (Table-top procedure)						OU-6 (Bomb procedure)					
	Bias	$RSD_{MV}/\sqrt{n}$	U_{VR}/k	u_{bias}	RSD_{MV}	U	Bias	$RSD_{MV}/\sqrt{n}$	U_{VR}/k	u_{bias}	RSD_{MV}	U
	A	B	C	D		E	A	B	C	D		E
Li							*2.8*	*2.0*	*1.9*	*4.0*	6.1	*14.6*
Be							*-5.1*	*4.2*	*5.3*	*8.5*	12.5	*30.2*
Sc	1.8	0.9	1.4	2.4	3.4	8.3	-3.0	2.1	6.5	7.5	6.3	19.5
V	3.6	0.8	0.9	3.8	3.2	9.9	1.7	1.8	1.9	3.1	5.3	12.3
Cr	-8.1	1.6	4.0	9.2	6.1	22.0	11.7	3.4	1.4	12.3	10.1	31.9
Co	1.3	1.4	1.9	2.7	5.3	11.9	-4.1	2.4	1.8	5.1	7.1	17.5
Ni	-1.7	1.1	1.9	2.8	4.3	10.3	7.0	2.3	1.5	7.5	9.3	20.5
Cu	1.3	1.1	0.9	1.9	4.3	9.4	6.4	2.3	5.6	8.9	7.0	22.5
Zn	3.5	1.2	0.7	3.8	4.8	12.2	-3.1	2.2	1.5	4.0	6.5	15.3
Ga	0.8	2.1	1.2	2.5	8.0	16.8	3.4	1.3	1.4	3.9	4.0	11.2
Rb	1.7	0.7	1.4	2.3	2.8	7.3	-3.5	2.6	1.6	4.6	7.7	18.0
Sr	1.2	0.8	0.6	1.6	3.2	7.2	-1.3	1.3	1.0	2.1	3.8	8.7
Y	0.0	1.2	1.2	1.7	4.8	10.2	-3.4	1.2	1.3	3.9	4.9	10.7
Zr	1.0	1.0	0.8	1.6	3.8	8.2	-1.3	1.7	1.6	2.7	5.2	11.7
Nb	-0.3	0.9	1.5	1.8	3.4	7.7	-4.1	2.2	1.9	5.0	6.5	16.4
Sn							0.4	1.0	3.1	3.3	3.0	8.9
Sb							*1.8*	*2.3*	*9.0*	*9.5*	7.0	*23.6*
Cs	0.0	2.1	2.7	3.4	8.1	17.6	-2.5	1.7	1.6	3.4	5.1	12.2
Ba	-0.5	0.6	0.6	1.0	2.2	4.8	-1.3	1.3	1.3	2.2	4.0	9.2
La	-1.4	0.6	1.2	1.9	2.4	6.2	-0.6	2.0	2.6	3.3	6.1	13.8
Ce	-0.3	0.6	0.6	0.9	2.2	4.8	-1.4	0.9	1.7	2.4	2.6	7.1
Pr	-2.4	0.4	0.8	2.6	1.7	6.2	-0.1	1.3	1.6	2.0	3.8	8.6
Nd	-0.6	0.4	0.9	1.1	1.6	3.9	-0.7	1.1	2.4	2.7	3.3	8.6
Sm	0.0	0.5	0.9	1.0	1.8	4.1	-0.2	1.1	3.3	3.5	3.3	9.7
Eu	-0.6	0.8	1.2	1.5	2.9	6.5	-0.7	1.2	1.8	2.3	7.4	8.7
Gd	-1.0	0.5	1.4	1.8	1.9	5.2	0.0	0.6	3.4	3.4	1.9	7.8
Tb	-1.3	0.5	1.6	2.2	2.0	5.9	-2.3	1.2	2.2	3.4	3.6	9.9
Dy	0.0	0.6	1.8	1.9	2.4	6.1	0.8	0.7	1.3	1.7	2.0	5.1
Ho	-1.2	0.6	1.9	2.3	2.5	6.8	-1.0	1.0	2.3	2.7	2.9	7.9
Er	0.0	0.6	1.2	1.3	2.4	5.5	3.1	0.9	3.5	4.8	2.6	10.9
Tm	0.0	0.9	1.8	2.0	3.5	8.0	*2.2*	*2.2*	*2.1*	*3.7*	6.5	*15.0*
Yb	-0.6	0.6	1.3	1.5	2.3	5.5	2.7	0.8	1.6	3.2	2.3	7.9
Lu	0.0	0.5	2.0	2.1	2.0	5.8	4.4	1.4	2.1	5.1	4.3	13.3
Hf	1.3	1.0	1.3	2.0	3.7	8.4	4.3	1.4	3.2	5.5	4.1	13.7
Ta	-1.5	1.1	2.0	2.8	4.1	9.9	-3.9	1.4	5.5	6.9	4.1	16.0
Pb	0.0	0.9	2.7	2.9	3.6	9.2	-2.8	1.2	1.3	3.3	3.6	9.7
Th	-1.8	0.7	1.3	2.3	2.6	6.9	-3.5	3.1	4.3	6.3	9.2	22.3
U	0.0	0.6	1.8	1.9	2.4	6.2	-1.0	1.8	2.2	3.0	5.3	12.1

Mo. Cd and W are absent because there are no reference values. Data of OU-6 in *italic* were calculated using informative values.

Example: La in BRP-1

A = Bias (%) = (MV-RV)*100/RV

    A = (42-42.6)*100/42.6 = -1.41 %

B = $RSD_{MV}/\sqrt{n}$ = 2.4/√15 = 0.61 %

C = (U_{RV}/k)*100/RV

    C = (1/2)*100/42.6 = 1.17 %

D = uncertainty of bias = u_{bias} (%) = $(A^2+C^2+D^2)^{1/2}$

    D = $(-1.41^2+0.61^2+1.17^2)^{1/2}$ = 1.93%

E = expanded measurement uncertainty = U (%) = $k*(u^2_{bias}+ RSD^2_{MV})^{1/2}$

    E = $2*(1.93^2+2.4^2)^{1/2}$ = 6.2%.

MV and RV = mean of results and reference values; n = number of dissolutions; SD_{MV} = standard deviation of the mean; U_{VR} = expanded uncertainty of the reference value; k = coverage factor

ANEXO IV

Artigo em preparação: Cotta AJB e Enzweiler J.

Determination of Cr, Ni, Cu, Zn, Sr and Sn in geochemical reference materials by isotope dilution inductively coupled plasma mass spectrometry.

Determination of Cr, Ni, Cu, Zn, Sr and Sn in geochemical reference materials by isotope dilution inductively coupled plasma mass spectrometry

Introduction

Reference materials (RM) play a crucial role in geochemical measurements. Its use comprehends the development and validation of analytical methods, the calibration of instruments and the establishment of quality control and assurance protocols. In summary, analysis of RM constitutes a major procedure to establish the traceability of measurements (Kane 2001, Kane and Potts 2002, 2007).

However, the successful use of a RM is compromised by the lack of reference values and by the indication of values with large uncertainties. For instance, RM are frequently analyzed to check the measurement bias, but to test the bias significance uncertainties related to both the measurement result and the reference value should be taken in account (ISO Guide 33, 2000). Obviously, the power of such test in detecting a significant bias diminishes as uncertainty of the RM increases. The indication of reference values with small uncertainties is also essential when RM are used for calibration purposes, because its uncertainties are directly transferred to the measurement result. In these cases, traceability cannot be supported in the absence of fitted-for-purpose uncertainties for each reference value (Kane and Potts 2002, 2007).

Only a few geochemical RM have been characterized following procedures that confer than the status of certified reference materials (CRM), in accordance with ISO Guide 35 (2006). As a result many non-certified MR were issued with insufficient characterization and/or with values having uncertainties that are overly large in comparison with the precision achieved by the

use of modern instruments. This is particularly true in the case of trace elements where advances in techniques now permit precise determinations at low concentrations.

Examples of this problematic situation occur to Cr, Ni, Cu, Zn, Sr and Sn in many RM of basaltic and granitic composition, especially to older RM, which characterization occurred with less precise methods than those currently available in most laboratories. This group of elements is frequently analyzed but most users of geochemical data do focus more on other sets of elements, like high field strength and rare earth elements (respectively HFSE and REE). Much attention has been given to the accurate measurement of REE and as a result such capability has been transferred to the characterization of RM. However, the same did not occur for Cr, Ni, Cu, Zn, Sr and Sn. Therefore, the development of accurate analytical methods to measure these elements is absolutely essential to further progresses in RM characterization.

For many trace elements the isotope dilution mass spectrometry (ID-MS) technique can provide precise and accurate results in different matrices (Heumann 1992, Klingbeil *et al*. 2001, Heumann 2004, Willbold and Jochum 2005). ID-MS measurements made by inductively coupled plasma mass spectrometry with quadrupole analyzer (ID-ICP-QMS) allows the determination of a group of elements in a single run with adequate precision to ICP-QMS many cases (Becker and Dietze1998, Heumann *et al*. 1998, Klingbeil *et al*. 2001, Pin *et al*. 2003, Vogl 2007).

In this work we apply ID-ICP-MS to measure Cr, Ni, Cu, Zn, Sr and Sn in a set of silicate rock RM, with the objectives of developing a valid measurement procedure and contributing with an accurate data set for further RM studies.

Experimental

Reagents

Pure water prepared by means of a Milli-Q water purification system (resistivity 18 MΩ cm, Millipore, USA) was used throughout the experiments. Concentrated acids (HF, HNO_3, HCl and $HClO_4$), obtained from Merck (reagent A.C.S.) were purified by sub-boiling distillation. Isotopic enriched tracers, with certified isotopic compositions, were obtained (^{53}Cr, oxide) from Oak Ridge National Laboratory (USA) and (^{61}Ni, ^{65}Cu, ^{68}Zn, ^{86}Sr and ^{122}Sn, solutions) from Alfa Aesar (USA). The ^{53}Cr oxide was dissolved by heating with few drops of perchloric acid in a capped 23 ml PFA vessel (Savillex, USA) for 30 minutes and the spike was stabilized in 2% HNO_3. The final concentration of Cr in the spike solution was checked by reverse ID-MS. Single element standard solutions (10.00 ± 0.03 µg ml^{-1}, High Purity Standards, HPS, USA, with densities informed by producer after contact), whose certified concentrations are traceable to the NIST SRM 3100 series, were gravimetrically diluted and used to prepare the mass discrimination calibration blend. All weighing were performed with an analytical balance (Sartorius, Germany). Plastic containers, pipette tips and tubes were cleaned with a mixture of 8% HNO_3 + 2% HCl and rinsed with pure water.

Sample analyses

Isotope ratios were measured with an *Xseries^{II}*, ICP-MS equipped with collision cell (CC) technology (Thermo, Germany). The instrument settings are outlined in Table 1. To attenuate possible polyatomic interferences (such as ^{35}Cl^{16}O^{1}H$^+$ on ^{52}Cr$^+$, ^{44}Ca^{16}O$^+$ on ^{60}Ni$^+$, ^{40}Ar^{23}Na$^+$ on

$^{63}Cu^+$, $^{40}Ar^{26}Mg^+$ on $^{66}Zn^+$, $^{40}Ar^{48}Ti^+$ on $^{88}Sr^+$, $^{40}Ar_3^+$ on $^{120}Sn^+$) the measurements were performed in collision cell mode, according to Cotta and Enzweiler (2010).

The measurements for isotope ratio calculations were acquired in peak jump mode, with 1 point per mass peak and dwell times established according to the expected signal intensity. Isotope ratios are the mean of 5 sets of 100 intensity ratios after dead time correction (Nelms *et al.* 2001) and background subtraction using 2% HNO_3. Samples were introduced by autosampler SC-FAST (Elemental Scientific, USA). The measurement sequence consisted in analyzing a blank and the calibration blend every five samples.

Table 1. Operation condition of the quadrupole ICP-MS and isotopes measured

Incident power	1.4 kW
Extraction	-210 to -160 V
Plasma Ar flow rate	13 l min^{-1}
Auxiliary Ar flow rate	0.8 l min^{-1}
Nebulizer flow	0.82 to 0.83 l min^{-1}
Measurements	5 x 100 scans
Hexapole bias	-17 V
Quadrupole bias	-14 V
7% H_2 in He	3.5 ml min^{-1}
Isotopes	Dwell time (ms)
$^{52,53}Cr$, $^{60,61}Ni$, $^{120,122}Sn$	30
$^{63,65}Cu$, $^{66,68}Zn$, $^{86,88}Sr$	20
$^{49}Ti^*$, $^{44}Ca^*$, $^{137}Ba^*$	10

* used in mathematical corrections.

The precision of isotope ratio measurement were mostly between 0.2 and 0.5%. Corrections were applied to account for interferences of oxides and hydroxides of Ca and Ti and of double charged Ba on Ni, Cu and Zn isotopes, as indicated in Table 2. The coefficients of these corrections were established by repeated analyzes of solutions containing the interfering element at levels corresponding to those found in the samples. For some RM the ratio $^{87}Sr/^{86}Sr$ was determined in non-spiked aliquots, in these measurements the overlap of ^{87}Rb on ^{87}Sr was

subtracted mathematically, as done for the polyatomic interferences. The impact of such corrections was also included in the uncertainty budget of the result.

Table 2. Mathematical corrections applied to account for interferences in target isotopes

Isotope	Equation
^{60}Ni	^{60}C-0.00020(2)*^{44}Ca
^{61}Ni	^{61}C-0.00024(3)*^{44}Ca
^{63}Cu	^{63}C-0.0021(1)*^{49}Ti
^{65}Cu	^{65}C-0.0023(1)*^{49}Ti-0.0010(1)*^{137}Ba
^{66}Zn	^{66}C-0.0024(1)*^{49}Ti-0.0008(1)*^{137}Ba
^{68}Zn	^{68}C-0.035(3)*^{137}Ba
^{87}Sr	^{87}C-0.400(2)*^{85}Rb

^{x}C represents the total count rates obtained for isotope x. The numbers in parentheses is the uncertainty, given as one standard deviation (1s), in the last digit of the correction coefficient.

Isotope dilution

Isotope dilution analysis relies on the alteration of the isotopic composition of an element in a sample by the addition of a known amount of an enriched isotope of the same element (called spike). Sample and spike(s) are mixed and a complete isotopic equilibration must be reached. This has important implications for application to determinations in rocks samples because they must be fully decomposed. On the other side, after the isotope equilibration further treatments admit small losses that are compensated with a loss of the spike in the same proportion, and thus does not influence the final results.

The general double ID-MS equation can be expressed by Eq. 1:

$$C_X = C_Z \frac{m_y}{m_x} \times \frac{m_{zc}}{m_{y_c}} \times \left(\frac{R_y - R_{xy} \times K}{R_{xy} \times K - R_z}\right) \times \left(\frac{R_{Bc} - R_z}{R_y - R_{Bc}}\right) \times \frac{\sum\limits_i R_{xi} \times K_i}{\sum\limits_i R_{zi} \times K_i} \qquad (1)$$

In double ID-MS technique the spike is characterized by a primary assay (or as in this study by a calibration standard), where C means concentration; m mass; R the isotope ratio a/b, between a, the most abundant isotope in the sample, and b the most abundant in the spike; x, y

and z refers to sample, spike and calibration standard; K is the mass discrimination factor, which was obtained dividing the calculated isotope ratio (R_{Bc}) by the mean of the measured isotope ratio ($R_{Bc(mean)}$) in the calibration blend, analyzed after and before the sample blend. The calculated ratio (R_{Bc}) was estimated using the amount of the spike added to a previously diluted calibration standard (CS) solution with assumed natural isotopic composition (Böhlke *et al.* 2005). The informed concentration and isotopic composition of the spike were also considered in the calculation of the isotope ratio (R_{Bc}) in the calibration blend (CS+spike). The calibration blend was run every five samples, and corrections for mass discrimination were applied using the bracketing technique (Briche *et al.* 2001).

The value of ratio, R_{Bc}, was estimated using Eq. 2:

$$R_{Bc} = \frac{C_z \times m_{z_c} \times A_z^a + C_y \times m_{y_c} \times A_y^a}{C_z \times m_{z_c} \times A_z^b + C_y \times m_{y_c} \times A_y^b} \qquad (2)$$

Where, A is the isotopic abundance; m_{zc} and m_{yc} are the mass of previously diluted CS and spike used to prepare the calibration blend. For Cr, Ni, Cu, Zn and Sn significant differences in the isotopic composition between sample and calibration standard are not expected, and Eq. (1) can be simplified to Eq. (3):

$$C_X = C_z \frac{m_y}{m_x} \times \frac{m_{z_c}}{m_{y_c}} \times \left(\frac{R_y - R_{xy} \times K}{R_{xy} \times K - R_z} \right) \times \left(\frac{R_{Bc} - R_z}{R_y - R_{Bc}} \right) \qquad (3)$$

However, such assumption ($\Sigma R_{xi} \approx \Sigma R_{zi}$) is not always true for Sr, since the pair Rb and Sr is involved in a long-lived natural radioactive decay scheme (^{87}Rb→^{87}Sr), which can change the

isotopic composition of the these elements in the sample. Thus, besides measuring the ratio ^{88}Sr/^{86}Sr in the sample+spike blend (R_{xy}), the ^{87}Sr/^{86}Sr ratio in the sample is also required to calculate the Sr concentration. To some of the RM analyzed the ^{87}Sr/^{86}Sr was taken from published data and in absence of such information, it was determined experimentally. As the

$$C_X = C_Z \frac{m_y}{m_x} \times \frac{m_{zc}}{m_{y_c}} \times \left(\frac{R_y - R_{xy} \times K}{R_{xy} \times K - R_z} \right) \times \left(\frac{R_{Bc} - R_z}{R_y - R_{Bc}} \right) \times \frac{\left(9.432 + \left({}^{87}Sr/{}^{86}Sr \right)_x \times K' \right)}{10.142} \times \left(\frac{m_{sam\ sol}}{m_{aliquot}} \right) \quad (4)$$

remaining isotopic ratios (^{88}Sr/^{86}Sr, ^{84}Sr/^{86}Sr) in the sample and all the ratios in spike are fixed, the Eq. (1) is rewritten to Eq. (4):

Where the values *9.432* and *10.142* correspond respectively to $[(^{88}Sr/^{86}Sr)_x + (^{86}Sr/^{86}Sr)_x + (^{84}Sr/^{86}Sr)_x = 8.375+1+0.057 = 9.432]$ and $[\Sigma R_{zi} = (^{88}Sr/^{86}Sr)_z + (^{87}Sr/^{86}Sr)_z + (^{86}Sr/^{86}Sr)_z + (^{84}Sr/^{86}Sr)_z = 10.142]$. Been *K'* is the mass discrimination factor for the $(^{87}Sr/^{86}Sr)_x$ ratio measured in a non-spiked aliquot of the sample. Given the relatively high concentration of Sr in the analyzed RM, it was more convenient to add the spike in just one aliquot ($m_{aliquot}$) of the sample solution ($m_{sam\ sol}$), instead of spiking the whole test portion before dissolution.

Following the isotope dilution Eq. 3 and 4, the concentration of the analytes in the samples were calculated. The combined measurement uncertainty associated with each determination was calculated combining the standard uncertainties of the different quantities involved in Eq. 3 and 4 using the spreadsheet method developed by Kragten (1994) and uncertainty propagation procedures according Eurachem/Citac guide (2000). The reported final result was calculated as the mean of all replicates analyzed with it resultant combined uncertainty. An example of the calculus is given in the appendix A.

Reference materials, dissolution procedures and spiking

A set of RM of silicate rocks were analysed in this study: BCR-2 (basalt), GSP-2 (granodiorite), AGV-1 (andesite), RGM-1 and RGM-2 (rhylotes) and G-3 (granite) all produced by the US Geological Survey (RGM-2 and G-3 are still under characterization process), GSR-1 (granite) provided by the Institute of Geophysical and Geochemical Prospecting (IGGE, China), OU-6 (slate) produced by the International Association of Geoanalysts (IAG, Kane 2004) and BRP-1 (basalt) produced in a joint project between Brazilian institutions and the USGS (Cotta and Enzweiler 2008) and distributed by Brazilian Geological Survey.

Test portions, ranging from 30 to 100 mg, were decomposed according validated procedures (Cotta and Enzweiler 2010) involving HF/HNO_3 dissolution in PFA vessels for basalts (Table-top) and in PTFE bombs for non-basaltic samples (Bomb). In order to minimize the consumption of the spikes of ^{53}Cr, ^{61}Ni, ^{65}Cu, ^{68}Zn and ^{122}Sn, only small test portions were spiked before dissolution, and when test portions of 100 mg where used, spikes were added to one weighted aliquot of the sample solution after dissolution. Independently of the test portion mass, the spike of ^{86}Sr was added to one aliquot of the sample solution, which was analyzed in separated to keep counts in pulse counting mode. The remaining analytes could be determined in the same aliquot. When samples were skiped prior dissolution, the smaller size of the test portion was 30 mg, to minimize errors during the weighting of small masses and because RM are not expected to be homogeneous in few tens of milligrams scale (Cotta and Enzweiler 2007). After dissolution, sample solutions were carefully diluted to achieve a nitric acid content of 2% (v/v) with final dilution factor larger than 1000 fold.

Three procedural blanks were prepared for each dissolution technique and measured using the same procedure as for the samples. The blank result was subtracted and the associate uncertainty included in the combined uncertainty of the final determination result.

The amount of spike added to the test portions or solution aliquots was carefully estimated aiming to minimize error magnification effects from overspiking or underspiking and to diminish as much as possible non-linearity effects and dead time corrections of the detector system (Heumann 1988). These two last effects can be canceled out by matching the signal intensity and isotope ratios of the CS+spike and sample+spike blends (Catterick *et al.* 1998). However, while it is possible to match the ratios for all the samples, the matching of concentrations requires the preparation of a calibration blend to each sample, which is not practical. Therefore, just one calibration blend was prepared containing mean analyte concentrations of the analysed sample solutions.

The impact of detector dead time is eliminated when ratios close to unit are measured. Therefore, the amount of spike added to the sample (and thus, the blends ratio) was chosen as a compromise between minimizing dead time and non-linearity problems and keeping error magnification factor low. This compromise is achieved by choosing ratios close to the unit without being too far from the optimum theoretical ratio. The Table 3 summarizes the data involved in these calculations.

Table 3. Isotopic composition of the sample, spike, and optimum and chosen ratios for the blends with respective error magnification factor

Isotope	Natural[*]	Spike	R_x	R_y	R_{opt} ($Q_{min.}$)	R_{Blends} (Q)
^{52}Cr	83.789 ± 0.009	2.65 ± 0.02	8.819 ± 0.008	0.0273 ± 0.0001	0.49 (1.12)	1.0 (1.15)
^{53}Cr	9.501 ± 0.009	97.20 ± 0.02				
^{60}Ni	26.223 ± 0.008	5.18 ± 0.003	23.005 ± 0.0007	0.0562 ± 0.0001	1.14 (1.10)	1.0 (1.11)
^{61}Ni	1.140 ± 0.001	92.11 ± 0.05				
^{63}Cu	69.15 ± 0.08	0.10 ± 0.04	2.241 ± 0.006	0.0010 ± 0.0003	0.05 (1.04)	0.3 (1.16)
^{65}Cu	1.14 ± 0.08	99.90 ± 0.04				
^{66}Zn	27.98 ± 0.04	1.80 ± 0.01	1.471 ± 0.005	0.0189 ± 0.0001	0.17 (1.25)	0.3 (1.32)
^{68}Zn	19.02 ± 0.06	95.40 ± 0.14				
^{88}Sr	82.580 ± 0.005	2.68 ± 0.01	8.375 ± 0.004	0.0280 ± 0.0001	0.48 (1.12)	1.0 (1.16)
^{86}Sr	9.860 ± 0.005	95.64 ± 0.19				
^{120}Sn	32.58 ± 0.05	1.10 ± 0.001	7.04 ± 0.02	0.01178 ± 0.00003	0.29 (1.09)	0.9 (1.16)
^{122}Sn	4.63 ± 0.02	93.40 ± 0.21				

Representative isotopic composition Böhlke *et al.* (2001). Uncertainties given as 1s. R_{opt} is the optimum theoretical isotope ratio to achieve minimum error magnification factor (Q_{min}). R_{Blends} is the ratio chosen to be used in the preparation of the blends (sample+spike and CS+spike) with its respective error magnification factor (Q). $R_{opt} = (R_x.R_y)^{1/2}$ and $Q = (R_{xy}(R_y-R_x))/((R_{xy}-R_x).(R_y-R_{xy}))$, where R_{xy}, R_x and R_y are defined as *b/a*.

For Cr, Ni, Sr and Sn the R_{opt} are favorable and therefore it was possible to select values for the ratios, which are equal or very close to unit without significant increase in the error magnification factor. This also diminished the consumption of the spikes of ^{53}Cr, ^{86}Sr and ^{122}Sn. However, for Cu and Zn the R_{opt} is not favorable for determination and its use would imply in significant corrections for dead time. Therefore, the ratio of 0.3 was selected since it diminishes the impact of dead time correction without increasing Q, as can be seen in the Figure 1, and again diminishes the amount of spike consumed. Note that for Cu and Zn the use of a ratio close to unit was avoided because it would imply in a great elevation in the error magnification factor.
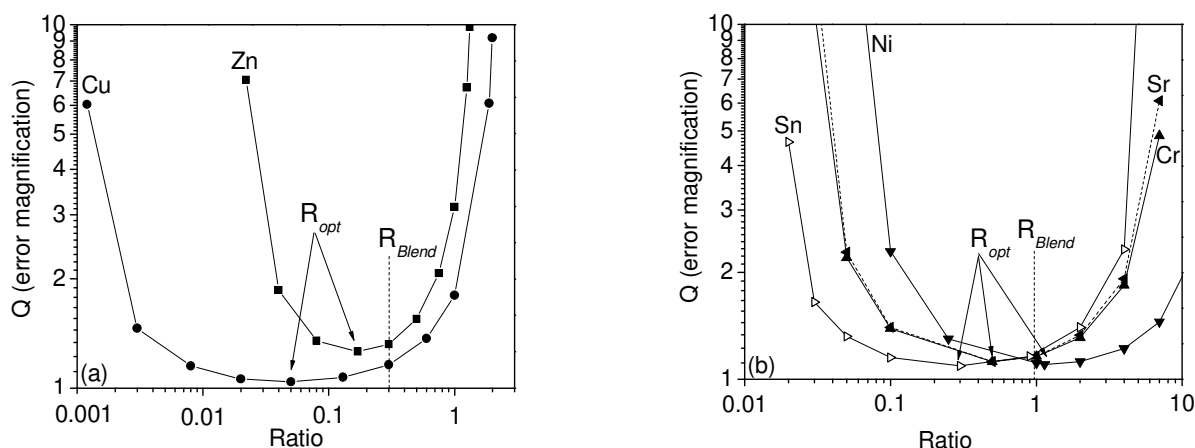
Figure 1. Error magnification for different ratios of Cu and Zn (a), Cr, Ni, Sr and Sn (b). The selected ratio(R_{Blend}) favors the measurement without significant elevation in Q (Heumann 1988).

Results

The key requirement to obtain reliable results by ID-ICP-MS is the accurate and precise determination of isotope ratios in the sample blend. However, during ICP-MS measurements the recorded value differs from the true ratio in the blend because of mass discrimination effect (Heumann *et al.* 1998). To correct such effect, a gravimetrically prepared calibration blend solution was analyzed repeatedly to calculate mass discrimination factors (K), as defined above.

The K factors showed no significant change over the measurement sequence, remaining stable within the isotope ratio precision ($\approx 0.3\%$), even though sensitivity had decreased up to 10 to 15% by the end of the measurements. The mass discrimination (*MD*) per mass unit, *MD=(K-1)*100/Δm*, varied from 6 to 3.4% for $^{52}Cr/^{53}Cr$ and $^{120}Sn/^{122}Sn$, respectively. The stability of K factors was essential to properly correct the isotope ratios measured in the sample blends and so to obtain results with small uncertainties.

In Table 4 results of individual determinations are presented with it combined standard measurement uncertainty. Test portion mass and the spiking technique (*i.e.* whether the spike was added before or after sample decomposition) are also indicated. Each test portion represents one different dissolution, spiking and analyses of the RM. The mean of the individual determinations, followed by the resultant combined standard measurement uncertainty (*u*), are presented together with reference value (RV) for each element.

The reference material AGV-1, despite no longer available, was analyzed because published values obtained by ID-MS are available for comparison for all elements determined in this study. These published values are presented for comparison.

Table 4. Individual results with respective combined standard measurement uncertainties for each test portion and mean value of all determinations with resultant combined uncertainty (in mg kg^{-1})

RM	Cr	RV	Ni	RV	Cu	RV	Zn	RV	Sr	RV	Sn	RV
BCR-2												
(30 mg, BD)	16.8±0.2		14.7±0.3		18.3±0.2		132±2		335±3		2.03±0.02	
(30 mg, BD)	16.4±0.2		14.7±0.3		18.7±0.2		133±2		334±2		2.04±0.02	
(100 mg, AD)	16.4±0.1		14.5±0.3		18.2±0.2		132±2		332±2		2.02±0.02	
(100 mg, AD)	16.4±0.1		14.5±0.3		18.4±0.2		130±2		334±2		2.03±0.02	
mean±u	*16.5±0.3*	*18±2*	*14.6±0.4*	*-*	*18.4±0.3*	*19±2[a]*	*133±3*	*127±9*	*334±3*	*346±12*	*2.03±0.03*	*-*
BRP-1[#]												
bottle 1	10.5±0.1		23.2±0.3		159.7±0.7		141.7±1.4		495±2		2.50±0.02	
bottle 1	10.8±0.1		23.6±0.4		159.8±0.6		140.9±1.4		502±2		2.48±0.02	
bottle 2	10.8±0.1		23.6±0.3		161.0±0.8		140.6±1.3		491±2		2.52±0.02	
bottle 2	10.4±0.1		23.4±0.3		159.2±0.8		141.2±1.5		487±2		2.46±0.02	
bottle 3	10.7±0.1		23.4±0.4		158.4±0.8		141.4±1.4		491±2		2.48±0.02	
bottle 3	10.6±0.1		23.7±0.4		160.5±0.7		140.7±1.3		492±2		2.50±0.02	
bottle 4	10.8±0.1		23.5±0.3		160.0±0.8		141.1±1.4		489±2		2.49±0.02	
bottle 4	10.5±0.1		23.2±0.2		159.2±0.8		141.4±1.4		486±2		2.47±0.02	
bottle 5	10.7±0.1		23.4±0.3		158.8±0.9		140.4±1.4		484±2		2.49±0.02	
bottle 5	10.6±0.1		23.2±0.3		158.5±0.8		140.6±1.4		486±2		2.48±0.02	
mean±u	*10.7±0.2*	*12.4±0.8*	*23.4±0.5*	*23.4±1.8*	*160±1*	*160±5*	*141±2*	*142±3*	*490±5*	*492±12*	*2.48±0.04*	*2.5±0.4[a]*
OU-6												
(50 mg, BD)	71.4±0.3		40.2±0.3		52.3±0.3		111±1		131.2±0.8		2.46±0.02	
(50 mg, BD)	71.2±0.4		41.2±0.3		48.3±0.3		115±1		131.7±0.8		2.44±0.02	
(100 mg, AD)	71.4±0.3		39.0±0.3		56.6±0.3		113±1		132.0±0.8		2.48±0.05	
mean±u	*71.3±0.4*	*70.7±4.1*	*40.1±0.7*	*40.2±2.2*	*52±2*	*40.4±2.9*	*113±2*	*111.4±4.6*	*132±1*	*131.7±5*	*2.46±0.04*	*2.67±0.27*
GSP-2	*obtained*		*obtained*		*obtained*		*obtained*		*obtained*		*obtained*	
(50 mg, BD)	20.7±0.2		16.9±0.2		42.6±0.3		116±3		233±1		6.20±0.03	
(50 mg, BD)	20.8±0.1		17.2±0.3		46.2±0.2		118±3		237±1		6.38±0.05	
(100 mg, AD)	21.0±0.2		17.1±0.2		47.7±0.3		117±3		236±1		6.51±0.04	
(100 mg, AD)	21.1±0.1		17.2±0.2		43.3±0.2		119±3		236±1		6.21±0.06	
(100 mg, AD)	20.8±0.2		17.4±0.2		42.6±0.2		118±3		236±1		6.49±0.04	
mean±u	*20.9±0.3*	*20±6*	*17.2±0.3*	*17±2*	*44.4±1.7*	*43±4*	*118±4*	*120±10*	*236±2*	*240±10*	*6.4±0.1*	*-*
GSR-1												
(70 mg, BD)	2.7±0.1		2.5±0.2		1.7±0.1		28±1		107.4±0.6		11.92±0.06	
(70 mg, BD)	2.7±0.1		2.5±0.2		1.5±0.1		26±1		105.7±0.6		11.80±0.08	
(100 mg, AD)	2.6±0.1		2.4±0.2		1.6±0.1		28±1		104.9±0.5		11.80±0.07	
(100 mg, AD)	2.6±0.1		2.6±0.2		1.6±0.1		28±1		105.9±1.4		11.91±0.06	
mean±u	*2.7±0.2*	*3.6±1.1*	*2.5±0.3*	*2.3±1.2*	*1.6±0.1*	*3.2±1.3*	*28±1*	*28±4*	*106±1*	*106±9*	*11.9±0.1*	*12.5±2*
AGV-1												
(50 mg, BD)	9.2±0.1		16.0±0.2		58.5±0.3		90±3		660±3		3.92±0.02	
(50 mg, BD)	9.1±0.1		16.0±0.2		59.5±0.4		91±3		660±3		3.90±0.03	
(100 mg, AD)	9.1±0.1		16.0±0.2		58.9±0.4		89±5		662±3		4.01±0.02	
(100 mg, AD)	9.1±0.1		16.1±0.2		58.6±0.4		94±3		660±3		3.96±0.02	
(100 mg, AD)	9.0±0.1		15.9±0.2		58.7±0.8		86±3		663±3		4.01±0.02	
(100 mg, AD)	9.1±0.1		16.1±0.2		59.4±0.4		93±3		659±3		3.98±0.03	
mean±u	*9.1±0.2*	*10±3*	*16.0±0.3*	*16[a]*	*58.9±0.8*	*60±6*	*91±5*	*88±9*	*661±4*	*660±9*	*3.96±0.04*	*4.2[a]*
Published values		*8.18±0.33[b]*		*15.7±0.6[b]*		*60.3±3.0[b]*		*86±7[b]*		*660±1[c]*		*4.16±0.24[d]*

The reference values (RV) are presented with standard deviation established during the respective characterization process.

The mass of each test portion mass and the spiking technique are indicated in parenthesis; BD means that spikes were added before dissolution, except ^{86}Sr, and AD means that spikes were added to one aliquot of the sample solution after dissolution.

For each analyte the resultant combined uncertainty of the mean of the results was calculates as $u = ((s_{results}/\sqrt{n})^2 + \Sigma s_i^2/n)^{1/2}$, where $s_{results}$ is the standard deviation calculated from the individual results, s_i are the combined standard measurement uncertainty of the individual determinations and n the number of results.

[#] 100 mg test portions of BRP-1 were dissolved in duplicate from five different bottles. Aliquots of the sample solutions were spiked and used for the determinations.

[a] informative value proposed by the RM provider. Published values: [b] Makishima *et al.* (2002) using ID-HR-ICP-MS. [c] Raczek *et al.* (2001) using ID-TIMS. [d] Lu *et al.* (2007) using ID-ICP-QMS. Uncertainty of published values [b, c, d] is given as one standard deviation.

Table 4. (*cont.*) Individual results with respective combined standard measurement uncertainties for each test portion and mean value of all determinations with resultant combined uncertainty (in mg kg^{-1})

RM	Cr	RV	Ni	RV	Cu	RV	Zn	RV	Sr	RV	Sn	RV
RGM-1												
(70 mg, BD)	3.5±0.1		4.6±0.2		10.5±0.1		34±3		103.6±0.6		3.81±0.02	
(70 mg, BD)	3.6±0.1		5.3±0.2		10.7±0.1		33±3		103.3±0.6		3.78±0.03	
(100 mg, AD)	3.8±0.1		5.0±0.2		10.7±0.1		32±3		103.4±0.5		3.93±0.03	
(100 mg, AD)	3.4±0.1		5.1±0.2		10.6±0.1		31±3		104.0±0.6		3.84±0.03	
mean±u	*3.6±0.2*	*3.7[a]*	*5.0±0.3*	*-*	*10.6±0.2*	*12±1.4*	*33±4*	*32[a]*	*103.6±0.8*	*110±10*	*3.84±0.05*	*4.1±0.4*
RGM-2												
(70 mg, BD)	3.3±0.1*		4.8±0.2		9.5±0.1		33±3		107.8±0.6		3.33±0.02	
(70 mg, BD)	6.0±0.1		5.7±0.2		9.9±0.1		30±3		107.6±0.6		3.31±0.03	
(100 mg, AD)	5.9±0.1		5.3±0.2		9.5±0.1		35±3		107.1±0.5		3.35±0.02	
(100 mg, AD)	5.8±0.1		5.0±0.2		9.6±0.1		32±3		107.4±0.7		3.37±0.02	
mean±u	*5.9±0.8*	*-*	*5.2±0.4*	*-*	*9.6±0.2*	*-*	*32±4*	*-*	*107.5±0.9*	*-*	*3.34±0.04*	*-*
G-3												
(50 mg, BD)	18.6±0.1		10.0±0.3		16.8±0.2		96±6		465±2		2.15±0.01	
(50 mg, BD)	18.4±0.1		10.2±0.2		16.9±0.1		99±7		462±2		2.19±0.02	
(100 mg, AD)	18.6±0.1		9.9±0.2		16.9±0.2		98±6		467±2		2.20±0.03	
mean±u	*18.6±0.2*	*-*	*10.1±0.3*	*-*	*16.8±0.2*	*-*	*98±7*	*-*	*465±3*	*-*	*2.18±0.03*	*-*

Test portion mass and spiking technique are indicated within parenthesis, BD means that spikes were added before dissolution, except [86]Sr, and AD means that spikes were added to one aliquot of the sample solution after dissolution.
* Result excluded from the calculation of the mean value, but not from the resultant combined uncertainty of the mean.
[a] informative value.

The combined standard measurement uncertainty of each determination includes uncertainty components associated to the precision of the isotope ratio measurements on sample (R_{xy}) and calibration (R_{Bc}) blends, concentration of the CS (C_z), all the masses (m_x, m_y, m_{yc}, m_{zc}, $m_{aliquot}$, $m_{sam\ sol}$) involved in Eq. 3 or 4, drift in the measured ratio ($R_{Bc(drift)}$), subtractions of interferences ($R_{xy(interferences)}$) and procedural blank (C_{blank}) and dead time corrections ($R_{xy(dead\ time)}$ and $R_{Bc(dead\ time)}$). Figure 2 presents the relative contribution of each component to the combined standard measurement uncertainty calculated for Cu in BRP-1, bottle 1 first replicate. In this example, the major contribution comes from the standard uncertainties of the isotope ratios measured in the sample and in the calibration blends, which together accounts by more than 75% of the budget, and thus are limiting factors for uncertainty of the result. The third and the fourth more important components were those related to the uncertainties in the concentration of the diluted calibration standard, used to prepare the calibration blend, and that associated to the correction of polyatomic interferences, both corresponding to less than 0.2% of the Cu

concentration in the sample. In Figure 2, the capability of the double ID-MS technique to negate uncertainties related to the concentration (C_y) and isotopic composition of the spike (R_y) and calibration standard (R_z) are also shown. In the appendix A the procedure used to calculate the combined standard measurement uncertainty is summarized and the relative contribution of each component presented, Table 5.
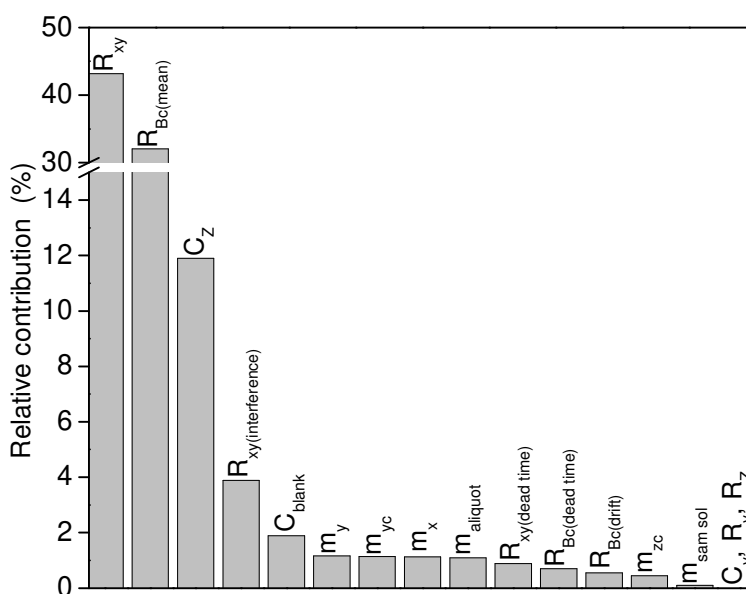

Figure 2. Relative contribution of each component for the combined standard uncertainty calculated for Cu in BRP-1. Details in appendix A.

Individual results were obtained with combined standard measurement uncertainty varying from approximately 0.5% for Sr, in all RM analyzed, to 7% for Cu in GSR-1. To most analytes the combined standard measurement uncertainties were better than 1%, except for Zn in granitic RM due significant interferences of double charged Ba on ^{68}Zn isotope, in these cases the uncertainties were near 10%. In contrast, in basalts (BRP-1 and BCR-2) and in OU-6 this interference was less intense and the combined standard measurement uncertainty was better than 2%. One indicative of the reliability of the interferences corrections applied for Zn comes from the agreement between the mean results obtained for AGV-1 (91±5 mg kg^{-1}) and the value

published by Makishima *et al*. (2002), 86±7 mg kg^{-1}, obtained using ID-MS technique with an high resolution instrument (HR-ICP-MS) to separate the interferences signal.

The smaller combined standard measurement uncertainty obtained for Sr reflects the absence of significant polyatomic and double charged interferences. The contribution of double charged Yb, oxides of Ge and hydroxides of Ga represent less than 0.01% of the Sr isotopes signal in these RM, which exempts the use of mathematical corrections. Additionally, Sr is present at elevated concentrations and the $^{88}Sr/^{86}Sr$ ratios were measured alone in a separated aliquot. The higher count rates ($\approx$ 0,5 Mcps) resulted in better precision (varying mainly from 0.1 to 0.2%, in contrast with 0.2 to 0.5% for other elements) and the complete matching procedure of signal intensities and isotope ratios between sample and calibration blends was applied. The contribution of radiogenic Sr, formed from the decay of $^{87}Rb \rightarrow {}^{87}Sr$, was only important to GSP-2 in which it represents 0.64% of the overall Sr content. For the other RM the amount of radiogenic Sr corresponds to less than 0.25%.

Averages of procedural blanks are presented in Table 6 (appendix A). The blank levels of Zn, Sr and Sn in all RM analyzed were negligible, but for Cr, Ni and Cu they represent up to 10% of the concentrations found in GSR-1, RGM-1 and RGM-2. Thus in these cases, the combined standard measurement uncertainty was dominated by the blank component. For the remaining RM, blank levels of Cr, Ni and Cu were none significant.

The individual results were used to calculate mean values for each analyte, Table 4. These mean values are indicated with a resultant combined uncertainty ($u=((s_{results}/\surd n)^2+\Sigma s_i^2/n)^{1/2}$), which takes into account the repeatability of the determinations ($s_{results}/\surd n$) and the pooled uncertainty of individual determinations ($\Sigma s_i^2/n$), following Briche *et al.* (2001). The resultant combined uncertainty of the mean varied from about 1 to 3% for most analytes, except for Zn due interferences, as discussed above.

In general, the mean of results agrees with reference values (RV), when the range delimitated by $RV \pm SD_{RV}$ is considered, were SD_{RV} is the standard deviation of the RV. Exceptions are the obtained value for Cu in GSR-1 and OU-6. The comparison of our result, 1.6 ± 0.1 mg kg^{-1}, with the RV of Cu in GSR-1, 3.2 ± 1.3 mg kg^{-1}, is difficult since it possesses a large SD_{RV}, indicating that the original data set used to establish the reference value presented a wide dispersion, probably because these data sets were obtained using procedures not fit to accurately measure Cu at low concentration. A similar difficulty probably occurred for Ni and Cu in GSR-1.

The difference between the mean of results, 52 ± 2 mg kg^{-1}, and RV for Cu in OU-6, 40.4 ± 2.9 mg kg^{-1}, can be attributed to the heterogeneous distribution of Cu in this RM, as reported by Kane (2004) during the certification of OU-6.

A systematic difference, of -1.5 and -1.7 mg kg^{-1}, in relation the RV was observed in the obtained results of Cr for BCR-2 and BRP-1, respectively. The similarity of these lower values can be traced to the use of BCR-2 as quality control sample sent to laboratories responsible for the characterization of BRP-1. After the characterization step, the quality of the reported results was judged comparing the reported values for BCR-2 and the interval delimited by $RV \pm 2SD_{RV}$. Data sets lying outside this range were considered for exclusion since traceability could not be assured. Thus, is highly probable that if there is a significant bias in the RV for Cr in BCR-2 compared to its "true" value, that bias was transferred to the RV of BRP-1, through the use of BCR-2 as quality control sample.

Although a unique result, even being obtained by ID, it does not prove the need to change a RV, accumulated evidence suggests that the true value of Cr in BRP-1 may be lower than the established RV. For instance, the mean of several results obtained by ICP-MS with conventional calibration curve technique (Cotta and Enzweiler, 2010), produced a mean value of 11.4 ± 0.7 mg

kg^{-1}; the results published by Jochum *et al*. (2009) and Regnery *et al*. (2010) using laser ablation HR-ICP-MS were 8.8±1.6 and 8.7±1.4 mg kg^{-1}, respectively, and the provisional mean value of 10.7±0.5 mg kg^{-1} proposed by the organizers of proficiency test (GeoPT25, IAG, 2009), during a round in which BRP-1 was analyzed and 63 laboratories submitted results for Cr. All those data support the conclusion that the mean value obtained in this study, 10.7±0.2 mg kg^{-1}, probably is closer to a "true" value of Cr in BRP-1. Such evidences suggest that the certified value of Cr in BRP-1 could be updated.

The mean value obtained for Cr in AGV-1 was 9.1±0.2 mg kg^{-1}, and is between the RV, 10±3 mg kg^{-1}, and the result published by Makishima *et al*. (2002), 8.18±0.33 mg kg^{-1}. For Ni, Cu, Zn and Sn our mean result agree within the experimental uncertainty (≈5%) with the values of Makishima *et al*. (2002) and Lu *et al*. (2007). It is worth noting that the measurement of Cr, Ni and Cu at high resolution to solve interferences resulted in larger uncertainties (expressed as one standard deviation of the instrumental precision) compared to those obtained in present investigation, where all significant sources of uncertainty were taken in account. The Sr mean results in AGV-1 and GSP-2, respectively 661±4 and 236±2 mg kg^{-1}, agrees within uncertainties with the values obtained by Raczek (2001), 660±1 and 238.0±0.2 mg kg^{-1}, using ID-TIMS.

Conclusion

Mean values with relatively small combined uncertainties were obtained by double ID technique with measurements on an ICP-QMS. Combined standard measurement uncertainties could have been diminished if interfering elements, especially for the determination of Zn, were removed before analyses. The use of collision cell was effective to diminish the overlap caused by polyatomic interferences on target isotopes used for quantification. Furthermore performing the measurements in collision cell mode provided satisfactory conditions to achieve stable mass bias correction factors and ultimately in precise and accurate results.

The lower results for Cr in BCR-2 and BRP-1 compared to the respective reference values suggests that traceability was not properly achieved for this element during the characterization of BRP-1 by the interlaboratory program. Therefore, we propose the inclusion of the ID-ICP-MS values in the set used to calculate the Cr reference value in BRP-1, the reconsideration of values originally taken off because they were outliers and the calculation of a new RV, which probably will be closer to the mean value obtained in this study, 10.7 ± 0.2 mg kg^{-1}.

Appendix A.

In this appendix we describe the procedure used to calculate the combined standard measurement uncertainty of individual determinations together with complementary data used in the calculation of concentration. To perform these calculations we followed the Eurachem/Citac Guide (2000), which recommends the use of the spreadsheet method for uncertainty calculation developed by Kragten (1994). The spreadsheet method is an approximate numerical method of differentiation, where the uncertainty, $u(y(x_1, x_2 ...x_n))$, for a expression $y(x_1, x_2,...x_n)$ is calculated simply as the difference between the values of y calculated for $[x_i + u(x_i)]$ and for x_i respectively. As follows:

$$u(y(x_1,x_2...x_n) = (\{y([x_1+u(x_1)],x_2...x_n) - y(x_1,x_2...x_n)\}^2 + ... + \{y(x_1,x_2,[x_i+u(x_n)]) - y(x_1, x_2...x_n)\}^2)^{1/2}$$

Table 5 contains the values of the input quantities, with its standard uncertainty, used to calculate the concentration of Cu in BRP-1 following equation (3).

The calculation starts by estimating the concentration of the diluted calibration standard solution used to prepare the calibration blend and it standard uncertainty. The commercial HPS calibration standard has a concentration (C_{HPS}) of 10.00 µg ml^{-1}, with overall uncertainty of 0.03 µg ml^{-1} (a coverage factor equal to 2 was assumed), and density (d) of 1.0061±0.0001 g ml^{-1}. From this calibration standard a mass (m_1) of 1.0150±0.0003 g was taken and diluted with 2% HNO$_3$ to 9.9149±0.0005 g (m_2). The obtained solution has a concentration (C_z), corrected by density, given by: Cz = C_{HPS}*m$_1$*d/m$_2$ = 1.0175 ±0.0016 µg g^{-1}, which standard uncertainty, $u(C_z)$, was estimated following:

$$u(C_z)= C_z \times \sqrt{\Sigma \left(\frac{u(x_i)}{x_i}\right)^2}$$

$$u(C_z)=C_z*[(0.03/2/10)^2+(0.0001/1.0061)^2+(0.0003/1.0150)^2+(0.0005/9.9149)^2]^{1/2}$$

$$u(C_z)= 0.0016 \text{ µg g}^{-1}.$$

The standard uncertainty on each mass was estimated using repeatability of weight measurements. Detector dead time was estimated measuring the ratio ^{88}Sr/^{86}Sr in five solutions of Sr with natural isotopic composition at different concentration to produce count rate in the range of 0.1 to 1.0 Mcps to the isotope ^{88}Sr. Dead time was established after plotting the measured isotope ratios versus the Sr concentration, for different dead times. The optimum dead time (50±3 ns) was that resulted in isotope ratios independent of concentration, according to (Nelms *et al.* 2001). The uncertainty associate to dead time correction was determined following: $u(R_{Bc(dead\ time)})=R_{Bc(DT=\ 50ns)}-R_{Bc(DT=53ns)}$, where $R_{Bc(DT=\ 50ns)}$ and $R_{Bc(DT=53ns)}$ are the R_{Bc} ratio calculated using a dead time correction of 50 and 53 ns, respectively. A similar procedure was used to obtain the uncertainty of dead time correction for the R_{xy} ratio.

The standard uncertainty, $u(R_{xy})$, corresponds to the standard deviation calculated for the 5 readings obtained in each measurement of the sample blend.

The uncertainty associated to the ratio R_{xy}, due the subtraction of interferences, $u(R_{xy(interferences)})$, was estimated using the uncertainty in the coefficients of the corrections applied. The $u(R_{xy(interferences)})$ was calculated as the difference between the isotope ratio R_{xy}, corrected for interferences using the equation shown in Table 3, and this ratio recalculated using the coefficient of the correction less it uncertainty to one isotope and the coefficient of the correction plus it uncertainty to the another isotope (R'_{xy}). It means that the ratio R'_{xy} was obtained using the

measured intensity of ^{63}Cu corrected for interferences using the equation: $^{63}Cu = ^{63}C-0.0020*^{49}Ti$, and the isotope ^{65}Cu the equation: $^{65}Cu=^{65}C-0.0024*^{49}Ti-0.0011*^{137}Ba$. The uncertainties associated to dead time correction and the subtraction of interferences were estimated using a conservative simplification of the formal procedure, which tends to produce an over estimative of these uncertainties.

Table 5. Summary of the component and respective numerical input used to estimate the standard measurement uncertainty of individual determinations; the example contains the data used to determine Cu in bottle 1of BRP-1. The last column presents the relative contribution (RC %) of each component

Component	Value ± u	C_x	$C_x{}'$	$(C_x{}'-C_x)^2$	RC (%)
$C_z \pm u(C_z)$ in mg kg^{-1}	1.0175±0.0016	159.72	159.97	0.063	11.9
$m_y \pm u(m_y)$ in g	0.2039±0.0001	159.72	159.80	0.006	1.2
$m_x \pm u(m_x)$ in g	0.2072±0.0001	159.72	159.64	0.006	1.1
$m_z \pm u(m_z)$ in g	0.9923±0.0003	159.72	159.77	0.002	0.4
$m_{yc} \pm u(m_{yc})$ in g	0.2052±0.0001	159.72	159.64	0.006	1.1
$m_{sam\ sol} \pm u(m_{sam\_sol})$ in g	20.9303±0.002	159.72	159.73	0.0002	0.04
$m_{aliquot} \pm u(m_{aliquot})$ in g	0.6284±0.0003	159.72	159.62	0.010	1.1
$A^a_z \pm u(A^a_z)$ in %	69.15±0.08	159.72	159.72	0.000	0.00
$A^b_z \pm u(A^b_z)$ in %	30.85±0.08	159.72	159.72	0.000	0.00
$R_z \pm u(R_z)$	2.241±0.006	159.72	159.72	0.000	0.00
C_y in mg kg^{-1}	4.263±0.009	159.72	159.72	0.000	0.00
$A^a_y \pm u(A^a_y)$ in %	0.10±0.03	159.72	159.72	0.000	0.00
$R_y \pm u(R_y)$	0.0010±0.0003	159.72	159.72	0.000	0.00
$A^b_y \pm u(A^b_y)$ in %	99.90±0.03	159.72	159.72	0.000	0.00
$R_{Bc(mean)} \pm u(R_{Bc(mean)})$	0.2723±0.0008	159.72	159.31	0.170	32.0
$R_{Bc(mean)} \pm u(R_{Bc(drift)})$	0.2723±0.0001	159.72	159.66	0.004	0.6
$R_{Bc(mean)} \pm u(R_{Bc(dead\ time)})$	0.2723±0.0001	159.72	159.66	0.004	0.7
$R_{xy} \pm u(R_{xy})$	0.2701±0.0009	159.72	160.20	0.228	43.2
$R_{xy} \pm u(R_{xy(dead\ time)})$	0.2701±0.0001	159.72	159.79	0.005	0.9
$R_{xy} \pm u(R_{xy(interferences)})$	0.2701±0.0004	159.72	159.86	0.021	3.9
$C_{blank} \pm u(C_{(blank)})$ in mg kg^{-1}	0.2±0.1	159.72	159.82	0.01	1.9
			$\Sigma(C_x{}'-C_x)^2 =$	0.529	
	Combined standard measurement uncertainty = $[\Sigma(C_x{}'-C_x)^2]^{1/2} =$			0.73	

C_x is the concentration of the analyte calculated using the values of the quantities as indicated and $C_x{}'$ is the concentration calculated using the quantities values plus it standard uncertainty. For instance, C_x is calculated with the value of 0.2039g for m_y and $C_x{}'$ is calculated using m_y = 0.2039+0.0001=0.2040g, where 0.0001g is the uncertainty of the mass 0.2039g.
The contribution of the blank to the uncertainty of the result was estimated taking: $C_x{}'=C_x+u(C_{blank})$.

The calibration blend was analyzed repeatedly during the measurement sequence, the $R_{Bc(mean)}$ is the mean of the values obtained for the ratio R_{Bc} after and before analyzing the sample blend. The uncertainty, $u(R_{Bc(mean)})$, corresponds to the higher standard deviation of these two measurements. The uncertainty associated to the drift in the $R_{Bc(mean)}$, it is $u(R_{Bc(drift)})$, was

estimated as the halved difference between the two ratios obtained for the calibration blend $(R_{Bc(drift)}=0.5*(R_{Bc(before\ sample)}-R_{Bc(after\ sample)})$. A similar procedure was used by Briche *et al.* (2001) to estimate the uncertainties associate to $R_{Bc(mean)}$ and $R_{Bc(drift)}$. The uncertainty associated to the blank subtraction is explained at the bottom of Table 5 with uncertainties listed in Table 6.

Table 6. Averaged blank concentration and it combined uncertainty, $u(C_{(blank)})$, (in mg kg^{-1})

Element	Table-top	Bomb
Cr	0.2±0.1	0.2±0.1
Ni	0.1±0.1	0.2±0.2
Cu	0.2±0.1	0.2±0.1
Zn	0.2±0.2	0.3±0.2
Sr	0.03±0.01	0.04±0.02
Sn	0.004±0.004	0.003±0.002

Blank concentrations as equivalent concentration in the sample for a dilution factor of 2000 fold.

To account for the amount of radiogenic Sr formed due the decay of $^{87}Rb \rightarrow ^{87}Sr$, the ratio $^{87}Sr/^{86}Sr$ of the RM was considered in Eq. (4). For some RM published values were used, Table 7, in absence of them the ratio $^{87}Sr/^{86}Sr$ was measured ([#]).

Table 7. Published and measured isotopic ratios for $^{87}Sr/^{86}Sr$ in geochemical RM

	BCR-2	GSP-2	AGV-1	G-3	RGM-1[*]	OU-6	BRP-1	GSR-1
$^{87}Sr/^{86}Sr$	0.704959(17)[a]	0.764962(17)[a]	0.703931(17)[a]	0.710019(6)[b]	0.704219(8)[c]	0.726(5)[#]	0.706(3)[#]	0.700(5)[#]

[a] Raczek *et al.* (2003), [b] Balcaen *et al.* (2005), [c] Weis *et al.* (2006), [*] the same value was assumed to RGM-2,
[#] measured in this study. Uncertainties, within parentheses, are given as one standard deviation.

References

Balcaen L., De Schrijver I., Moens L. and Vanhaecke F. (2005)
Determination of 87Sr/86Sr isotope ratio in USGS silicate reference materials by multi-collector ICP-mass spectrometry. International Journal of Mass Spectrometry, 242, 251-255.

Becker J.S. and Dietze H.J. (1998)
Inorganic trace analysis by mass spectrometry, Spectrochimica Acta Part B, 53, 1475-1506.

Böhlke J.K., de Laeter J.R., De Bièvre P., Hidaka H., Peiser H.S., Rosman K.J.R. and Taylor P.D.P. (2005)
Isotopic compositions of the elements, 2001. Journal of Physical and Chemical Reference Data, 34, 57-67.

Briche C.S.J.W., Harrington C., Catterick T. and Fairman B. (2001)
Orthodox uncertainty budgeting for high accuracy measurements by isotope dilution inductively coupled plasma-mass spectrometry. Analytica Chimica Acta, 437, 1-10.

Catterick T., Fairman B. and Harrington C. (1998)
Structured approach to achieving high accuracy measurements with isotope dilution inductively coupled plasma mass spectrometry .Journal of Analytical Atomic Spectrometry, 13, 1009-1013.

Cotta A.J.B., Enzweiler J., Wilson S.A., Pérez C.A., Nardy A.J.R. and Larizzatti J.H. (2007)
Homogeneity of the geochemical reference material BRP-1 (Paraná Basin Basalt) and assessment of minimum mass. Geostandards and Geoanalytical Research, 31, 379-393.

Cotta A.J.B. and Enzweiler J. (2008)
Certificate of analysis of the reference material BRP-1 (Basalt Ribeirao Preto). Geostandards and Geoanalytical Research, 32, 231-235.

Cotta A.J.B. and Enzweiler J. (2010, *in press***)**
Classical and new procedures of whole rock dissolution for trace elements analysis by ICP-MS. Geostandards and Geoanalytical Research.

Eurachem/Citac Guide (2000)
Quantifying uncertainty in analytical measurement (second edition), 120pp.
(*http://measurementuncertainty.org/pdf/QUAM 2000-1.pdf*)

Heumann K.G. (1988)
Isotope dilution mass spectrometry in Inorganic Mass Spectrometry, ed. F. Adams, R. Gijbels and R. Van Grieken, John Wiley & Sons, New Yore, 1988, 301-376.

Heumann K.G. (1992)
Isotope-dilution mass-spectrometry. International Journal of Mass Spectrometry and Ion Processes, 118, 575-592.

Heumann K.G., Gallus S.M., Radlinger G. and Vogl J. (1998)
Precision and accuracy in isotope ratio measurements by plasma source mass spectrometry.Journal of Analytical and Atomic Spectrometry, 13, 1001-1008.

Heumann K.G. (2004)
Isotope-dilution ICP-MS for trace element determination and speciation: From a reference method to a routine method?. Analytical and Bioanalytical Chemistry, 378, 318-329.

IAG (2009)
GeoPT25 - An international proficiency test for analytical geochemistry laboratories – Report on round 25 (Basalt, HTB-1), 30pp. (*http://www.geoanalyst.org/geopt/GeoPT25Report.pdf*)

ISO Guide 33 (1989)
Uses of certified reference materials. International Organisation for Standardisation (Geneva), 12pp.

ISO Guide 35 (2006)
Certification of reference materials- General and statistical principles (third edition). International Organization for Standardization (Geneva), 64pp.

Jochum K.P., Stoll B., Friedrich J.M., Amini M., Becker S., Dücking M., Ebel D.S., Enzweiler J., Hu M., Kuzmin D., Mertz-Kraus R., Müller W.E.G., Regnery J., Sobolev A., Wang X. and Zhan X. (2009)
Laser ablation-inductively coupled plasma-mass spectrometry and its application in geochemistry, cosmochemistry and environmental research. Rock and Mineral Analysis, 28, 53-68.

Kane J.S. (2001)
The use of reference materials: A tutorial. Geostandards Newsletter-The Journal of Geostandards and Geoanalysis, 25, 7-22.

Kane J.S. and Potts P.J. (2002)
Traceability in geochemical analysis. Geostandards Newsletter-The Journal of Geostandards and Geoanalysis, 26, 171-180.

Kane J.S. (2004)
Report of the International Association of Geoanalysts on the Certification of Penrhyn Slate, OU-6. Geostandards and Geoanalytical Research, 28, 53-80.

Kane J.S. and Potts P.J. (2007)
ISO best practices in reference material certification and use in geoanalysis. Geostandards and Geoanalytical Research, 31, 361-378.

Klingbeil P., Vogl J., Pritzkow W., Riebe G. and Müller J. (2001)
Comparative studies on the certification of reference materials by ICPMS and TIMS using isotope dilution procedures. Analytical Chemistry, 73, 1881-1888.

Kragten J. (1994)
Calculating standard deviations and confidence intervals with a universally applicable spreadsheet technique. Analyst 119, 2161-2166.

Lu Y.H., Makishima A., Nakamura E. (2007)
Coprecipitation of Ti, Mo, Sn and Sb with fluorides and application to detennination of B, Ti, Zr, Nb, Mo, Sn, Sb, Hf and Ta by ICP-MS.Chemical Geology, 236, 13-26.

Makishima A., Kobayashi K. and Nakamura E. (2002)
Determination of chromium, nickel, copper and zinc in milligram samples of geological materials using isotope dilution high resolution inductively coupled plasma-mass spectrometry. Geostandards and Geoanalytical Research, 26, 41-51.

Nelms S.M., Quetel C.R., Prohaska T., Vogl J. and Taylor P.D.P. (2001)
Evaluation of detector dead time calculation models for ICP-MS. Journal of Analytical and Atomic Spectrometry, 16, 333-338.

Pin C., Joannon S., Bosq C., Le Fèvre B. and Gauthier P.J. (2003)
Precise determination of Rb, Sr, Ba and Pb in geological materials by isotope dilution and ICP-quadrupole mass spectrometry following selective separation of the analytes. Journal of Analytical and Atomic Spectrometry, 18, 135-141.

Raczek I., Jochum K.P. and Hofmann A.W. (2003)
Neodymium and strontium isotope data for USGS reference materials BCR-1, BCR-2, BHVO-1, BHVO-2, AGV-1, AGV-2, GSP-1, GSP-2 and eight MPI-DING reference glasses. Geostandards Newsletter-The Journal of Geostandards and Geoanalysis, 27, 173-179.

Raczek I., Stoll B., Hofmann A.W. and Jochum K.P. (2001)
High-precision trace element data for the USGS reference materials BCR-1, BCR-2, BHVO-1, BHVO-2, AGV-1, AGV-2, DTS-1, DTS-2, GSP-1 and GSP-2 by ID-TIMS and MIC-SSMS. Geostandards Newsletter-The Journal of Geostandards and Geoanalysis, 25, 77-86.

Regnery J., Stoll B. and Jochum K.P. (2010)
High-resolution LA-ICP-MS for accurate determination of low abundances of K, Sc and other trace elements in geological samples. Geostandards and Geoanalytical Research, 34, 19-38.

Vogl J. (2007)
Characterisation of reference materials by isotope dilution mass spectrometry. Journal of Analytical Atomic Spectrometry, 22, 475-492.

Vogl J., Quetel C.R., Ostermann M., Papadakis I., Van Nevel L. and Taylor P.D.P. (2000)
Contribution to the certification of B, Cd, Mg, Pb, Rb, Sr and U in a natural water sample for the International Measurement Evaluation Programme Round 9 (IMEP-9) using ID ICP MS. Accreditation and Quality Assurance, 5, 272-279.

Weis D., Kieffer B., Maerschalk C., Barling J., de Jong J., Williams G., Hanano D., Pretorius W., Mattielli N., Scoates J.S., Goolaerts A., Friedman R.M. and Mahoney J.J. (2006)
High-precision isotopic characterization of USGS reference materials by TIMS and MC-ICP-MS. Geochemistry Geophysics Geosystems, 7, 1-30.

Willbold M. and Jochum K.P. (2005)
Multi-element isotope dilution sector field ICP-MS: A precise technique for the analysis of geological materials and is application to geological reference materials. Geostandards and Geoanalytical Research, 29, 63-82.